

**BACK ANALYSIS OF SLOPE FAILURE AT
WALIPANNA, SOUTHERN EXPRESS WAY**

I.A.N.D Idirimanna

(138813L)

Degree of Master of Science in Foundation Engineering and Earth
Retaining Systems

Department of Civil Engineering

University of Moratuwa

Sri Lanka

May 2018

**BACK ANALYSIS OF SLOPE FAILURE AT
WALIPANNA, SOUTHERN EXPRESS WAY**

I.A.N.D Idirimanna

(138813L)

Thesis submitted in partial fulfillment of the requirements for the degree of Master of
Engineering in Foundation Engineering and Earth Retaining Systems

Department of Civil Engineering

University of Moratuwa

Sri Lanka

May 2018

DECLARATION OF THE CANDIDATES AND SUPERVISORS

I declare that this is my own work and this dissertation does not incorporate without acknowledgement any material previously submitted for a Degree or Diploma in any University or other institute of higher learning and to the best of my knowledge and belief it does not contain any material previously published or written by another person except where the acknowledgement is made in the text.

Also, I hereby grant to University of Moratuwa the non-exclusive right to reproduce and distribute my thesis/dissertation, in whole or in part in print, electronic or other medium. I retain the right to use this content in whole or part in future works (such as articles or books).

Signature of the candidate:.....

Date:.....

IdirimannaI.A.N.D.

“I have supervised and accepted this dissertation for the submission of the degree”

Signature of the supervisor:.....

Date:.....

Prof. Kulathilake S.A.S.
B.Sc. Eng. Hons (Moratuwa), Ph.D. (Monash), C.Eng., MIE(SL),
Department of Civil Engineering,
University of Moratuwa,
Sri Lanka

ABSTRACT

Slope failures due to excessive rainfall are a common geotechnical hazard in tropical countries where residual soils are abundant. These soils possess significant matric suctions in dry seasons and are in a stable state. Heavy infiltration of rainwater causes destruction of matric suctions, development of perched water table conditions and rise of ground water table. Thus shear strength is reduced causing slopes to fail. In order to understand the mechanism of rainfall induced slope stability it is necessary to model this process with a reasonable accuracy.

Sri Lankan residual soil formations are formed by weathering of the metamorphic parent rock and have inherited significant abrupt variations in engineering characteristics as; soil water characteristic curves (SWCCs), variation of permeability with water content and unsaturated shear strength parameters.

Cut slope at chainage of 42+340 to 42+400 in Walipanna at southern expressway failed after few days of rain. The back analysis of failure indicated that the safety margin is less than unity when saturated shear strength parameters of soil were used in the analysis. Infiltration of the rainfall that was recorded in nearby rain gauges was modeled using the SWCC and permeability function derived from the tests conducted on undisturbed samples recovered from the site.

The presence of relict joints was confirmed during the rectification work and the combination of the relict joints and failed surface drainage system would have contributed to the failure. The results of the analysis also revealed that if the drainage measures are in position in perfect working order this failure would not have occurred. Those measures were found to be capable of tolerating even a rainfall of much higher intensity than that actually occurred.

The modeling of infiltration revealed that the rise of ground water table is quite significant at the toe of the wall. Therefore when natural slopes are excavated into steeper profiles it is recommended to have a series of sub horizontal drains at the toe level even if the ground water table is found to be lower than the toe level. Also, the importance of routine maintenance of the drainage systems of all slopes is highlighted very strongly.

Key Words :Slope stability; Matric Suction; Unsaturated soil; Infiltration.

DEDICATION

This thesis is dedicated to my loving parents Mr H.B Idirimanna and
Mrs.F.R.Wickramasinghe.

For their endless love, support and encouragement

ACKNOWLEDGEMENT

I wish to express my deepest gratitude to Prof. S.A.S. Kulathilake, Senior Professor of the Department of Civil Engineering for his enormous support, valuable suggestions, diligent efforts and strong encouragement given to me throughout the thesis work. His deep insight and vast experience in the field of Geotechnical Engineering, contributed greatly to the success of this work.

It is a great privilege to thank Dr. L.I.N. de Silva, Senior Lecturer of the Department of Civil Engineering for providing all the necessary guidelines and direction as the Course coordinator of M.Eng program.

I should really pay my sincere gratitude to Eng. (Dr) Asiri Karunawardena, Director General of National Building Research Organization (NBRO), for his guidance and continuous support throughout the masters. I appreciate the enormous support given by Mr. R.M.S. Bandara, Head, Landslide Research and Risk Management Division of National Building Research Organization. I also owe many thanks to Mr.P.Dharmasena, Senior Engineer and Ms. N Vasanthan, Engineer, NBRO for their valuable contribution in the research work, giving valuable ideas and encouragement throughout the project. Special thanks are due to all staff members at NBRO

Finally yet importantly, I appreciate my husband for lending his devoted time to me during the last few years to read for the MSc and encouraging me to complete this final hurdle.

TABLE OF CONTENTS

	Page
DECLARATION OF THE CANDIDATES AND SUPERVISORS	i
ABSTRACT.....	iii
DEDICATION	iv
ACKNOWLEDGEMENT	v
TABLE OF CONTENTS.....	vi
LIST OF FIGURES	ix
List of Tables	xiv
LIST OF ABBREVIATIONS.....	xv
LIST OF APPENDICES	xvi
1. CHAPTER 01: Introduction.....	1
1.1 Background.....	1
1.2 Problem identification	3
1.3 Objectives	3
1.4 Methodology Applied.....	4
1.5 Thesis Outline.....	5
2. CHAPTER 02: Literature Review	6
2.1. Landslide Causal factors and Triggering factors.....	6
2.2 Classification of Landslides.....	7
2.2.1 Different form of Slides.....	8
2.3 Assessment of the stability of a slope.....	9
2.3.1 Spencer’s Method for slope stability analysis	12
2.4 Residual soil formations	14
2.5 Basic constituents of an unsaturated soil.....	18
2.5.1 Shear strength parameters of an Unsaturated soil.....	19
2.5.2 Hydraulic properties of Unsaturated Soil	20

2.6 Modelling the process of infiltration using SEEP/W Software.....	25
2.6.1 Infiltration through a Homogeneous slope	26
2.6.2 Infiltration through a slope with Weathered rock overlying by Residual soil	27
2.6.3 Influence of the Infiltration on Slope Stability	28
2.6.4 Effectiveness of surface drainage on infiltration	30
2.7 Determination of characteristics of Unsaturated soils.....	33
2.7.1 Development of Permeability function.....	35
2.7.2 Development of Soil Water Characteristic Curve (SWCC)	36
2.7.3 Direct shear test with tensiometers	38
CHAPTER 03: Initial design, the failure and rectification of failure at Welipenna..	40
3.1 Background.....	40
3.2 Geology and Sub soil profile	41
3.3 The initial design of the cut slope.....	43
3.4 Description of the failure.....	45
3.4.1 Nature of the failure.....	45
3.4.2 Possible reasons of failure	48
3.5 Rectification Design	49
3.5.1 Rectification measure of Soil nailing and Anchoring.....	50
3.5.2 Constructed Surface and Sub surface drainage	50
3.5.3 Gravity retaining wall	51
3.5.2 Construction Sequence	51
CHAPTER 04: Back analysis of slope failure	53
4.1 Preparation of Infiltration model	53
4.1.1 Rainfall data for the preparation of Infiltration model	53
4.1.2 Input parameters of Hydraulic properties of unsaturated soil.	54
4.1.3 Boundary conditions and mesh properties.....	55
4.1.4 Type of Analysis.....	56

4.1.5 Modeling of Infiltration behavior	56
4.2 Results of Infiltration analysis	58
4.2.1 Without surface drainage measures	58
4.2.1.2 Homogeneous Residual soil with Relict joints.....	61
4.2.2 Infiltration analysis for slope with surface drainage improvement	64
4.2.3 Infiltration analysis for slope with rainfall of high intensity	65
4.3 Slope Stability analysis.....	67
4.3.1 Sub soil profile and shear strength parameters	67
4.3.2 Analysis Type	68
4.4 Results of slope stability Analysis.....	69
4.4.1. Slope without any surface drainage improvement.....	69
4.4.1.1 Slope without Relict joints.....	69
4.4.1.2. Slope with Relict joints.....	78
4.4.2 Slope with surface drainage improvement.....	86
4.4.2.1 Slope without Relict joints.....	86
4.4.2.2 Slope with surface drainage improvement and with relict joints	92
4.4.4 Stability of the slope with higher rainfall intensity of 20mm/hr	101
CHAPTER 05: Conclusions	105
5.1 Failure at Walipanna in Southern Expressway.....	105
5.2 Identification of causes of failure	105
5.3 Rectification process.....	107
5.4 Concluding comments/ Lessons learnt.....	107
5.5 Key Findings.....	108
06: References.....	109
07: Appendices.....	112

LIST OF FIGURES

	Page
Figure 2.1: Fall; a toppling mechanism along discontinuities.....	7
Figure 2.2: Rotational Slide.....	8
Figure 2.3: Translational slide.....	9
Figure 2.4: Forces acting on a slice in the Spencer method	12
Figure 2.5: Variation of the FOS with respect to moment and force equilibrium....	14
Figure 2.6: Degree of Weathering and the Nature of the weathered product varies within a short distance	16
Figure 2.7 : Whitish zones encountered in a failure mass.....	16
Figure 2.8: Closely spaced rock Joints-remain as “Relict Joints” after weathering...	17
Figure 2.9: Toppling (Fall) Mode of failure could take place through relict joints ..	17
Figure 2.10 Four phases of Unsaturated soil	18
Figure 2.11: planar surface for the shear strength equation for unsaturated soils	20
Figure 2.12: Idealized soil–water characteristic curve (after Fredlund and Rahardjo, 1993).....	22
Figure 2.13: Geometry of analysed slope, selected sections and boundary conditions	25
Figure 2.14: Pore water pressure distribution of uniform soil profile with 5mm/hr rainfall (after Sujeewan & Kulathilake 2011)	26
Figure 2.15: Pore water pressure distribution of uniform soil profile with 20mm/hr rainfall (after Sujeewan & Kulathilake 2011)	27
Figure 2.16: Geometry of 1:1 two layers slope and selected sections(after Sujeewan & Kulathilake 2011)	27
Figure 2.17: Pore water pressure distributions of slope with Weathered rock overlying by Residual soil for 20mm/hr rainfall (after Sujeewan & Kulathilake 2011).....	28
Figure 2.18: Critical failure surface – homogeneous soil slope at initial stage (Case 1 Kulathilake & Sujeewan 2011)	29
Figure 2.19: Critical failure surface – two layers of soil slope at initial stage (Case 2 Kulathilake & Sujeewan 2011)	29

Figure 2.20: Critical failure surface – homogeneous slope at later stage (Case 1 Kulathilake & Sujewan 2011)	29
Figure 2.21: Critical failure surface – two layers of soil slope at a later stage (Case 2 Kulathilake & Sujewan 2011)	29
Figure 2.22: Variation of factor of safety with duration of rainfall (after Sujeevan and Kulathilaka 2011)	30
Figure 2.23 – Pore water pressure distribution for 5mm/hr rainfall with vegetation layer of permeability 10^{-7} m/s.....	31
Figure 2.24: Pore water pressure distribution for 20mm/hr rainfall with vegetation layer of permeability 10^{-7} m/s.....	31
Figure 2.25: Shape of a typical failure surface without vegetation cover	32
Figure 2.26: Shape of a typical failure surface with vegetation cover	32
Figure 2.27: Variation of factor of safety with drainage improvement, Kulathilake and Kumara (2013).....	33
Figure 2.28: Particle size distribution for Sandy Silt, Vasanthan (2016).....	34
Figure 2.29: Typical arrangement of permeability test, Vasanthan (2016).....	35
Figure 2.30: Graph of Hydraulic conductivity Vs Matric suction for wetting path - Sandy Silt, Vasanthan (2016).....	36
Figure 2.31: Typical arrangement of 5-bar pressure plate apparatus used for the research (Vasanthan 2016)	37
Figure 2.32: The variation of volumetric water content with matric suction (SWCC) for SANDY SILT for various methods, Vasanthan (2016).....	38
Figure 2.33: Typical arrangement of Direct shear apparatus used for the research, Vasanthan (2016).....	39
Figure 2.34: The variation of apparent cohesion with average matric suction, Vasanthan (2016).....	39
Figure 3.1: Location map – 1:50,000 scale	40
Figure 3.2 – Joint sets in the bedrock exposed at the top of the slope	41
Figure 3.3 – Typical drilling records indicating boudinage structures.....	42
Figure 3.4 – Water oozing out of relict joints during drilling	42
Figure 3.5: Photograph of the site before any cutting	43

Figure 3.6: Stability of the cut slope at 1:1.2 gradient – Section at 42+380 Critical failure surface (Design report – STDP).....	44
Figure 3.7: Berm drains and cascade drains	45
Figure 3.8 – Initial Crack and downward movement of soil	46
Figure 3.9– Movements of soil at the top and Movement of Cascade Drain.....	46
Figure 3.10– Debris of Failure Has Covered the road section towards the Galle	47
Figure 3.11 – Debris of Failure Has Covered the road section towards the Galle ...	47
Figure 3.12 –A Zone of whitish Feldspar rich clay in the failure surface.....	48
Figure 3.13 – Simulated failure surface (Rectification report – NBRO)	49
Figure 3.14 – Proposed stabilization with soil nailing subsurface drainage and toe wall	50
Figure 3.15: The location of soil nails, cable anchors and long horizontal drains ...	51
Figure 3.16: View after completing the rectification (Dharmasena et.al 2015).....	52
Figure 4.1: Peak rainfall from Bombuwawa and Beddegama Rain Gauges	54
Figure 4.2: SWCC used for analysis - Sandy Silt, wetting path, Vasanthan(2016). 54	
Figure 4.3: K function used for the analysis, Vasanthan (2016)	55
Figure 4.4: Slope with applied Boundary conditions	56
Figure 4.6: Pore water distribution vs depth in sections A-A to F-F for the idealized rainfall.....	59
Figure 4.7: Figure shows the rain infiltration through slope profile	60
Figure 4.8: Analyzed slope with relict joints.....	61
Figure 4.9: K function used for the material in relict joints	61
Figure 4.10: SWCC used for the material in relict joints	61
Figure 4.11: Pore water distribution vs depth in sections A-A to F-F	62
Figure 4.12: Rain infiltration through slope profile and relict joints	63
Figure 4.13: Pore water distribution vs depth in sections A-A and E-E for slope without relict joints and with surface drainage improvement (Permeability of vegetation layer = 10^{-7} m/s).....	64
Figure 4.14: Pore water distribution vs depth in sections A-A and E-E for slope with relict joints and with surface drainage improvement vegetation layer = 10^{-7} m/s). 64	
Figure 4.15: Pore water distribution vs depth in sections A-A and E-E for slope without surface drainage improvement and 20mm/hr rainafall	66

Figure 4.16: Pore water distribution vs depth in sections A-A and E-E for slope with 10^{-7} m/s permeable vegetation layer and 20mm/hr rainfall.....	66
Figure 4.17: Pore water distribution vs depth in sections A-A and E-E for slope with 10^{-8} m/s permeable vegetation layer and 20mm/hr rainfall.....	66
Figure 4.18: Slope stability analysis of the initial day	71
Figure 4.19: Slope stability analysis of the 1 st day.....	71
Figure 4.20: Slope stability analysis of the 2 nd day.....	72
Figure 4.21: Slope stability analysis of the 3 rd day	72
Figure 4.22: Slope stability analysis of the 4 th day.....	73
Figure 4.23: Slope stability analysis of the 5 th day.....	73
Figure 4.24: Slope stability analysis of the initial day	75
Figure 4.25: Slope stability analysis of the 1 st day.....	75
Figure 4.26: Slope stability analysis of the 2 nd day.....	76
Figure 4.27: Slope stability analysis of the 3 rd day	76
Figure 4.28: Slope stability analysis of the 4 th day.....	77
Figure 4.29: Slope stability analysis of the 5 th day.....	77
Figure 4.30: Slope stability analysis of the initial day	79
Figure 4.31: Slope stability analysis of the 1 st day.....	79
Figure 4.32: Slope stability analysis of the 2 nd day	80
Figure 4.33: Slope stability analysis of the 3 rd day	80
Figure 4.34: Slope stability analysis of the 4 th day.....	81
Figure 4.35: Slope stability analysis of the 5 th day.....	81
Figure 4.36: Slope stability analysis of the initial day	83
Figure 4.37: Slope stability analysis of the 1 st day.....	83
Figure 4.38: Slope stability analysis of the 2 nd day.....	84
Figure 4.39: Slope stability analysis of the 3 rd day	84
Figure 4.40: Slope stability analysis of the 4 th day.....	85
Figure 4.41: Slope stability analysis of the 5 th day.....	85
Figure 4.42: Slope stability analysis of the initial day	87
Figure 4.43: Slope stability analysis of the 1 st day.....	87
Figure 4.44: Slope stability analysis of the 2 nd day.....	88
Figure 4.45: Slope stability analysis of the 3 rd day	88

Figure 4.46: Slope stability analysis of the 4th day.....	88
Figure 4.47: Slope stability analysis of the 5 th day.....	89
Figure 4.48: Slope stability analysis of the initial day	90
Figure 4.49: Slope stability analysis of the 1 st day.....	90
Figure 4.50: Slope stability analysis of the 2 nd day	91
Figure 4.51: Slope stability analysis of the 3 rd day	91
Figure 4.52: Slope stability analysis of the 4th day.....	91
Figure 4.53: Slope stability analysis of the 5 th day.....	92
Figure 4.54: Slope stability analysis of the initial day	93
Figure 4.55: Slope stability analysis of the 1 st day.....	94
Figure 4.56: Slope stability analysis of the 2 nd day	94
Figure 4.57: Slope stability analysis of the 3 rd day	94
Figure 4.58: Slope stability analysis of the 4th day.....	95
Figure 4.59: Slope stability analysis of the 5 th day.....	95
Figure 4.60: Slope stability analysis of the initial day	96
Figure 4.61: Slope stability analysis of the 1 st day.....	97
Figure 4.62: Slope stability analysis of the 2 nd day	97
Figure 4.63: Slope stability analysis of the 3 rd day	97
Figure 4.64: Slope stability analysis of the 4th day.....	98
Figure 4.65: Slope stability analysis of the 5 th day.....	98
Figure 4.66: FOS distribution of Slope without surface drainage improvement	99
Figure 4.67: FOS distribution of Slope with surface drainage improvement.....	100
Figure 4.68: FOS distribution of Slope for 20mm/hr continuous rain	102
Figure 4.69: Slope stability analysis of the initial day	103
Figure 4.70: Slope stability analysis of the 1 st day.....	103
Figure 4.71: Slope stability analysis of the 2 nd day	103
Figure 4.72: Slope stability analysis of the 3 rd day	104
Figure 4.73: Slope stability analysis of the 4 th day	104
Figure 4.74: Slope stability analysis of the 5 th day.....	104
Figure 5.1: Different forms of analysis done.....	106

LIST OF TABLES

Table 2.1: Weathering profile	15
Table 2.2: Summary index property test for Sandy Silt	34
Table 3.1 – Shear Strength Parameters from undisturbed samples	43
Table 4.1: Shear strength parameters of the soil profile	68
Table 4.2: Shear strength parameters of the filling material in relict joints	68
Table 4.3: Minimum Factor of Safety for Circular slip surfaces – Without relict joints.....	70
Table 4.4: Minimum Factor of Safety for non-circular slip surfaces – without relict joints.....	74
Table 4.5: Minimum Factor of Safety for Circular slip surfaces – With Relict joints	78
Table 4.6: Minimum Factor of Safety for Non Circular slip surfaces – With Relict joints.....	82
Table 4.7: Minimum Factor of Safety for Circular slip surfaces – Without relict joints – For rainfall recorded at Bombuwawa and Beddegama	86
Table 4.8: Minimum Factor of Safety for non-circular slip surfaces – without relict joints.....	89
Table 4.9: Minimum Factor of Safety for Circular slip surfaces – With Relict joints - Peak rainfall from Bombuwawa and Beddagama Rg	92
Table 4.10: Minimum Factor of Safety for Non circular slip surfaces – With Relict joints.....	96
Table 4.11: Summary of the minimum Factor of Safety values – Slope without surface drainage improvement	99
Table 4.12: Summary of the minimum Factor of Safety values – Slope with surface drainage improvement	100
Table 4.13: Minimum Factor of Safety - 20mm/hr continuous rain.....	101

LIST OF ABBREVIATIONS

Abbreviation	Description
CH	Chainage
KU	Kasetsart University
NBRO	National Building Research Organization
SM	SILTY SAND
SWCC	Soil Water Characteristic Curve
STDP	Southern Transport Development Project

LIST OF APPENDICES

Appendix	Description	Page
Appendix A:	Location plan of the bore holes which were drilled from the berms, after failure	112
Appendix B:	The details of the borehole logs.....	114
Appendix C:	Five boreholes CD1 –CD5 which were drilled in the natural slope along the vicinity of the road segment.....	120
Appendix D:	Data of the rain gauge stations closest to the location as Bombuwala and Beddegama.....	126

1. CHAPTER 01: INTRODUCTION

1.1 Background

Rainfall-induced slope failure creates one of the most common geotechnical hazards in tropical regions such as Sri Lanka. These disasters cause significant impact to the economy of the country and create number of negative social impacts such as; loss of human life, damage to the property and also damage to the natural environment and wild life.

Two-thirds of Sri Lankan land area is covered with residual soils, which are formed by the in-situ weathering of the parent rock. In these slopes the degree of weathering can vary in an abrupt manner due to the differences in the mineralogical structure of the parent rock, which is metamorphic. It leads to the formation of a soil of highly heterogeneous nature.

The intense rainfall is the major triggering factor for slope failures under these conditions. Rainwater infiltration into soil depends on several factors such as soil structure – presence of relict joints, soil type, presence of soil moisture, status of the soil air, infiltrating water quality and slope tillage. It also it depends on the period of rainfall occurrence such as continuous rainfall for days or intermittent rainfall for hours by hours/ days by days.

Safety margins of these slopes are high during the periods of dry weather due to the prevailing matric suctions the negative pore water pressures. The pore water pressure distribution with depth prior to the rainfall is hydrostatic below the ground water table and negative above it in the unsaturated soil mass. As a result of heavy rainfall, significant infiltration takes place and soil at the surface is getting nearly saturated. As an unsaturated soil approaches saturation, the matric suction term goes towards zero. This loss of matric suction would reduce the apparent cohesion and caused to decrease the soil shear strength.

At the mean time, the wetting front progresses downwards as rainfall continues and water infiltrated downward will cause a rise of the ground water table. Towards the

toe of the slope the infiltration would cause much greater destruction of the matric suction profile and perched water table conditions could develop at surface level. Those changes would trigger slopes failures.

The systems of joints in the parent rock remain as zones of weakness and high permeability in the residual soil formed. They are termed as relict joints. The presence of relict structures in a sloping layered soil formation adds further complexity to the problem. This results in an inconsistency in the saturation profiles developed for a homogenous soil. Therefore, special attention should be paid in the modelling process when handling unsaturated soils with relict joints.

Vegetation will have a positive contribution to the stability of the slope by limiting the infiltration of rainwater and providing immediate shear strength enhancement and modifying the saturated soil water regime. Also there will be a positive impact from roots of vegetation to the slope stability and some of these roots will be acting like soil nails.

A rainfall induced slope failure occurred in a cut slope at chainage of 42+340 to 42+400 in Walipanna at southern expressway. After prolonged rainfall that continued for several days in western part of the country, the slope became unstable and collapsed on 2nd November 2012.

The slope is formed of residual soils where the parent rock is metamorphic. Due to weathering under high ambient temperature and high rainfall conditions and the differences in the mineralogical structure in the parent rock the weathered product is highly variable. Rocks with no or slight weathering were embedded in a matrix of soil (boudinage structures). Five different joint systems were identified in the rocks in the area and adversely oriented relict joints filled with water were identified during the rectification process.

The failure was back analysed by simulating the events that have taken place preceding the failure. Two rain gauges located in the region have the records of rainfall occurred prior to the failure. The sub soil parameters of the slope were determined through laboratory experiments after the failure and previous investigations.

1.2 Problem identification

The residual soil slopes have a deep groundwater table with a significant portion of unsaturated zone above the water table. Infiltration of rainwater through this unsaturated zone and subsequent changes in shear strength of unsaturated soils causes reduction in the stability of a slope resulting slope failures.

However, still saturated soil properties are generally used for slope stability analysis. The unsaturated portion of the soil profile above the groundwater table where the pore pressures are negative is usually ignored. But, prior to mitigation of these rain induced slope failure where the groundwater table is deep and failure surfaces are shallow it is essential to study the transient suction distribution in response to the infiltration of rainfall to get an insight into the failure mechanism. Such comprehensive analyses have not been done in Sri Lanka.

As such, one of a main purpose of this research is to model the process closely using actual site specific characteristics of the unsaturated soils obtained through recent laboratory investigations.

1.3 Objectives

Objectives of this study are,

- To determine the effect of infiltration of rainfall and the resulting variation of the matric suction on the safety margin of a slope that is initially unsaturated.
- To study the effect of system of relict joints on the process of infiltration and therefore the safety margin of a slope.
- To study the effectiveness of surface drainage measures in minimizing the destructive effects of rainwater infiltration and maintaining the stability
- Back analyse the failure that took place at Walipanna in the Southern Expressway in the presence of relict joints and possible disturbances in the surface drainage.

1.4 Methodology Applied

The failure that occurred at 42+340 to 42+400 at Walipanna in the Southern Expressway was back analysed by simulating the events that took place preceding the failure.

The rainfall data over a week preceding the failure was obtained from rain gauge stations closest to the location as Bombuwala and Beddegama. The prominent soil type which was recognized at the site is Sandy Silt. Hydraulic characteristics of sandy silt; hydraulic conductivity function and soil water characteristic curve (SWCC) were obtained through laboratory tests done by Vasanthan (2016). The saturated shear strength parameters of the soil encountered were determined through laboratory tests.

The geometry of the slope prior to the failure is known and structural geology of the slope were identified by visual observations and observations made during the rectification work. Main geological structures are boudinage structures (unweathered rock in a matrix of soil) and systems of relict joints.

The infiltration of rainwater and the resulting changes in the pore pressure regime of the slope was simulated using the SEEP/W software and outcomes were incorporated into the slope stability analysis in SLOPE/W. Analyses were done using the Spencer's method and both the grid and radius approach and block specified method were adopted to evaluate the variation of the Factor of Safety during 5 days prior to the failure.

The effects of surface drainage measures of concrete paved berm drains and vegetation cover were taken into account in the slope stability analysis by incorporating 100mm thick low permeable layer as 10^{-20} m/s over the berms and 10^{-7} m/s and 10^{-8} m/s over the soil surface respectively. With the improvement of surface drainage with vegetation, significant reduction of the infiltration and further increasing of FOS could be identified. The failure in the drainage system that leads to the failure was modeled thereafter.

Further, stability of the slope was determined with a greater rainfall intensity of 20mm/hr continuous rain for 5 days, which is higher than the actual rainfall recorded during the failure time. The analysis revealed that, properly maintained surface

drainage improvement will provide a positive impact on slope stability even with rainfalls of high intensity.

1.5 Thesis Outline

Chapter 2 of the thesis reviews the available literature related to the;rainwater infiltration in an unsaturated soil and its influence on stability of the slope. Unsaturated characteristics of soil and different techniques of determination, variation of pore pressure regime of the slope with rainfall infiltration and theory related to slope stability analysis were highlighted.

Chapter 3 presents the initial design of the cut slope of 42+340 to 42+400 at Walipanna in the Southern Expressway, where the failure occurred and the new rectification design. Certain observations made during the rectification which create evidences of geological structures were also described.

Chapter 4 presents the back analysis of the slope failure with variation of the geotechnical/geological and physical properties. Infiltration models were prepared using SEEP/W software and subsequent stability analyses were done using SLOPE/W software. Both circular mode of failure and non circular mode of failures were analysed.

Chapter 5 summarizes the findings and makes suggestions for the further progress in this research area.

2. CHAPTER 02: LITERATURE REVIEW

The combination of adverse causal factors will indicate the susceptibility of a sloping ground to landslides. In such sites with high susceptibility in tropical countries the landslides would be triggered by rainfall of different intensity and duration. In this chapter a review of literature in the relevant areas is presented.

2.1. Landslide Causal factors and Triggering factors

Basic definition of the landslide is given as; “The downward movement of a rock, debris, or earth under gravity” (Cruden, 1991).

Many factors contribute to the instability of slopes or landslides. The rainfall is the major triggering factor for landslides in most tropical countries like Sri Lanka. Snow falls, snow melt etc, are also triggering factors in some Asian countries. Earthquakes are a triggering factor in some other countries.

According to Cruden & Varnes (1996), Wiczorek (1996) these causes for landslides (causal factors) can be mainly divided in to four categories as;

- a) Physical processes – Including rainfall, snow melt, earthquakes etc.
- b) Man made (human) processes – Including improper excavations of the slopes, loading of the slope, vegetation removal, improper mining activities, etc.
- c) Ground condition (geological) – Including weathering profile, adversely oriented structural discontinuities, etc
- d) Geomorphological processes - Including fluvial erosion of the slope, deposition loading of the slope, etc

The causal factors can also be divided into two as: external causes (increasing the applied shear stresses) and internal causes (reduces the shear strength) according to Varnes (1978) and Popescu (1993). Slope geometry, Vibrations, Ground water level fluctuation etc can be categorized as external causes while progressive failure, internal erosion, weathering of rock/soil belongs to the category of internal causes.

Natural slopes can be placed in three main categories according to physical state of stability as;

1. Stable,
2. Marginally stable,
3. Actively unstable (Popescu 1993-1994).

The factors which cause to transition of the stability from 1st state to 2nd state are called as preparatory causes while the causes which make the transition of the stability from 2nd state to 3rd state are called as the triggering causes.

2.2 Classification of Landslides

The downward movement of soil, debris or rock under gravity can be classified into three groups based on their mechanism as; Slides, Falls and Flows. Slides are the topic under consideration in this research.

In a slide there is a discrete shear boundary and failing mass will be moving intact along that boundary. The fall is basically a toppling mechanism taking place along discontinuities when they are adversely oriented. Falls normally take places from steep faces of soil or rock and the falling material is immediately separated from the parent rock or soil (Figure 2.1).

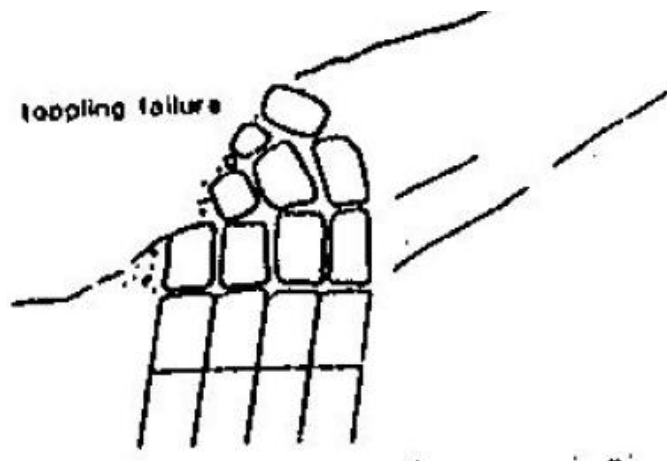


Figure 2.1: Fall; a toppling mechanism along discontinuities

In a flow, material has disintegrated and movement is not concentrated at the boundary. All the materials above the boundary flows down. A slope movement that initiate as a slide may be converted to a flow with further progression. Under condition of extreme rainfall such condition have developed in Sri Lanka. Flow of all the soil up to the bed rock level is a common sight.

Accumulated material collected in falls may end up as a flow creating a phenomenon of debris flow. The fundamental principals of shear strength in soils are applied to the study of initiation of movement in the form of a slide. The destruction has to be prevented prior to the initiation of a slide.

2.2.1 Different form of Slides

Slides can be either Rotational or Translational.

Rotational Slide – Circular shape slip surface

A landslide on which the surface of rupture is curved upward (spoon-shaped) and the slide movement is more or less rotational about an axis that is parallel to the contour of the slope is referred to s a rotational slide. The head of the displaced material may move almost vertically downward, and the upper surface of the displaced material may tilt backwards toward the scarp. If the slide is rotational and has several parallel curved planes of movement, it is called a slump. The surface of rotation can be either circular or non-circular. In the case of a slope formed of uniform soil the failure surface would be circular (Figure 2.2).

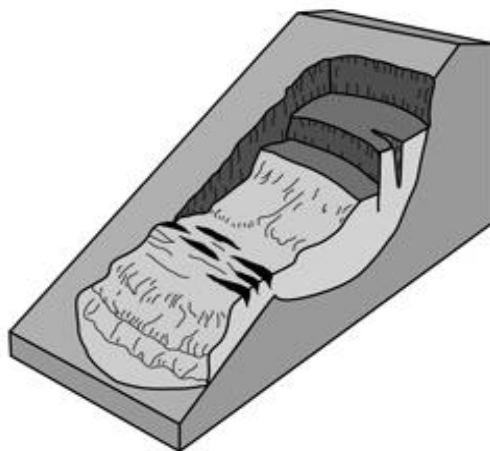


Figure 2.2: Rotational Slide

Translational slide

The mass in a translational landslide moves downward and outward, along a relatively planar surface with little rotational movement or backward tilting. This type of slide may progress over considerable distances if the surface of rupture is sufficiently inclined, in contrast to rotational slides, which tend to restore the slide equilibrium. The material in the slide may range from loose, unconsolidated soils to extensive slabs of rock, or both. Translational slides commonly fail along geologic discontinuities such as faults, joints, bedding surfaces, or the contact between rock and soil (Figure 2.3).

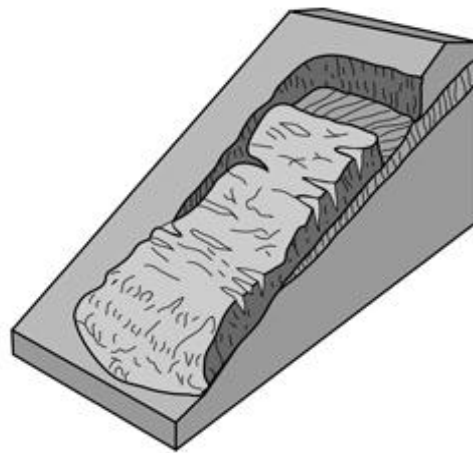


Figure 2.3: Translational slide

2.3 Assessment of the stability of a slope

The assessment of the stability of slope in a quantified approach is critically important. The stability of a slope is mostly assessed by the computation of a factor of safety through a mechanistic approach. The forces causing instability and forces restoring stability are compared to obtain a factor of safety. Alternatively, there is an approach of evaluation of the probability of failure.

Mechanistic analyses of landslides are done by two alternate techniques

1. Limit equilibrium method
2. Finite Element method

Limit equilibrium approach is the most widely used technique. In that the safety margin is estimated for an assumed mode of failure (trial failure surface). By considering a wide range of possible trial failure surfaces and estimating the safety factor for each one of them, the lowest value is taken as the Factor of Safety of the slope. The corresponding trial failure surface would be the most critical failure surface.

The shape of the most critical failure surface depends on the prevailing sub soil conditions and conditions triggering failure. It was found that in uniform soil conditions the failure surface would be mostly circular. In non uniform conditions it would be non circular, finding the path of least resistance through weakest layers.

When the failure soil mass is uniform, equilibrium can be considered taking it as one body and methods such as “Friction Circle Method” and associated charts such as “Taylors Charts” were developed. In non uniform soils the presence of layers of different shear strength properties has to be recognized. The usual practice is to divide the mass into a series of vertical slices.

In early stages of the development of limit equilibrium methods based on slices Fellenius (1936), assumed the failure surface to be circular. Subsequent researches such as Bishop (1955), Morgenstern-Price (1965), Spencer (1967), and Sarma (1973) have developed methods that have the capability of analysing both non circular and circular mode of failure.

The factor of safety of the slope is fundamentally defined as;

$$FOS = \frac{\text{Shear Strength}}{\text{Shear stress mobilized for equilibrium}}$$

$$F = \frac{\tau_f}{\tau_m} \tag{Eq (01)}$$

Where, τ_f = Shear Strength, τ_m = Shear stress mobilized for equilibrium.

In a saturated soil, the shear strength is expressed as;

$$\tau_f = c' + (\sigma - u) \tan \phi' \tag{Eq (02)}$$

For an unsaturated soil, the shear strength is expressed as;

$$\tau_f = c' + (\sigma - u_a)\tan\phi' + (u_a - u_w)\tan\phi^b \quad \text{Eq(03)}$$

Factor of Safety has to be evaluated for a sufficient number of trial failure surfaces in a systematic manner to arrive at the factor of safety corresponding to the slope. When the basic statics are considered in the method of slices the system of forces is statically indeterminate. It is made determinate by many different assumptions on inter slice forces.

Different researches Bishop (1955), Morgenstern-Price (1965), Spencer (1967), and Sarma (1973) developed methods making varying assumptions to eliminate this indeterminacy. Some assumptions may not be very sound theoretically but has lead to a simple analysis procedure, Fellenius (1936), Bishop's Simplified (1955) and Janbu's Simplified (1954) are such simple methods. Some assumptions are very sound theoretically but the analysis process is made quite complex, Spencer (1967) and Janbu's rigorous are two in this category. It would be necessary to use Computer Software to handle the iterative processes needed in such analysis.

Ideally it is necessary to consider both the force and moment equilibrium of the failure mass in the computation of factor of safety. Simpler method such as Fellenius method consider only moment equilibrium. Bishop's simplified method also consider only the moment equilibrium and applicable only for circular failure surfaces. On the other hand Janbu's simplified method considers only the force equilibrium

A more advanced method such as Spencer method is formulated to consider both force and moment equilibrium. It follows an iterative process of computations until the FOS values on force equilibrium and moment equilibrium are similar for the failure surface considered.

Considering these findings Spencer's method was used for the analysis of stability in this research when the failure surface is likely to be either circular or non circular.

2.3.1 Spencer's Method for slope stability analysis

The Spencer method was developed in 1967 and both shear and normal interslice forces are considered as Figure 2.4. It has two factor of safety equations one is respect to moment equilibrium and other in respect to force equilibrium.

This method adopts a constant ratio between the interslice shear and normal forces, and through an iterative procedure altered the interslice shear to normal ratio until the two factor of safety values were the same.

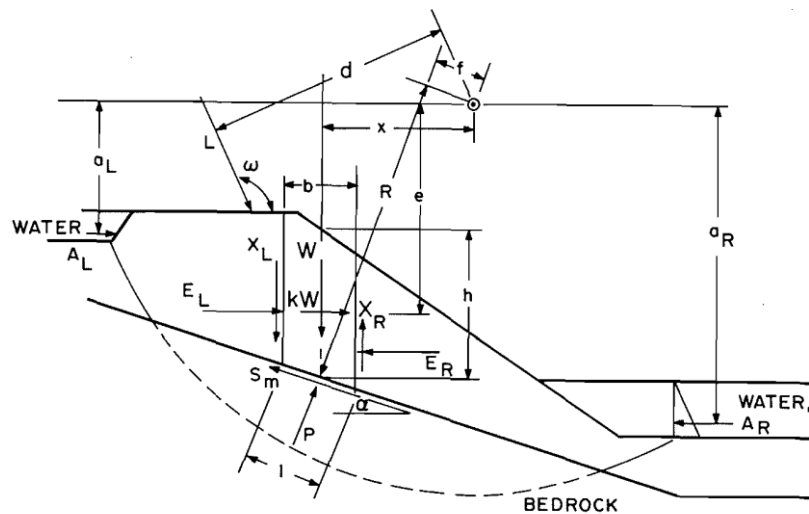


Figure 2.4: Forces acting on a slice in the Spencer method

Spencer (1967) derived two factor of safety equations. One is based on the summation of moments about a common point and the other on the summation of forces in a direction parallel to the interslice forces. The factor of safety equation is based on moment equilibrium can derived by,

$$F_m = \frac{\sum [c'IR + (P - ul)R \tan \phi']}{\sum Wx - + \sum Pf + \sum kWe + -Aa - Ld}$$

Eq 04

Where;

W = total weight of the slice

P=total normal force on the base of the slice

c' = effective cohesion

l = slice length

ϕ' - effective angle of internal friction

u = Pore water pressure

R = moment arm

f = distance to normal forces from the center of rotation

x = horizontal distance from slice to the center of rotation

e = vertical distance from centroid of slice to the center of rotation

L = line load

The factor of safety equation based on force equilibrium can also be derived by summing forces in a horizontal direction.

$$F_f = \frac{\sum [c' \cos \alpha + (P - ul) \tan \phi' \cos \alpha]}{\sum P \sin \alpha + \sum kW + -A - L \cos \omega} \quad \text{Eq (05)}$$

Interslice shear forces are related by:

$$X = E \tan \theta$$

$$\tan \theta = X_L/E_L = X_R/E_R \quad \text{Eq (06)}$$

Where, θ = angle of the resultant interslice force from horizontal, X = Interslice shear force, E = Interslice normal force

Spencer's method yields two factors of safety for each angle of side forces. However, at some angle of the interslice forces, the two factors of safety are equal and both moment and force equilibrium are satisfied (Figure 2.5). Iteration were done until this condition is achieved.

Spencer's Method also assumes that the normal forces on the bottom of the slice act at the center of the base –which has very little influence on the final solution.

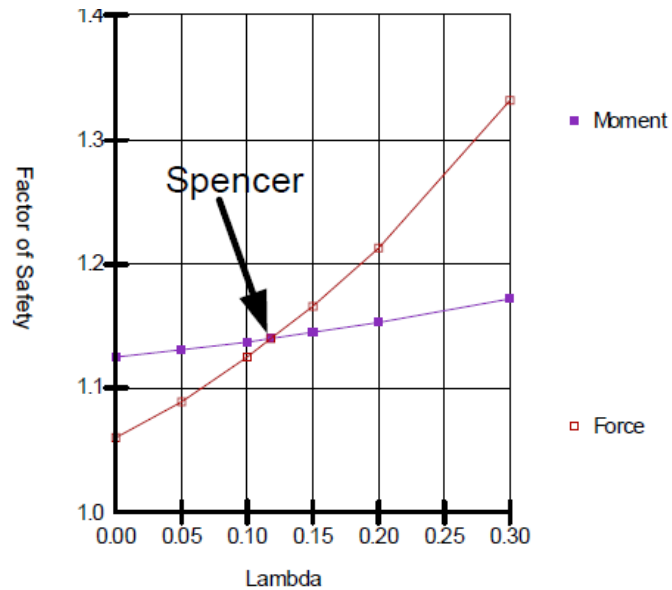


Figure 2.5: Variation of the FOS with respect to moment and force equilibrium

Although Spencer (1967) originally presented his method for circular slip surfaces, (Wright1969) showed that the method could readily be extended to analyses non-circular slip surfaces. Spencer's Method requires computer software to perform the calculations. Because moment and force equilibrium must be satisfied for every slice and the calculations are repeated for a number of assumed trial factors of safety and interslice force inclinations. Complete and independent hand-checking of a solution using Spencer's Method is impractical (US Army Corps of Engineers -2003). ‘

2.4 Residual soil formations

Most slopes in Sri Lanka are formed by residual soils. Residual soils are formed by in situ weathering of parent material and remains at the place where it was originally formed.

The parent rocks in these slopping grounds are mainly metamorphic. Soils which are formed by the in-situ weathering of the metamorphic parent rock are characterized by the heterogeneous nature inherited from the difference in its mineralogy and the process of variable weathering under tropical conditions. The standardweathering profile is given in the table 2.1 may not be present always in Sri Lankan residual soil formations.

Table 2.1: Weathering profile

(After Nurly and Azman)

Term	Description
Residual soil	All rock material is converted to soils. The mass structure and the material fabric texture are fully destroyed. The materials are generally silty and clayey and show homogeneous color.
Completely weathered	All material rock is decomposed to soil. Material partially preserved. The material is sandy and friable if soaked in water or squeezed by hand.
Highly weathered	The rock material is in the transitional stage to form soil. Material condition is either rock or soil. Materials completely discolored but the fabric is completely preserved. Mass structure partially present.
Moderately weathered	The rock material shows partial discoloration. The mass structure and material structure is completely preserved. Discontinuity is commonly filled by iron rich material fragment or block corner can be chipped by hand.
Slightly weathered	Discoloration along discontinuity and may be part of rock material texture are completely preserved. The material is generally weaker but fragment corners cannot be chipped by hand.
Fresh rock	No visible sign of rock material weathering. Some discoloration on major discontinuity surfaces.

However, with the terrains of residual soils formed by weathering of metamorphic rock, it is common to see sudden variation in the level of weathering instead of the gradual classes of weather prescribe in Table 2.1.



Figure 2.6: Degree of Weathering and the Nature of the weathered product varies within a short distance

Sometimes Charnokitic rocks in the original formation remain unweathered while Gneissic rock has completely weathered. This leaves boudinage structures (unweathered rock) in a matrix of soil in the slope. If the original rock has a high Feldspar content the weathered product would be clay; weaker in shear strength as shown by the whitish zone in Figure 2.6.

A whitish zone is seen in the failure surface in Figure 2.7 also.



Figure 2.7 : Whitish zones encountered in a failure mass

Another feature to be note is that, the initial systems of joints that exists in the parent rock remain as it is in the weathered product of residual soils, (figure 2.8). These joints are then referred to as relict joints. The initial joints could be either clean and tight or opened up and in-filled with loose material. Accordingly similar condition would exist in the relict joints present in residual soils.



Figure2.8: Closely spaced rock Joints-remain as “Relict Joints” after weathering

Water could also be present there. Therefore, the relict joints in residual soils are the planes of weakness. Failures in the form of falls – block of residual soils bounded by adversely oriented system of joints can be seen slopes of residual soil. The soil forming the block that has fallen is of high shear strength, but the failure has taken place along the relict joints (Figure 2.9).



Figure 2.9: Toppling (Fall) Mode of failure could take place through relict joints

2.5 Basic constituents of an unsaturated soil

The most of the slopes formed in residual soils of Sri Lanka has a low ground water table specially during the periods of dry weather. Hence in the study of instability of the slopes it is essential to understand the shear strength, permeability and water retention characteristics of an unsaturated soil.

Soil below the ground water table is completely saturated. Above the ground water table part of the voids would be filled with air and hence unsaturated. In a fine grained soil due to capillary rise, soil would be saturated to some height above the ground water table.

Saturated soil is a two phase system, namely solid and water, whereas unsaturated soil consists of four phases as:

1. Solid
2. Water
3. Air
4. Contractile skin (Figure 2.10)

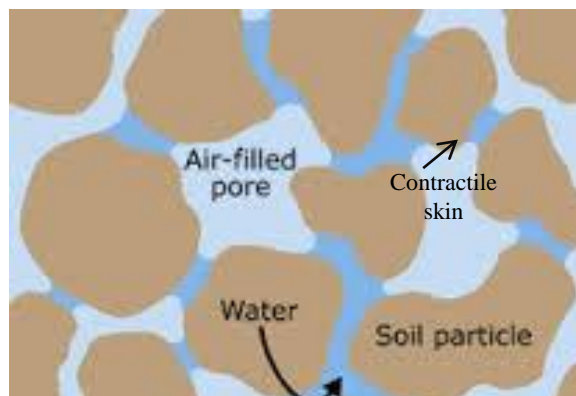


Figure 2.10 Four phases of Unsaturated soil

Contractile skin is the air-water interface which has air in one side and water in other side. This pore air phase has relatively high pressure than pore water phase. The phenomenon is, generally soil particle have an origin of silica mineral which is more likely to absorb water rather than air. As the result, air molecules exist in separate to the soil particles and totally surrounded by water while subject to compression and experience a relatively high pressure than water molecules.

Therefore, a molecule with the contractile skin subjects to an unbalanced force towards the interior of the water. This pressure difference between pore air pressure and pore water pressure is defined as matric suction or negative pore water pressure.

In order to stay in equilibrium a tensile pull is generated along the contractile skin. It's called surface tension, T_s and also contractile skin exists in a concave curvature toward the larger pressure. The pressure difference across the surface; matric suction can be related to the surface tension and the radius of curvature.

$$u_a - u_w = 2T_s/R \quad \text{Eq (07)}$$

Where, $u_a - u_w =$ matric suction or the difference between pore-air and pore-water pressures acting on the contractile skin.

2.5.1 Shear strength parameters of an Unsaturated soil

Stability of a slope depends on the shear strength generated along the sliding surface. Soil material can be taken as Mohr-Coulomb material in which the shear strength is expressed in terms of the cohesion “c” and the friction angle “ ϕ ”.

Shear strength equation for unsaturated soils incorporating the negative pore water pressure can be expressed as' (*Fredlund et al. 1978*);

$$\tau_f = c' + (\sigma_n - u_a) \tan \phi' + (u_a - u_w) \tan \phi^b \quad \text{Eq(08)}$$

$c' + (\sigma_n - u_a) \tan \phi'$ is termed apparent cohesion “ c_a ”

$$c_a = c + (u_a - u_w) \tan \phi^b \quad \text{Eq(09)}$$

where, $(u_a - u_w)$ – Prevailing matric suction

Where, τ_f -shear strength of unsaturated soil; c' -effective cohesion; $(\sigma_n - u_a)$ - net normal stress; σ_n - total normal stress; u_a -pore-air pressure; ϕ' - effective angle of internal friction; $(u_a - u_w)$ -matric suction; u_w -pore-water pressure; and ϕ^b -angle indicating the rate of increase in shear strength relative to the matric suction.

Figure 2.11 represent the equation 08,of shear strength in an unsaturated soil in a planer surface

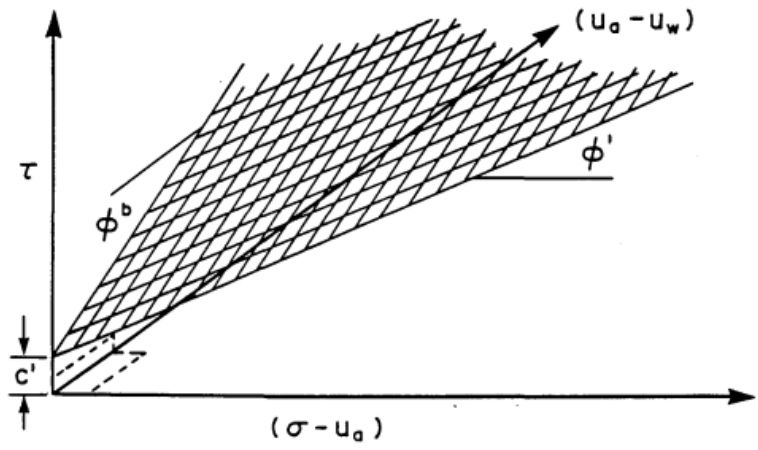


Figure 2.11: planar surface for the shear strength equation for unsaturated soils

During the dry season, the soil to a greater depth of the slope is in an unsaturated state and prevailing matric suction gives rise to a reasonably high apparent cohesion making the slope quite stable. As a result of heavy rainfall, significant infiltration takes place and soil is getting nearly saturated losing a greater part of the matric suction. Thus the shear strength of soil get reduced. This process of infiltration into the soil can be modeled using the relevant characteristics of soils.

Recently researched have found that the ϕ^b , the rate of increase in shear strength relative to the matric suction is not a constant. Former researchers Gan et al., (1988), Escario, V. & Juca, J., (1989), Vanapalli et al., (1996) and Jotisankasa et al., (2010) have found that angle of shearing resistance due to suction, ϕ^b displayed a non-linear relationship. According to the Vasanthan (2016); the angle of shearing resistance due to suction, ϕ^b was developed using pressure plate test and direct shear test results. Initially, ϕ^b is equals to ϕ' and then decreases to a constant value such that, $\phi^b < \phi'$. It could be seen that the ϕ^b value is not a constant.

2.5.2 Hydraulic properties of Unsaturated Soil

For unsaturated soil, soil properties are generally highly non-linear. Darcy’s law applies to unsaturated soils in the sense that the flux is proportional to the hydraulic head gradient. Flow of water takes place through only the voids filled with water and some of the water infiltrated goes in as storage. The coefficient of permeability cannot be assumed to be constant since the volume of water in soil can change significantly

depending on the soil suction. Soil suction can be characterized by Soil Water Characteristic Curves.

Thus, SWCC and coefficient of permeability are the most important hydraulic properties of unsaturated soils, in modeling the infiltration of rainwater.

Soil Water Characteristic Curve

Soil-water characteristic curve (SWCC) is one of the fundamental properties of unsaturated soils. It is defined as the relationship between water content and matric suction for the soil (Williams 1982). The water content defines the amount of water contained within the pores of the soil. In soil science, volumetric water content is most commonly used.

$$\text{Volumetric water content } \theta = \frac{V_w}{V_s} \quad \text{Eq(10)}$$

Where, V_w - Volume of water, V_s - Volume of soil

It is related to the more commonly used gravimetric water content (w) by,

$$w = \frac{W_w}{W_s} \quad \text{Eq(11)}$$

$$\theta = \frac{wGs}{1+e} = \frac{S_r e}{1+e} \quad \text{Eq(12)}$$

Soil water characteristic curve (SWCC) is the basic function which facilitates further analysis of advance infiltration and slope stability. It has relationship to almost all properties of soil such as, shear strength parameters, hydraulic conductivity, unfrozen water content, specific heat, thermal conductivity, water storage, diffusion and adsorption.

Figure.2.12 shows an idealized SWCC with two characteristic points: A^* and B^* . Point A^* corresponds to the air-entry value $((u_a - u_w)_b)$, and B^* corresponds to the residual water content (θ_r) .

Air entry value (A^*)

This is the point at which air starts to enter the soil. Means soil begin to unsaturated from the saturated state.

Residual water content (B^*)

Water content, where a larger suction is required to remove the remaining volume of water. At here soil begin to dry from the unsaturated state.

As shown in Figure 2.12, prior to A^* , the soil is saturated or nearly saturated, so it can be treated as a saturated soil with a compressible fluid due to the existence of sealed air bubbles. Beyond B^* , there is little water in the soil, so the effects of water content or negative pore-water pressure on soil behavior may be negligible.

Therefore, the soil beyond these two unsaturated stages is not the key focus of unsaturated soil behavior (*Bao et al. 1998*). What is of great concern in unsaturated soils is the stage between A^* and B^* , in which both air and water phases are continuous or partially continuous, and hence the soil properties are strongly related to its water content or negative pore-water pressure. It can be seen from Figure.2.12 that the SWCC between A^* and B^* is nearly a straight line on a semi logarithmic scale. The linear part of the SWCC can be approximately represented with the air-entry value $((u_a-u_w)_b)$, the saturated and residual volumetric water content, and the desaturation rate of the SWCC (i.e. the slope of the linear part).

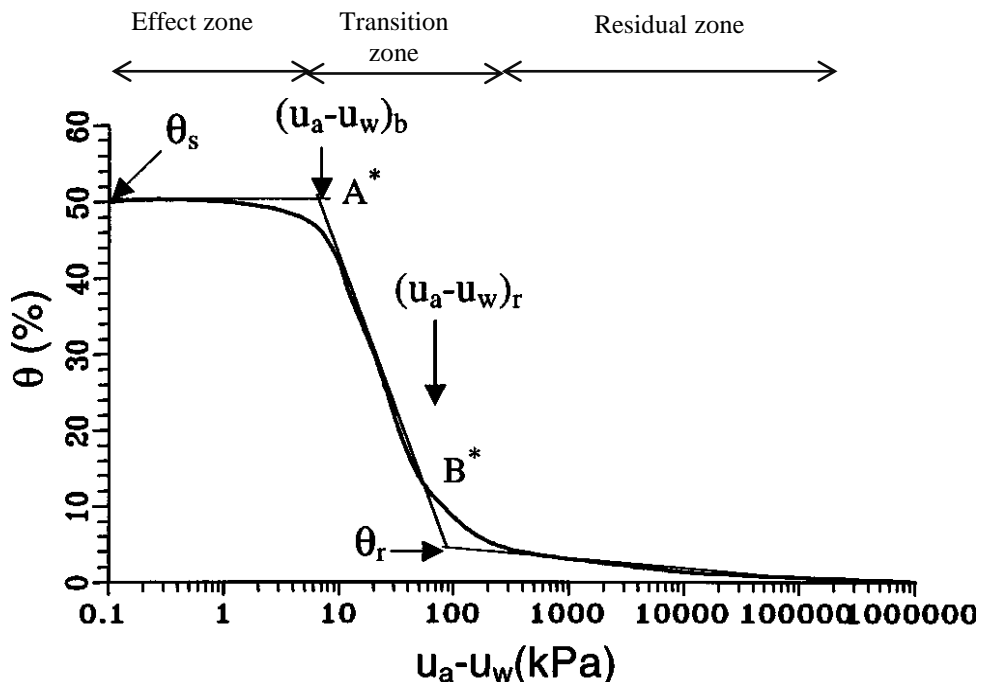


Figure 2.12: Idealized soil-water characteristic curve (after Fredlund and Rahardjo, 1993)

Hydraulic Conductivity function/ Permeability function

Infiltration of rainwater leads to development of perched water table or positive pore water pressure at shallow depth in soil slopes as a result of existing layer of much lower permeability. With high permeable soil layers infiltration leads to sudden raising of the main groundwater level. Therefore, the coefficient of permeability of unsaturated soil has greater concern for analysis of flow in saturated/ unsaturated soil in slope stability studies.

Hydraulic Conductivity function is the graph of coefficient of permeability for unsaturated soil with respect to negative pore water pressure. As the matric suction change, the distance between the air water interface and soil particle is changed resulting changes of the degree of saturation or volumetric water content. For an unsaturated soil, the coefficient of permeability depends on the degree of saturation.

Therefore determination of the variation of coefficient of permeability with matric suction is very important.

Coefficient of permeability of a deformable unsaturated soil can be determined using the tensiometer at the laboratory.

2.5.3 Theoretical formulation of process of infiltration

The flow of water through both saturated and unsaturated soil follows Darcy's Law which states that:

$$q = ki \quad \text{Eq(13)}$$

Where: q = the specific discharge, k = the hydraulic conductivity, and i = the gradient of total hydraulic head. Darcy's Law was originally derived for saturated soil, but later research has shown that it can also be applied to the flow of water through unsaturated soil as well. The only difference is that under conditions of unsaturated flow, the hydraulic conductivity is no longer a constant, but varies with changes in water content and indirectly varies with changes in pore-water pressure.

Darcy's Law is often written as:

$$v = ki \quad \text{Eq(14)}$$

Where, v = the Darcian velocity. The actual average velocity at which water moves through the soil is the linear velocity, which is equal to Darcian velocity divided by the porosity of the soil. In unsaturated soil, it is equal to Darcian velocity divided by the volumetric water content of the soil. (GEO-SLOPE International Ltd. -2007 Seep/W)

According to the Darcy-Buckingham equation, horizontal and vertical water flux (q_x and q_z) in unsaturated soil are expressed as equation 15 and equation 16:

$$q_x = -k(\psi) \left(\frac{\partial \psi}{\partial x} \right) \quad \text{Eq(15)}$$

$$q_z = -k(\psi) \left(\frac{\partial \psi}{\partial z} + 1 \right) \quad \text{Eq(16)}$$

Where $k(\psi)$ is the hydraulic conductivity as a function of negative pore water pressure ψ (Matric Suction). The equation for continuity of water is expressed as

$$\frac{\partial \theta}{\partial t} = - \left(\frac{\partial q_x}{\partial x} + \frac{\partial q_z}{\partial z} \right) \quad \text{Eq(17)}$$

Where, t is time, Substituting Equation -15 and Equation -16 into Equation -17 yields the two-dimensional, vertical and horizontal flow equation for soil water (Richard's Equation):

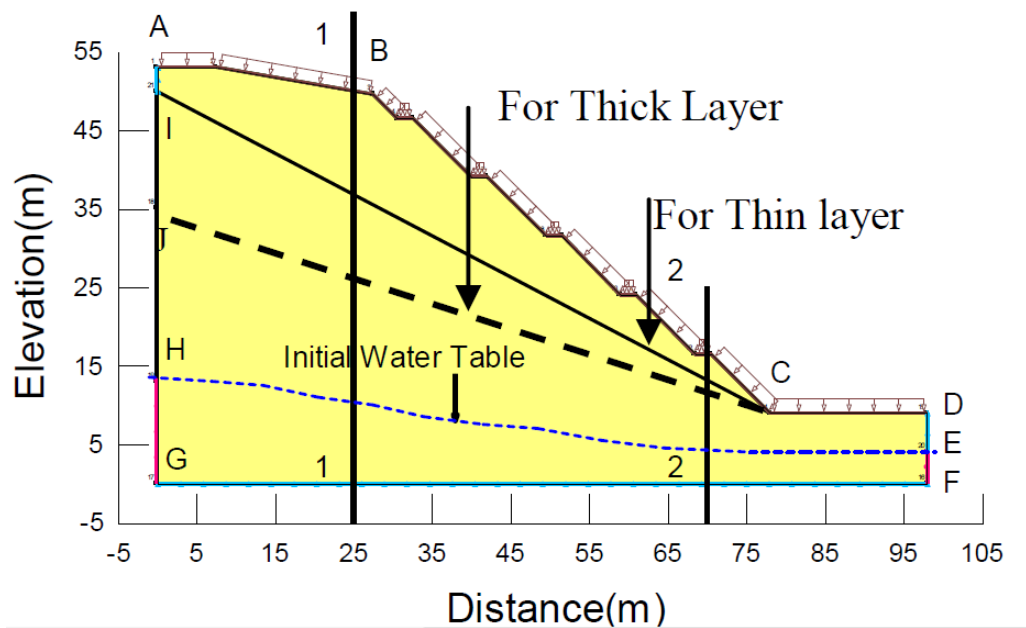
$$\frac{\partial}{\partial z} \left(K(\psi) \frac{\partial \psi}{\partial z} \right) + \frac{\partial}{\partial x} \left(K(\psi) \frac{\partial \psi}{\partial x} \right) + \frac{\partial}{\partial z} (K(\psi)) = c(\psi) \frac{\partial \psi}{\partial t} \quad \text{Eq(18)}$$

Where $c(\psi) = \partial \theta / \partial \psi$ is the water capacity function defined as the slope of the Soil Water Characteristic Curve. Solving Equations requires the SWCC and hydraulic conductivity function. Geoslope Seep/W software solved the equation with a finite element formulation.

2.6 Modelling the process of infiltration using SEEP/W Software

The process of infiltration into a slope made of an unsaturated soil was modeled by Kulathilake and Sujeevan (2011) considering a typical cut slope from Southern Transport Development Project

The typical cut slope considered is presented in Figure 2.13. Slopes of gradient 1:1 and 1:2 were considered.



Boundary Conditions

AB, BC, CD = I_r (Rainfall intensity)

AH, DE, FG = $Q = 0 \text{ m}^3/\text{s}$ (No flow Boundary)

EF, GH = h_t (Total head at sides)

Figure 2.13: Geometry of analysed slope, selected sections and boundary conditions

Slopes made of; uniform residual soil, a thick layer of residual soil underlain by weathered rock, a thin layer of residual soil underlain by weathered rock was considered. The weathered rock layer was of much lower permeability.

The groundwater table is at some depth in the residual soil. The pore water pressure is increasing hydrostatically below the ground water table. Above the ground water table the pore water pressures are negative. The negative value was considered to increase linearly towards the ground surface. Two cases were analysed; a profile with linear increase and a profile with linear increase with an upper limit for matric suction at

100kN/m². Infiltration into these slope profiles at the intensities of rainfall 5mm/hr and 20mm/hr were considered.

2.6.1 Infiltration through a Homogeneous slope

Sujeewan and Kulathilaka (2011), presented the pore water pressure distributions for Section 1-1 and Section 2-2 for rainfall intensities of 5mm/hr and 20mm/hr. (Figure 2.14 and Figure 2.15 respectively).

With a 5mm/hr rainfall, as rain progressed, matric suction is just lost and pore water pressure values approach zero at the top level (Section 1-1, Figure 2.14(a)) and water table has arisen at the lower levels (Section 2-2, Figure 2.14(b)).

With a 20mm/hr rainfall, not only the matric suctions were lost but also positive pore water pressures were developed at the top level – a perched water table condition. (Section 1-1, Figure 2.15 (a)). The development of the positive pore water pressure and the rise of the ground water table were more significant at lower levels (Section 2-2, Figure 2.15 (b)).

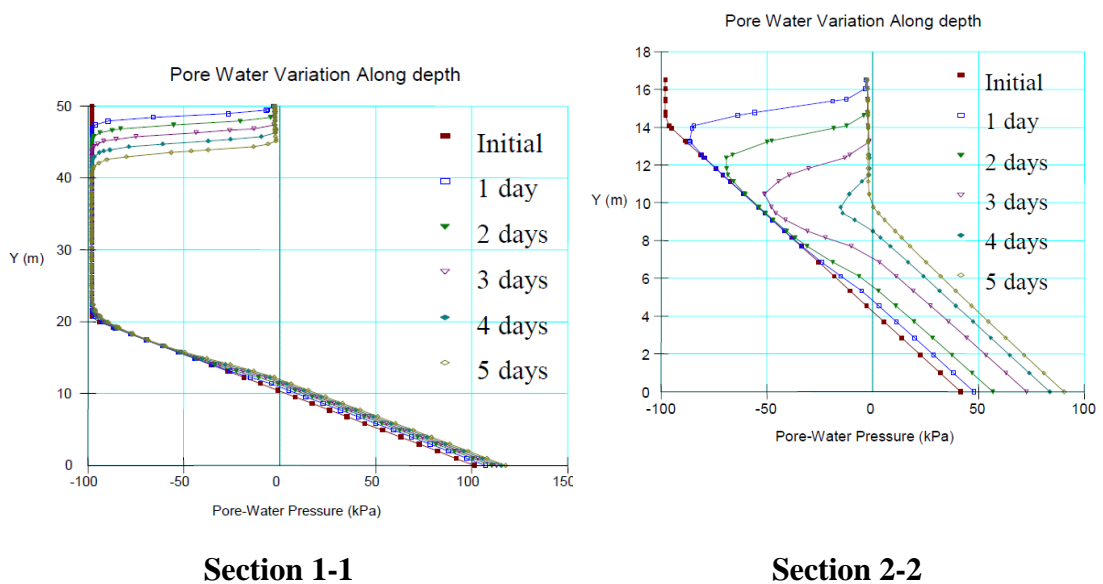


Figure 2.14: Pore water pressure distribution of uniform soil profile with 5mm/hr rainfall (after Sujeewan & Kulathilake 2011)

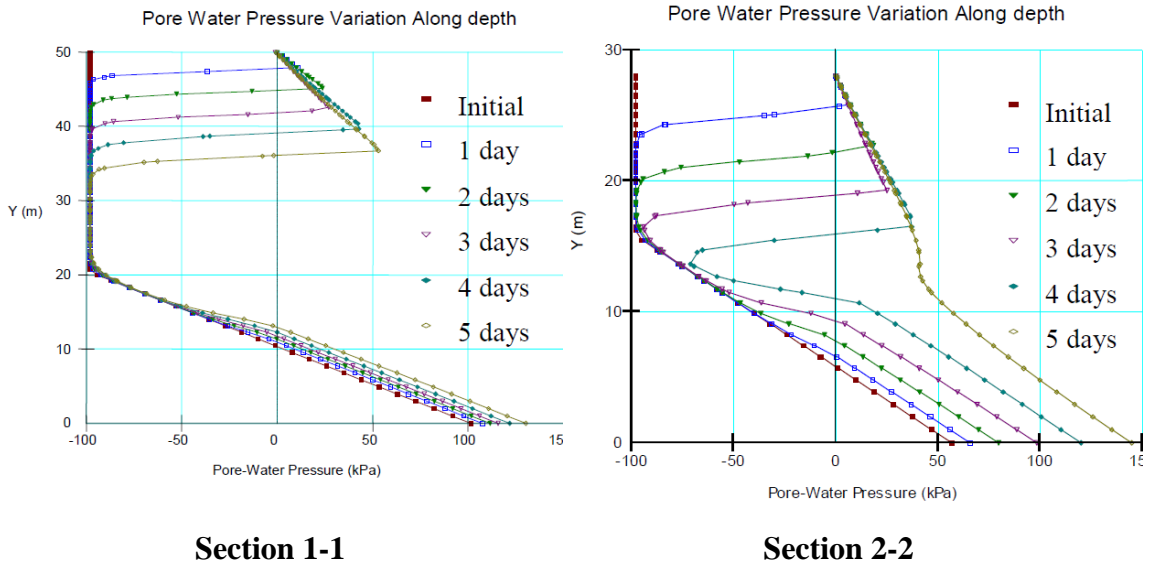


Figure 2.15: Pore water pressure distribution of uniform soilprofile with 20mm/hr rainfall (after Sujeewan & Kulathilake 2011)

2.6.2 Infiltration through a slope with Weathered rock overlying by Residual soil

When a highly weathered rock layer is underlying the residual soil, the downward movement of water is hampered and water gets accumulated at the boundary. It makes high positive pore water pressure with hydrostatic gradient above that boundary. In the meantime there is no rise in ground water table due to this barrier effect. Sujeeven and Kulathilake (2011) presented the pore pressure distributions for a rainfall of intensity 20 mm/hr, .Figure 2.16

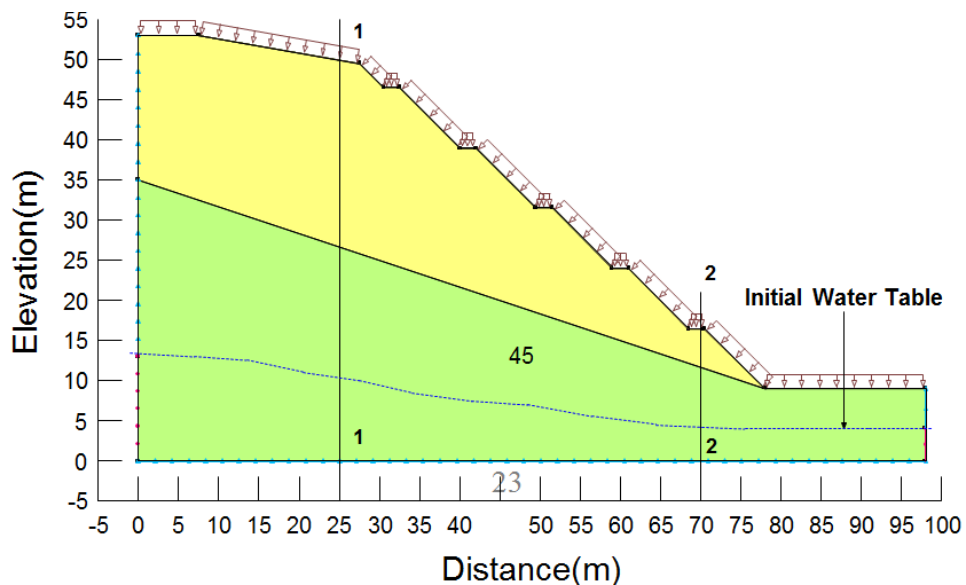


Figure 2.16: Geometry of 1:1 two layers slope and selected sections(after Sujeewan & Kulathilake 2011)

Pore water pressure distribution through slope with residual soil overlying weathered rock under 20mm/hr rainfall by Sujeeven and Kulathilake (2011) is illustrated in figure 2.17.

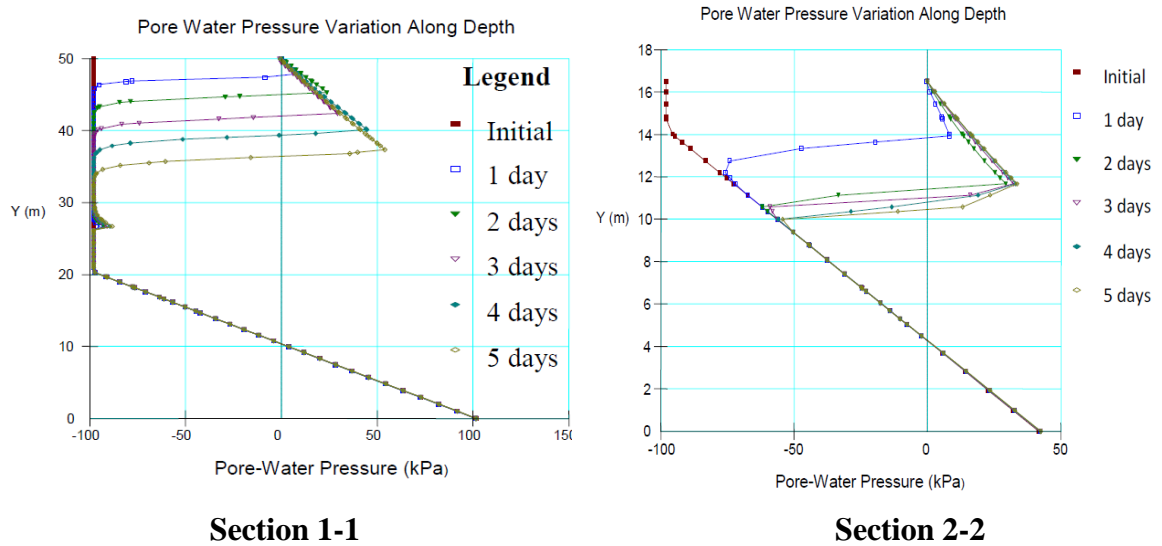


Figure 2.17: Pore water pressure distributions of slope with Weathered rock overlying by Residual soil for 20mm/hr rainfall (after Sujeevan & Kulathilake 2011)

2.6.3 Influence of the Infiltration on Slope Stability

The minimum factor of safety and the corresponding most critical failure surface at different time of the rainfall were obtained through the analysis by Kulathilake and Sujeeven (2011). Analysis was done using the Geoslope Slope/W software incorporating the pore water pressures derived from Seep/W analysis. Stability of the slope will be influenced by various rainfall parameters and different stratum of soil slope.

The shape of the critical failure surface was corresponding to the duration of the rainfall. At the initial stages of the rainfall or during the dry season, the prevailing high matric suctions near the surface induces greater shear strength. As such, critical failure surfaces are quite deep as shown in Figure 2.18 and Figure 2.19 for the uniform slope and two layered slope respectively. With the rainfall infiltration the loss of matric suction and development of perched water table has developed near the surface. This loss of matric suction would reduce the apparent cohesion and it is

significant closer to the ground surface. As such, the critical failure surfaces corresponding to the latter stages are much shallower as illustrated by Figure 2.20 and Figure 2.21.

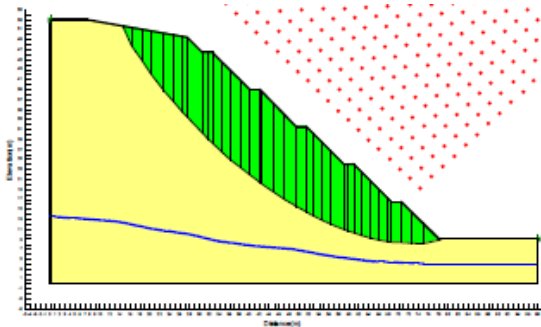


Figure 2.18: Critical failure surface – homogeneous soil slope at initial stage(Case 1 Kulathilake & Sujeevan 2011)

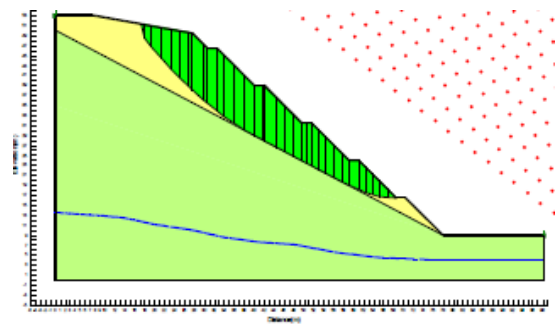


Figure 2.19: Critical failure surface – two layers of soil slope at initial stage(Case 2 Kulathilake & Sujeevan 2011)

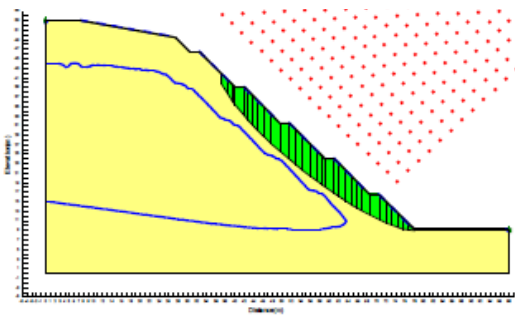


Figure 2.20: Critical failure surface – homogeneous slope at later stage(Case 1 Kulathilake & Sujeevan 2011)

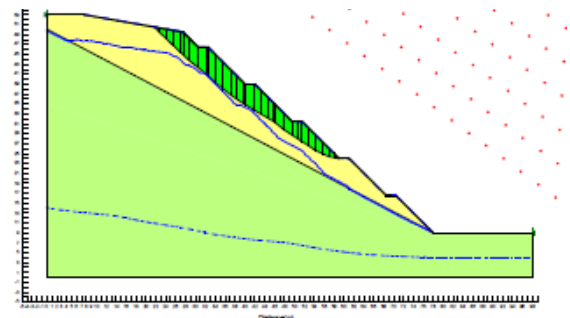


Figure 2.21: Critical failure surface – two layers of soil slope at a later stage(Case 2 Kulathilake & Sujeevan 2011)

It was found that the rainfalls of greater intensity are more unfavorable. But rainfall of intensity much greater than the saturated permeability of the soil will contribute to runoff. Therefore, in such situations, the values of factor of safety were also not changed considerably.

According to the analysis done by Kulathilake and Sujeevan (2011), when a layer of much lower permeability (less weathered rock) underlies the residual soil, it will obstructs the infiltration and create a negative effect on the stability of the slope.

Kulathilaka and Sujeevan (2011) presented the reduction of the safety margins of the slope with the rainfall, for the three idealized geological conditions as, uniform

residual soil (case 1), thick layer of residual soil underlain by weathered rock (Case 2) and a thin layer of residual soil underlain by weathered rock (Case 3), (Figure 2.22).

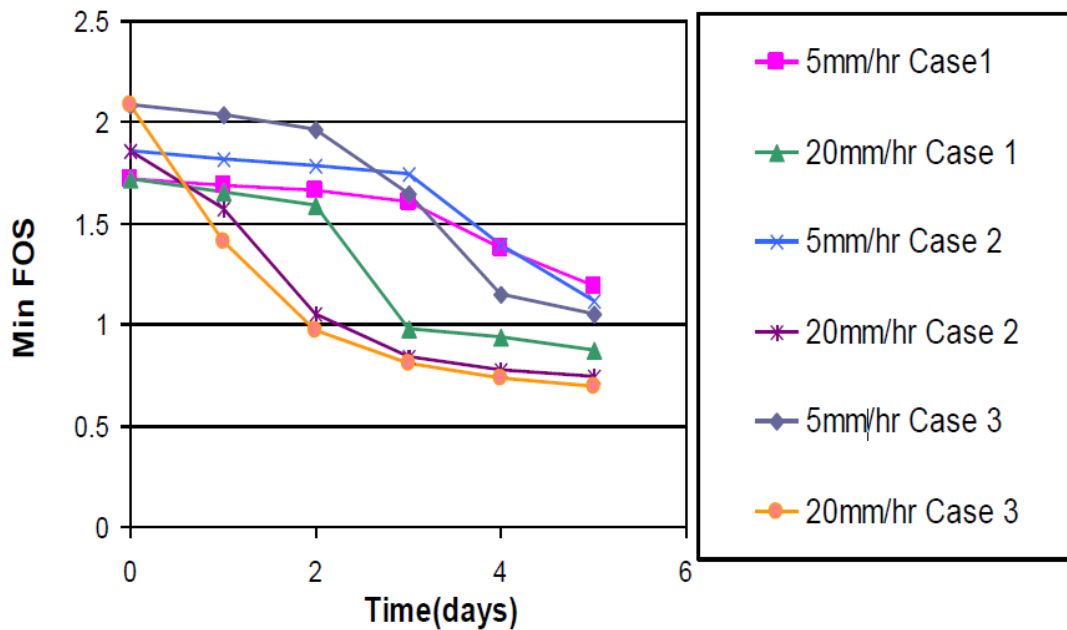


Figure 2.22: Variation of factor of safety with duration of rainfall (after Sujeevan and Kulathilaka 2011)

2.6.4 Effectiveness of surface drainage on infiltration

Kulathilake and Kumara (2013) showed how the destruction of matric suction could be prevented by use of proper drainage measures and vegetation cover. The study was done for a typical cut slope from the Southern Transport Development Project. The slope was idealized with 3 geological conditions of; homogeneous residual soil, thick layer of residual soil underlain by weathered rock and a thin layer of residual soil underlain by weathered rock. The influence of surface drainage measures were modeled with the software Seep/W by incorporating a 100mm thick layer of very low permeability 10^{-20} m/s over the berms for represent the berm drains and a thin layer of low permeability over the slope surface for represent the vegetation cover. A parametric study was done by varying the permeability of the thin vegetation layer over the range 10^{-7} m/s to 10^{-9} m/s. According to the results of the site specific analysis, 100mm thick vegetation cover with sufficiently low permeability of 10^{-7} m/s along with berm drains and cascades cause a significant reduction in infiltration.

Figure 2.23 and Figure 2.24 show the pwp distribution of above condition with the different rainfall intensities of 5mm/hr and 20mm/hr rain. The matric suction profiles for section 1-1 and section 2-2 for both rainfall is not very different. With the presence of a vegetation layer of low permeability near the surface, the infiltration of water is restricted and the excess rainfall has contributed to runoff. Complete loss of matric suction is prevented at both section 1-1 and section 2-2. Some matric suction remained even after 5 days of rainfall. The rise of water table at section 2-2 is also prevented. These distribution should be compared with Figure 2.14 and Figure 2.15.

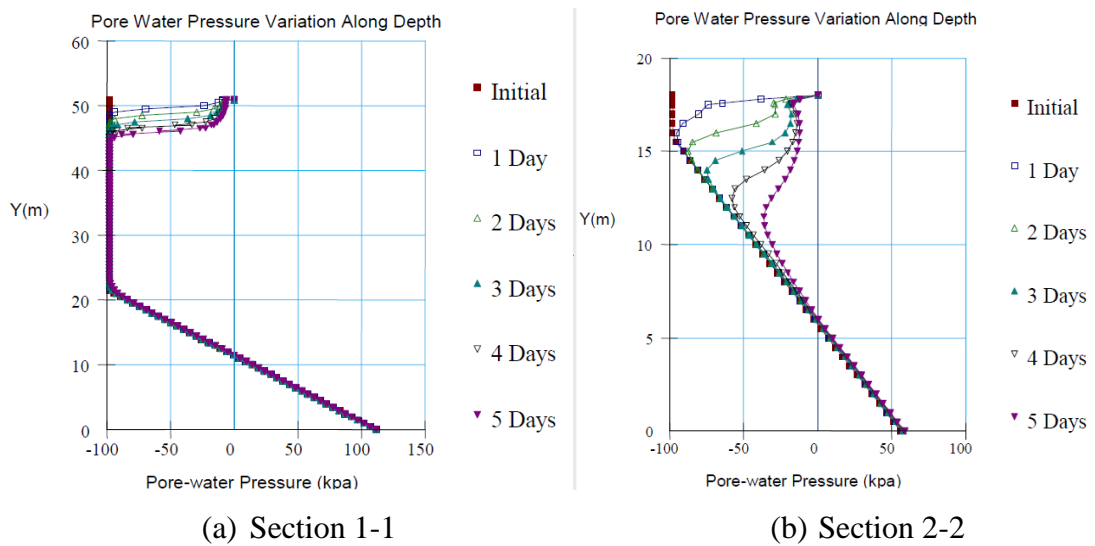


Figure 2.23 – Pore water pressure distribution for 5mm/hr rainfall with vegetation layer of permeability 10^{-7} m/s

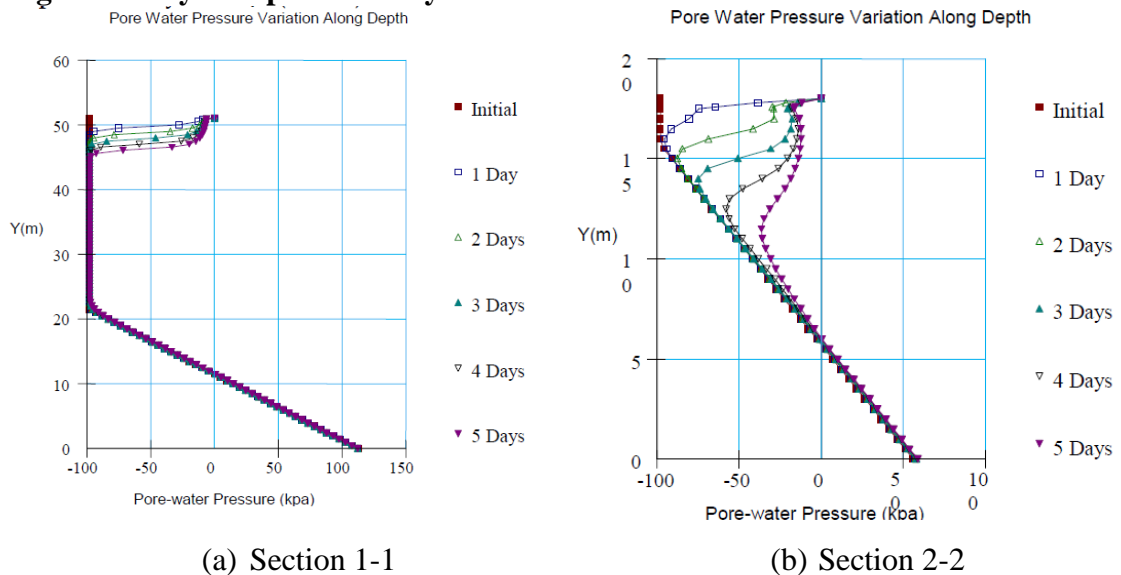


Figure 2.24: Pore water pressure distribution for 20mm/hr rainfall with vegetation layer of permeability 10^{-7} m/s

Comparison of Figure 2.25 and Figure 2.26 show how the critical failure surface is becoming deeper with the FOS improving; when use the vegetation and surface drainage improvement. As the result it could ensure that the slope remains stable during prolog rainfall.

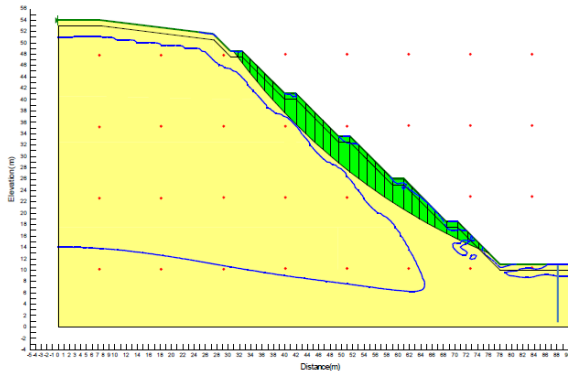


Figure 2.25: Shape of a typical failure surface without vegetation cover

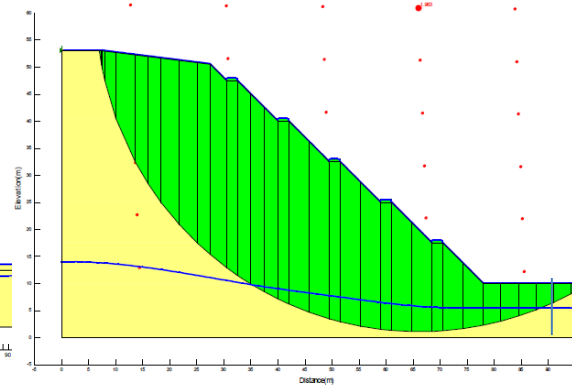


Figure 2.26: Shape of a typical failure surface with vegetation cover

The effectiveness of the berm drains and vegetation cover in maintenance of a sufficient safety margin in the slope even with a prolonged rainfall is illustrated through Figure 2.27. For the uniform slope, the variation of factor of safety under conditions of; slope with sealed berm drains only and slope also with vegetation cover of permeability 10^{-7} m/s are compared in Figure 2.27. It could be seen that the vegetation cover which reduced the infiltration and loss of maric suction had been effective in maintaining a significant margin of safety during the prolonged rainfall. When there is no protective vegetation cover, the factor of safety reduced significantly as the rain persists. When the vegetation cover is present the reduction of the factor of safety with the prolonged rainfall is very minimal. The difference of the factor of safety values corresponding to rainfall intensities of 5 mm/hr and 20 mm/hr is negligible. The surface vegetation layer of low permeability has restricted the infiltration and major part of the rainfall has ended as runoff.

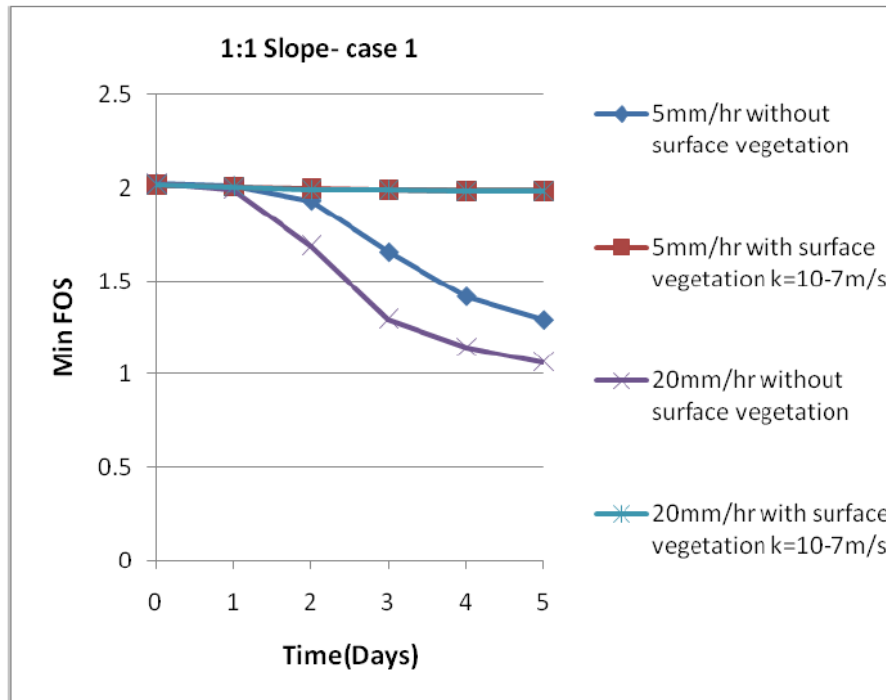


Figure 2.27: Variation of factor of safety with drainage improvement, Kulathilake and Kumara (2013)

2.7 Determination of characteristics of Unsaturated soils

The analyses reported in Sujeevan and Kulathilake (2011) were done using the characteristics of unsaturated soils reported in literature. As such there is a need to determine such parameters of Sri Lankan soils. In this project for the back analysis of the failure at 42+340 to 42+400, there was the need to determine the unsaturated parameters relevant to the slope

Vasanthan (2016) did a number of experiments to determine these parameters. For the purpose of determine these characteristics; two undisturbed box samples were obtained from the slope behind the escarpment of the failed segment prior to the rectification process. The basic soil characteristics such as particle size distribution, Aterberg limit etc were obtained on these and the soil were analysed.

According to the soil classification, main type of soil was recognized as Sandy Silt. Particle size distribution was obtained using the wet sieving technique is presented in Figure 2.28. Index properties of the soil are summerized in Table 2.2.

2.7.1 Development of Permeability function

Permeability function is the variation of permeability with matric suction. The undisturbed sample used for the permeability function test was instrumented with three tensiometers at different heights on different plan locations (Figure 2.29). For the determination of wetting method, the top surface of the sample was continuously wetted by water dripping at a constant rate from burette. In the drying method the water was allowed to evaporate from the surface of the sample. The flow of water was estimated by the loss of weight of the sample.

Matric suction and weight of the sample were monitored throughout the test. It is assumed that soil specimen remains at constant volume throughout the test.

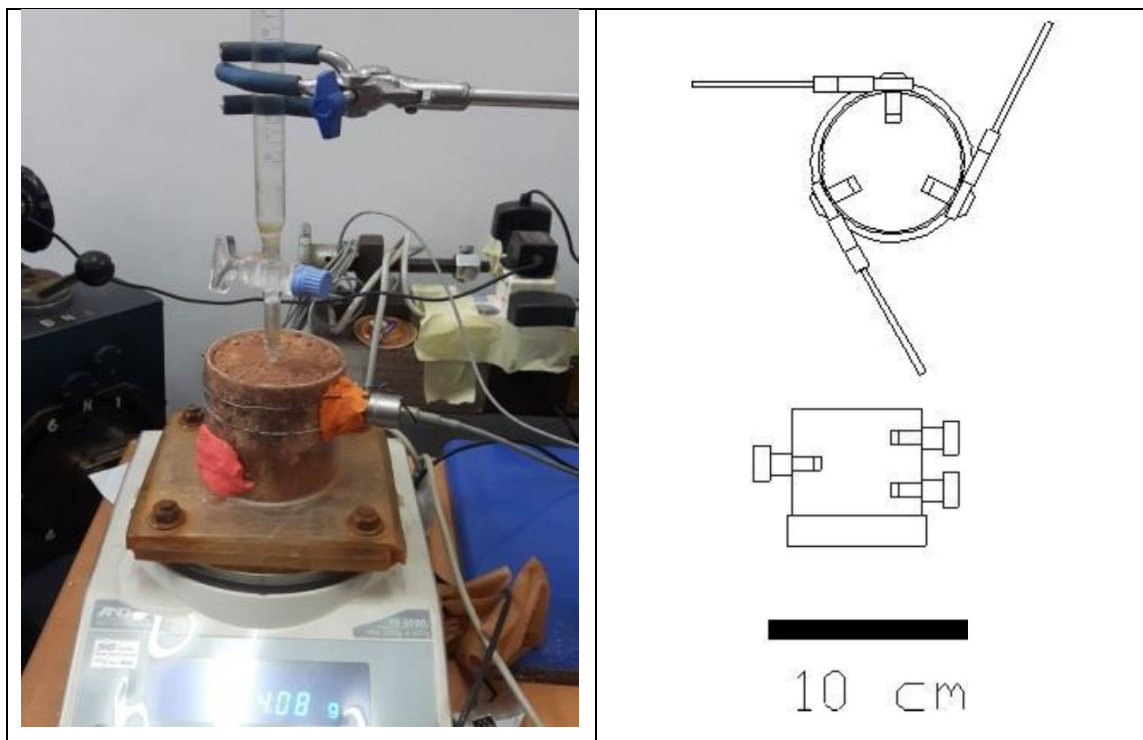


Figure 2.29: Typical arrangement of permeability test, Vasanthan (2016)

$$i = d(z - s/\gamma_w) / dz \quad \text{Eq (19)}$$

Where I = hydraulic gradient, z = elevation head of each tensiometer relative to the base of the sample, s = matric suction, and γ_w = unit weight of water.

$$v = dV_w / Adt \quad \text{Eq (20)}$$

Where v =flux velocity, dV_w = change of volume of water in soil sample which can be calculated from change in soil mass during test, A = cross section area of sample, and dt = elapsed time.

$$k = v / i \quad \text{Eq (21)}$$

Where k =Permeability

The results of permeability function obtained are shown in Figure 2.30 for the site of 42+340 to 42+400 in Walipanna at southern expressway.

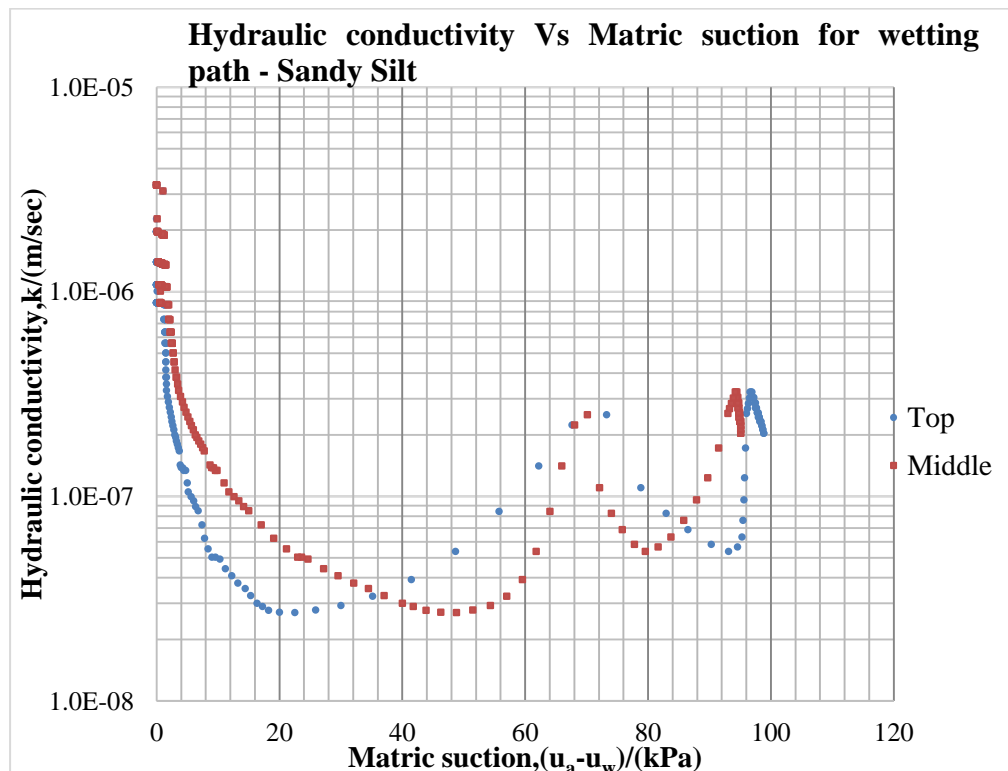


Figure 2.30: Graph of Hydraulic conductivity Vs Matric suction for wetting path - Sandy Silt, Vasanthan (2016)

2.7.2 Development of Soil Water Characteristic Curve (SWCC)

Soil water characteristic curve of a soil can be obtained by using a pressure plate apparatus and also using tensiometers. SWCC was developed by Vasanthan (2016) for the Sandy Silt soil encountered at the site of the failed slope .

A 5 bar pressure plate apparatus was used for the studies. Essential components of the pressure plate apparatus are; pressure vessel, ceramic pressure plate cell, a pressure control and supply system (Figure 2.31).



Figure 2.31: Typical arrangement of 5-bar pressure plate apparatus used for the research (Vasanthan 2016)

Undisturbed specimen used in this study with a dimension of 54.6mm of inner diameter and 10mm of height were kept within a PVC ring. Then the samples were kept on the ceramic pressure plate cell with filter paper placed at the bottom. The assembly was mounted on the pressure vessel and immersed in water for several hours allowing the sample to be saturated. After saturation, excess water on the surface of the cell was removed and air pressure was applied to generate a predetermined matric suction in the sample. Ceramic pressure plate cell, which is called a high air entry disk, has small pores relatively uniform in size. When the disk is saturated by water, air cannot pass through the disk until the air pressure exceeds a certain value due to its ability to resist the air flow.

This air pressure is referred to as the air entry value. The sample was allowed to reach an equilibrium state with a predetermined matric suction by applying the appropriate air pressure. The air entry values of the disks used in these tests are 300kN/m^2 and 500kN/m^2 . The bottom side of the air entry disk was open to the atmosphere and the water pressure is atmospheric (100kN/m^2). By applying an air pressure greater than 100kN/m^2 in the chamber, a predetermined matric suction could be generated.

Once the specimen reached such matric suction, the water content was determined. Achieving the matric suction value can be confirmed by observing constant volume

change through outflow tube. Average volumetric water content was determined by obtaining the weights of all samples under equilibrium conditions for each level of matric suction.

Alternatively, the matric suction, air void ratio relationship can be obtained from permeability test data and direct shear test data. The SWCC obtained for the soil samples at 42+340 to 42+400 using all these technics are presented in figure 2.32.

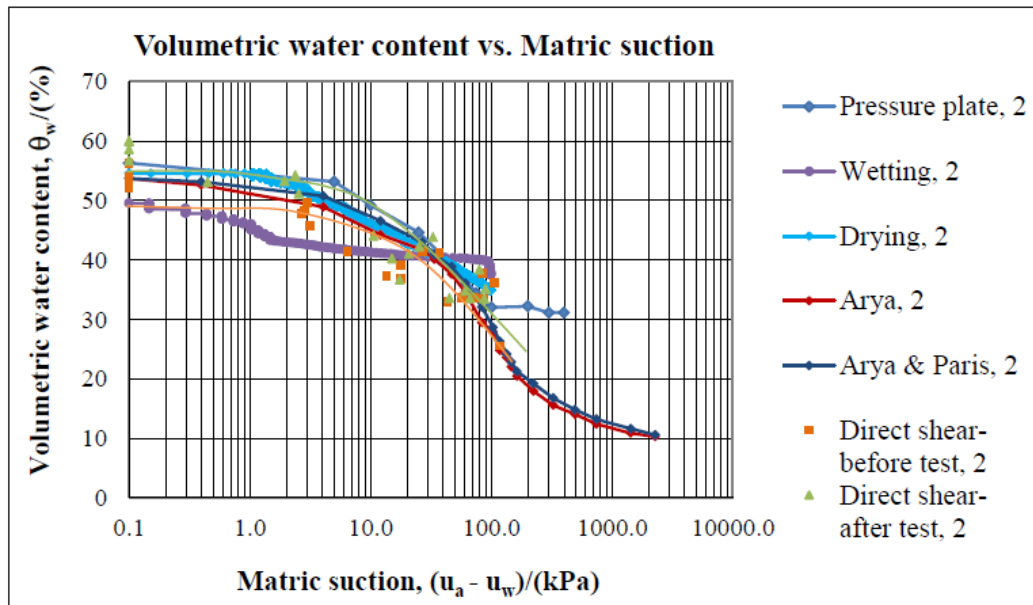


Figure 2.32: The variation of volumetric water content with matric suction (SWCC) for SANDY SILT for various methods, Vasanthan (2016)

2.7.3 Direct shear test with tensiometes

Testing procedure

Assembly of direct shear test was done and tensiometer was attached to the soil specimen, Figure 2.33. After some time was allowed to reach the equilibrium condition, normal loads were applied and tests were initiated under drained condition. The shearing was done at a rate of 0.125mm/min which ensured consolidation based on the value of coefficient of consolidation. Normal load intensities of 50, 100, 150 and 200kN/m² were applied. Tests were done with different level of saturation as; 50%,65%, 72%, 81%, 92% and 100% (fully saturated) were performed.

CHAPTER 03: INITIAL DESIGN, THE FAILURE AND RECTIFICATION OF FAILURE AT WELIPENNA

The failure occurred at the cut slope at chainage of 42+340 to 42+400 in Walipenna at Southern expressway was backanalysed in this research. Information on; site location, site characteristics, the initial design the failure and rectification process are presented in this chapter.

3.1 Background

After prolong rainfall that continued for several days in western part of the country, the cut slope at chainage 42+340 to 42+400 in the Southern express way became unstable and failed on 2nd November 2012. This interrupted the flow of traffic towards the Galle for more than five hours in the Southern express way.

The landslide area is located in between Dodangoda and Walipenna interchanges belongs to Dodangoda DS division in Kaluthara district. The slope is a terraced slope with an average inclination of 40°. The location map is presented in Figure 3.1.

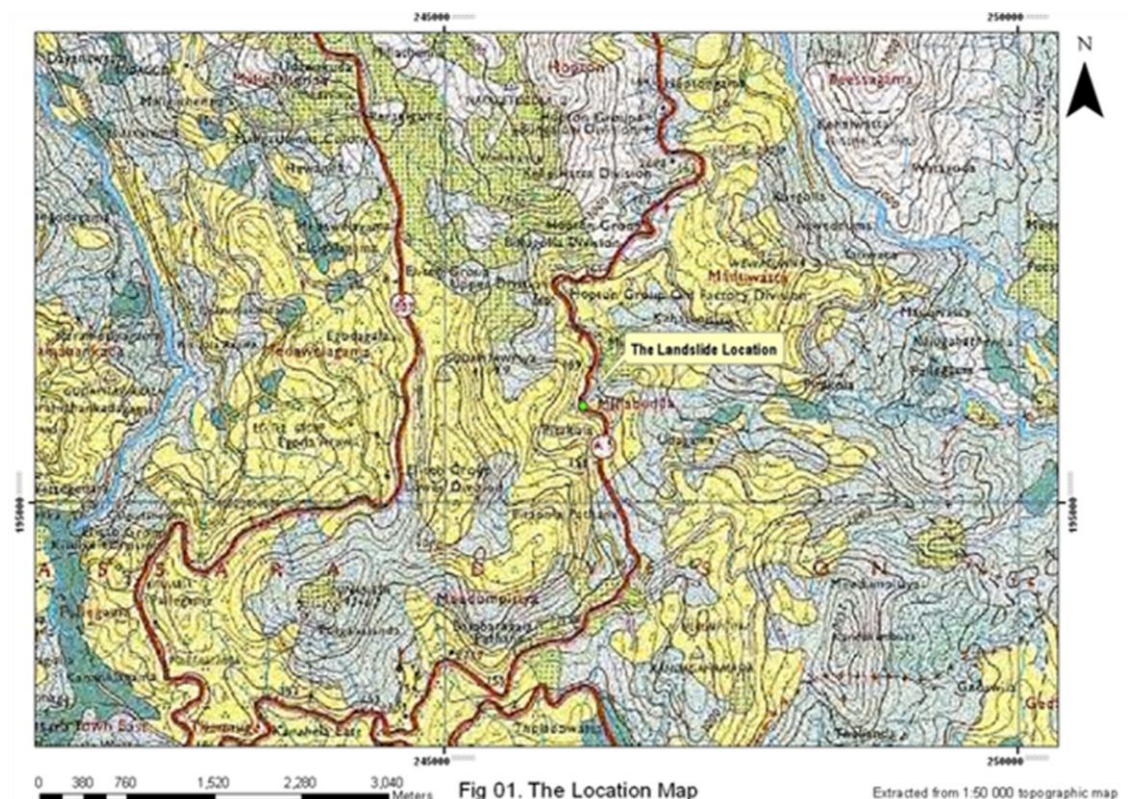


Figure 3.1: Location map – 1:50,000 scale

3.2 Geology and Sub soil profile

This slope was formed of unsaturated residual soils. An investigation with four boreholes had been done during the design stage of the cut slope. After the failure, seven further bore holes were drilled from the berms at locations shown in Annex 1. Based on the information gathered in the borehole investigation, the sub soil is found to be silty sands and sandy silts. The ground water table was above the road level according to the continuous water level measurements made in the seven boreholes. The details of the borehole logs are presented in Annex 2.

Type of the bedrock is garnet biotite gneissic. Outcrops of the bedrock can be seen at the top of the slope at 42+350 to 42+400. The bedrock is dipping into the slope at a very steep (80°) angle. Five different joint systems were identified in the rocks in the area as Figure 3.2.



Figure 3.2 – Joint sets in the bedrock exposed at the top of the slope

Residual soil had been formed as a result of the weathering of the gneissic rock. Due to weathering under high ambient temperature, high rainfall conditions and due to the differences in the mineralogical structure in the Metamorphic parent rock the weathered product is highly variable. As result, rocks with no or very slight weathering can be seen embedded in a matrix of soil. These are referred to as boudinage structures. This boudinage structures could be identified during the drilling for soil nailing in rectification process. A typical condition with boudinage structures encountered during drilling is presented in Figure 3.3.

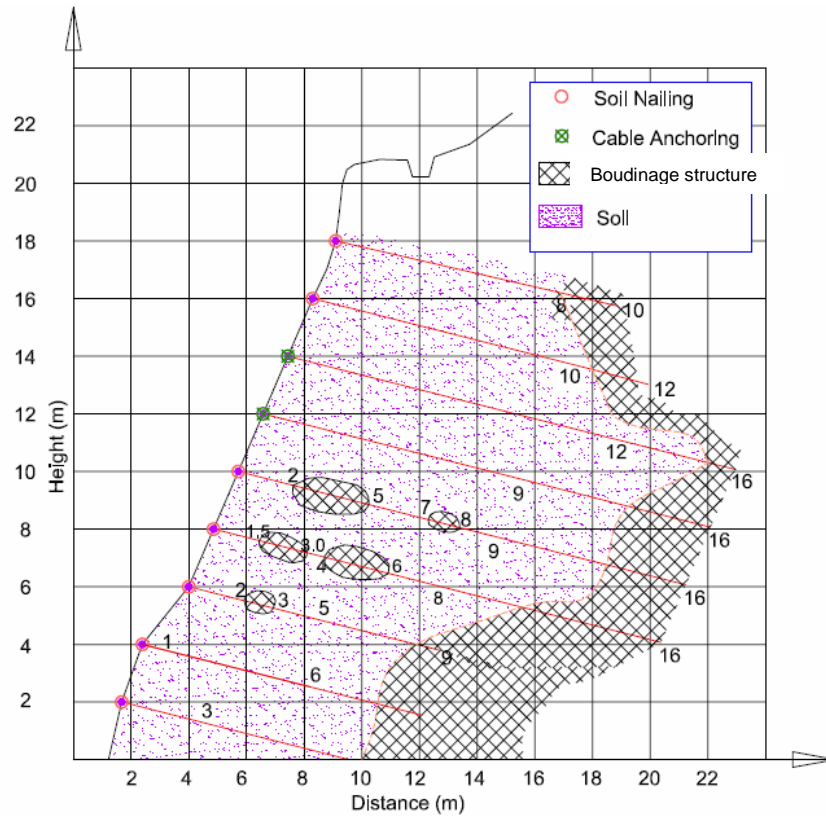


Figure 3.3 – Typical drilling records indicating boudinage structures

Adversely oriented relict joints filled with water were identified during the rectification process. During the drilling for soil nailing for rectification, the water trapped in the relict joints released under very high pressure covering the workers in mud. This implies that there is water under high pressure in relict joints. This water will move into the soil around making it saturate. The presence of pore water under higher pressure itself is having adverse effects on stability. (Figure 3.4).



Figure 3.4 – Water oozing out of relict joints during drilling

3.3 The initial design of the cut slope

During the constructions of Southern Transport Development Project (STDP) the hilly area in between the chainage of 42+380 to 42+440 was subjected to deep cuts. The deepest sections are in between the chainage 42+380 and 42+440.

Therefore, the stability of the proposed cuttings had been assessed and safe slope gradient for proposed cuttings had been determined. A photograph of the site before any cutting is presented in Figure 3.5.



Figure 3.5: Photograph of the site before any cutting

Five boreholes CD1 –CD5 (shown in Annex 3), were drilled in the natural slope along the vicinity of the road segment. This data also indicated that the sub soil is sandy silt. The ground water table is at or below the bottom level of the proposed cut (road level). Consolidated undrained triaxial tests with pore water pressure measurements were conducted on two specimen obtained from a box sample. Soil specimens were saturated prior to the testing. The Shear Strength parameters corresponding to two specimens are presented in Table 3.1.

Table 3.1 – Shear Strength Parameters from undisturbed samples

Sample No	Location	Soil Description	Moist. Content	Dry density kg/m^3	c'	ϕ'
04	42+380	Lateritic Soils	Mc=25.9%	$\gamma_d=1440$	35 kN/m^2	32°
05	42+420	Lateritic Soils	Mc=40.3%	$\gamma_d=1010$	9 kN/m^2	32°

Design of the cut slope was done using the sub soil parameters derived based on the SPT N values of five boreholes, laboratory testing data, visual descriptions of the soils, and the experience on similar type of soils. Accordingly the slope was analysed at shear strength parameters of; $c'=10 \text{ kN/m}^2$ and $\phi'=32^\circ$.

Geoslope SLOPE/W 2004 software was used in the analysis and several proposed geometries of, cutting the slope at gradients of 1:1.2, 1:1.3 and steep cut with soil nailing were checked. Consequently, it was designed to cut the slope at the gradient of 1:1.2 keeping berms at every 7.5m height difference as Figure 3.6. This yields a Factor of Safety of 1.2.

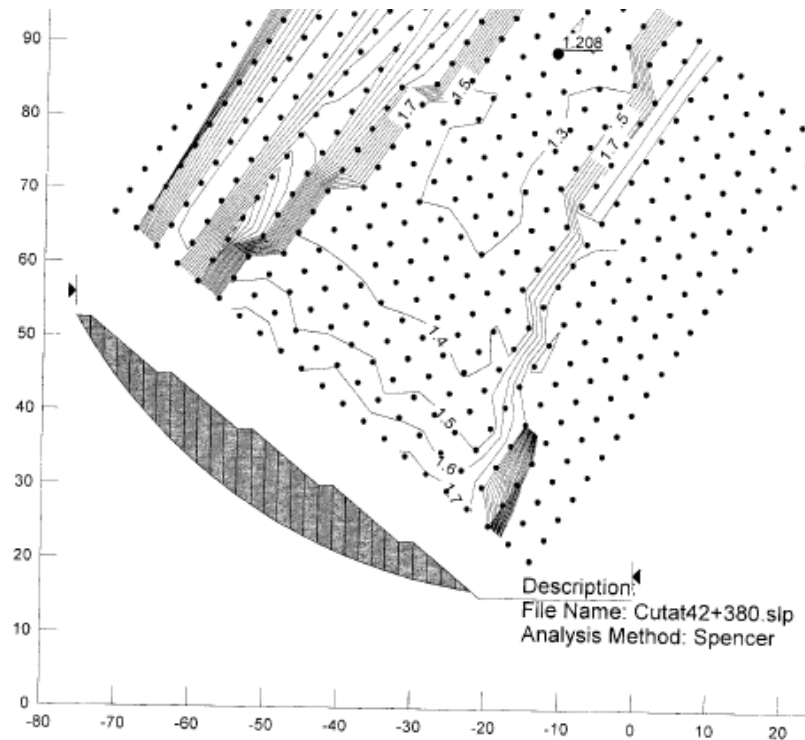


Figure 3.6: Stability of the cut slope at 1:1.2 gradient – Section at 42+380 Critical failure surface (Design report – STDP)

In order to minimize the infiltration and the loss of matric suction or development of perched water table, surface drainage of the area had been well developed with concrete paved berm drains on each berm and cascade drains to collect water from berm drains and free flowing of water runoff down the slope. Together, the slope is covered with grass cover to control the erosion (Figure 3.7). The grass cover also deflects the water flow as runoff while minimizing infiltration.



Figure 3.7: Berm drains and cascade drains

3.4 Description of the failure

3.4.1 Nature of the failure

After several days of rainfall a failure occurred in the slope upto a height of 3rd berm level (there were five berms altogether). This is a medium scale landslide that occurred over a length about 50m along the road and extends over a height about 20 m. The slip surface is quite shallow.

On the day of failure, cracks appeared on crown of the terraced slope around 9.30 am (Figure 3.8). The cracking of the cascade drain just above this level and possible leakage of water to the slope for quite some time could also be seen. Below the level of the crack in the slope the berm drains have also cracked (Figure 3.9). Cracks widened within the day and eventually failure occurred by 3 pm. The soil mass has been moved toward the carriageway and debris with an approximate flow length of 30 m from toe of the modified slope are accumulated on the 10m wide road reservation and whole road section towards the Galle (Figure 3.10, Figure 3.11).

The road itself was not damaged, but rather had been covered by a mass of soil that flowing. The affected portion of the road was about 70m long. That segment of the

expressway was closed and public were warned after the observation of the initial crack.



Figure 3.8 – Initial Crack and downward movement of soil



Figure 3.9– Movements of soil at the top and Movement of Cascade Drain



Figure 3.10– Debris of Failure Has Covered the road section towards the Galle



Figure 3.11 – Debris of Failure Has Covered the road section towards the Galle

3.4.2 Possible reasons of failure

The failure that occurred in this slope was triggered by the excessive rainfall that prevailed in the area over the days preceding the failure. Some cracks that existed in the drainage system (cascade drains) could be detected only after the catastrophic failure. As a result of heavy rainfall, significant infiltration has taken place. Water has seeped through the cracks making the soil nearly saturated. Thus the shear strength of soil has reduced.

Zones of whitish feldspar rich clays could be identified at limited locations around the mid level of the left escarpment (Figure 3.12). This weak material may also have contributed significantly to the failure of the slope. The shear strength of this material under saturated condition would be much lower than the saturated shear strength determined at the design stage.

The failure also has been facilitated further by excessive infiltration of rainwater into a system of adversely oriented relict joints. Relict joints would be filled with loose material /weak material which was observed in the failure escarpment and water infiltrated into relict joints could facilitate saturation of the slope material. Further, there would be pore pressure built up in relict joints. In such situations the sliding will take place along the critical failure surface and the ground water table need not rise to higher level. The observation after the failure was similar. The debris were not having lot of moisture. However, just prior to the failure water getting released under high pressure or oozing out of water near the toe has been observed. This could be attributed to the perched water table condition developed closer to the toe of the slope.



Figure 3.12 –A Zone of whitish Feldspar rich clay in the failure surface

3.5 Rectification Design

State of the stability of slope during failure was back analysed using SLOPE/W 2004 software. It was not possible to model the infiltration and account to the complete process at this stage. For the back analysis the unsaturated nature of the soil, that reduction of the apparent cohesion was simulated approximately by assigning weak zone of soil near the surface. Shear strength parameters of this weak zone was reduced to $c'=7 \text{ kN/m}^2$ and $\phi'=30^\circ$. Based on the experimental results obtained other areas were idealized to be formed of a uniform material of $c'=10 \text{ kN/m}^2$ $\phi'=32^\circ$. The most critical failure surface obtained was having a factor of safety of 0.993 (Figure 3.13). The obtained failure surface is shallow and somewhat close to that actually observed.

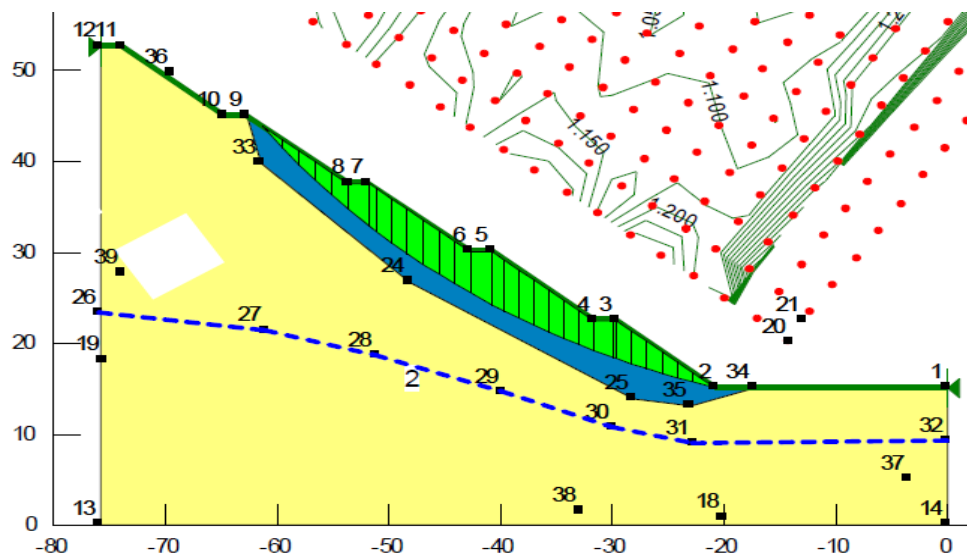


Figure 3.13 – Simulated failure surface (Rectification report – NBRO)

The analysis of slope after failure indicated that that the slope profile that remains after failure is not safe unless high matric suction values prevail. Therefore, to incorporate the worst situation, the rectification design was done using saturated shear strength parameters.

According to the analysis of stability of the slopes in the site it would be necessary to install slope reinforcement to enhance the safety margin of the slope to an acceptable value as Figure 3.14. It is also necessary to minimize the infiltration and facilitate the rapid dissipation of pore water pressures.

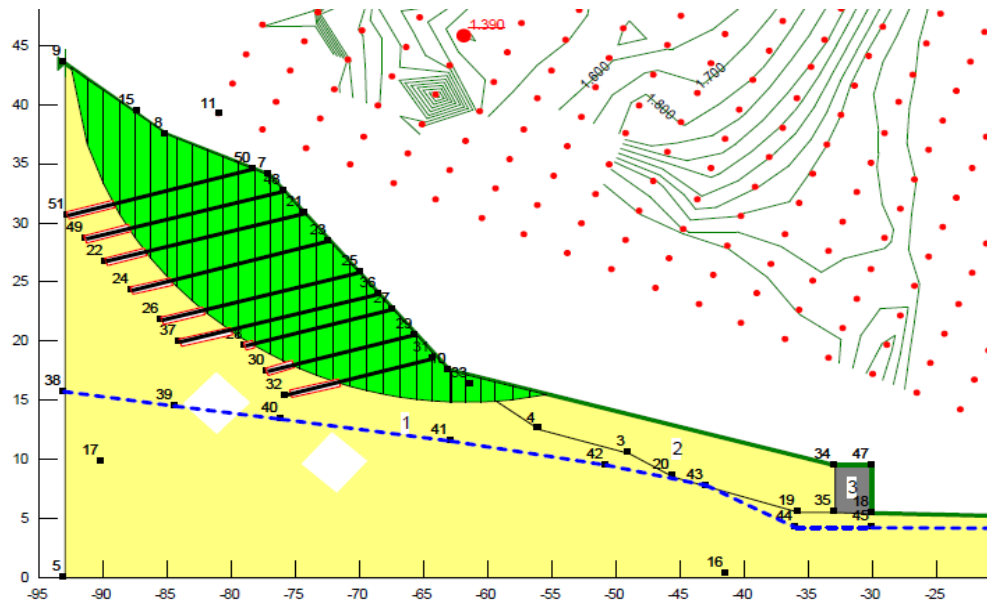


Figure 3.14 – Proposed stabilization with soil nailing subsurface drainage and toe wall

Therefore, it was proposed to strengthen the slope by reinforcing at the upper level and providing a gravity retaining wall at the toe. Surface drains were reconstructed and number of sub surface drains were done to facilitate the movement of water trapped in the slope.

3.5.1 Rectification measure of Soil nailing and Anchoring

The drilled and grouted soil nails were constructed as the main stabilizing measure. The diameter of the drill holes were 125 mm. The reinforcement inserted were 25 mm diameter tor steel bars at most locations. At some locations bars of diameter 32 mm were used.

Soil nailing design involved nails of 16m length at the highest location. Later it was decided to use cable anchors in place of those long nails. The other nails were length of 12m. Cable anchors used were pre-tensioned to 180 kN. Thereafter all the nail heads and cable anchoring heads were connected by a system of beams and the complete surface was shotcreted.

3.5.2 Constructed Surface and Sub surface drainage

Surface drainage improvement was done by repairing all failed berm drains and cascade drains.

The surface of the nailing area had been shotcreted. To minimize the build up of positive pore water pressures behind the shotcreted area, short drains of length around 2.0m were provided in a grid of 1.5 X 1.5m.

To minimize the rising of ground water table during heavy prolong rainfall and minimize the activation of deep seated slip surfaces, long drains of length around 12m were provided in 5m horizontal spacing.

3.5.3 Gravity retaining wall

In addition to the above strengthen measures, to having a toe support a gabion wall has been constructed. The wall was of height 4.5m.

The location of soil nails, cable anchors and long horizontal drains are presented in the elevation diagram in Figure 3.15.

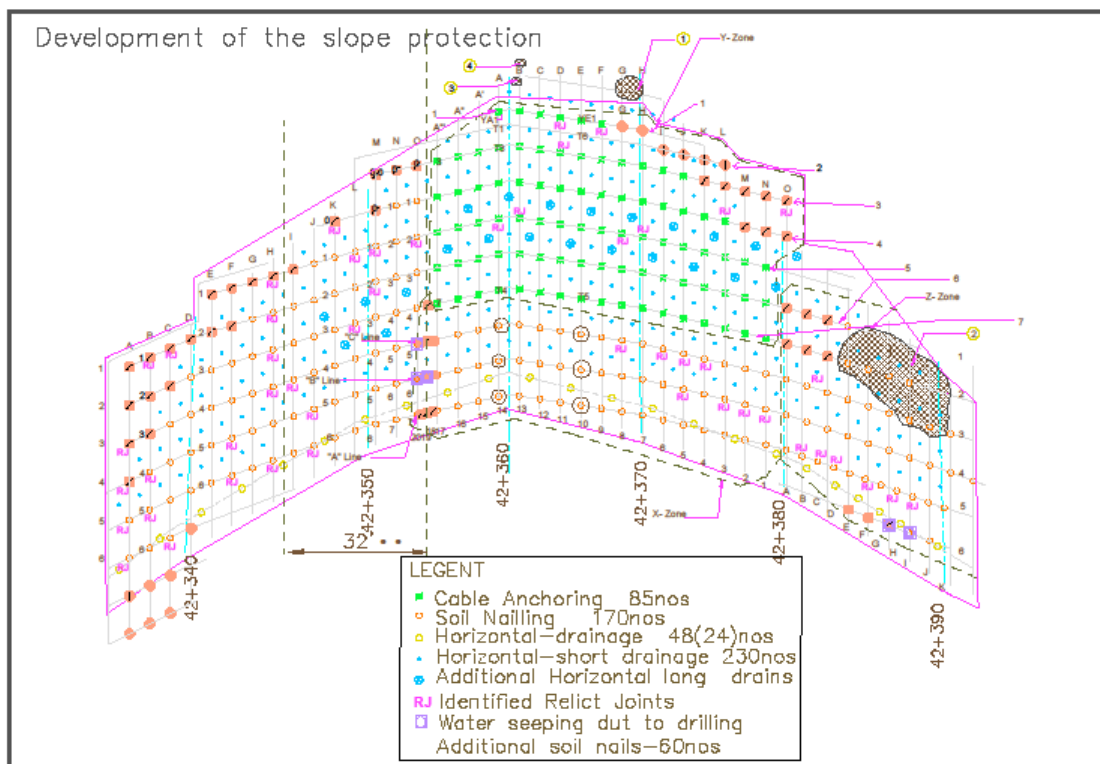


Figure 3.15: The location of soil nails, cable anchors and long horizontal drains

3.5.2 Construction Sequence

During the grouting for soil nailing there was further evidence about the inter connection of drill holes through the system of relict joints. The grout forced into one

hole was seen coming out from another non grouted holes. As such, special attention was paid to the construction sequence. The drilling for sub horizontal drains were done only after the completion of Soil nailing. If sub horizontal drains were done initially they could have got filled up with the grout impelled to soil nailing holes. The slope after completion of all rectification measures is presented in Figure 3.16



Figure 3.16: View after completing the rectification (After Dharmasena et.al 2015)

CHAPTER 04: BACK ANALYSIS OF SLOPE FAILURE

4.1 Preparation of Infiltration model

The failure that occurred at 42+340 to 42+400 at Walipanna in the Southern Expressway was back analysed by simulating the events that took place preceding the failure. The failure occurred after few days of rain and the two rain gauges located in the region have the records of rainfall.

The slope geometry prior to the failure is known. The saturated shear strength parameters of the soil encountered were determined through laboratory tests. The unsaturated characteristics necessary for modeling were determined through laboratory tests done by Vasanthan (2016).

The process of infiltration was modeled with SEEP/W (2007) software using this set of data. SEEP/W based on a Finite Element formulation has capability to analyze the infiltration behavior in both saturated and unsaturated soil. It needs main input parameters of Hydraulic conductivity functions, Soil Water Characteristic curves and rainfall intensities. Slope geometry, Material properties, Mesh properties, Boundary conditions, Time intervals and Analysis types are the other input parameters.

4.1.1 Rainfall data for the preparation of Infiltration model

The rainfall data over a week preceding the failure was obtained from the Meteorology department. Data of the rain gauge stations closest to the location as Bombuwala and Beddegama are presented in Annex D. Based on the data total accumulated rainfall at Bombuwala rain gauge station during the week preceding the failure was 431.5mm. At the Baddegama rain gauge station this value was 245.3mm. At both locations no heavy rain was recorded on the day of the landslide, 2nd November. At the landslide location itself no rainfall was recorded on that day.

For the back analysis, actual peak rainfall measured on five days preceding the failure at each rain gauge stations have been idealized and applied using appropriate slope boundary conditions. Figure 4.1 shows the idealized rainfall. Rainfall is not extreme during the failure, but prolonged rainfall with low intensity, where maximum recorded rainfall was 7mm/hr.

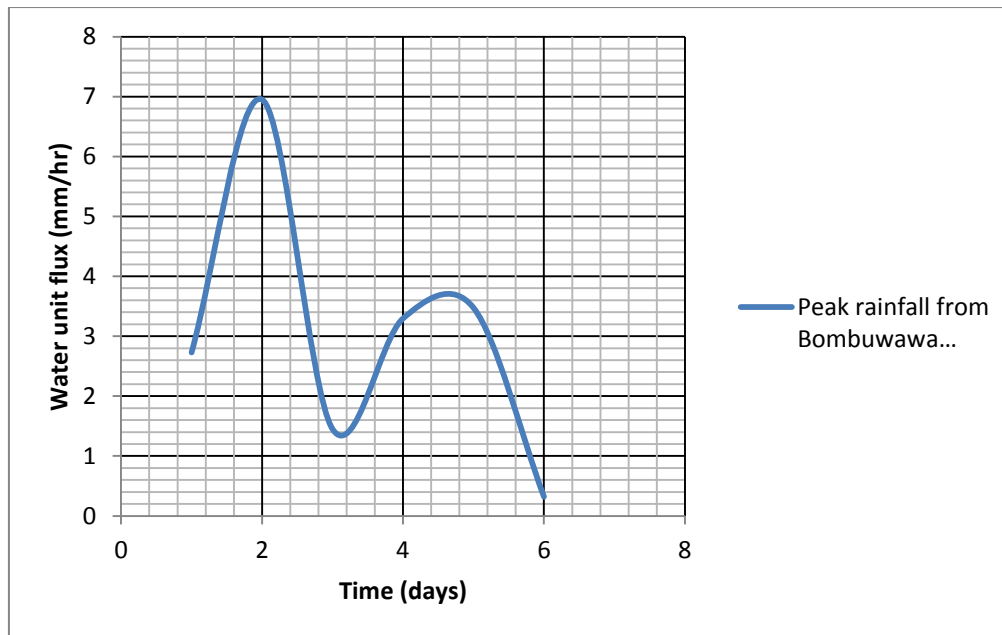


Figure 4.1: Peak rainfall from Bombuwawa and Beddegama Rain Gauges

4.1.2 In put parameters of Hydraulic properties of unsaturated soil.

As hydraulic properties of the unsaturated soil, Hydraulic conductivity function and soil water characteristic curve (SWCC) obtained by Vasanthan (2016) were used. The soil water characteristic curve (SWCC) and hydraulic conductivity function for the sandy silt for wetting path, which was used for the analysis are shown in Figure 4.2 and Figure 4.3 respectively. Saturated hydraulic conductivity of the soil is $3.3 \times 10^{-6} \text{ m/s}$ and saturated volumetric water content is 0.518.

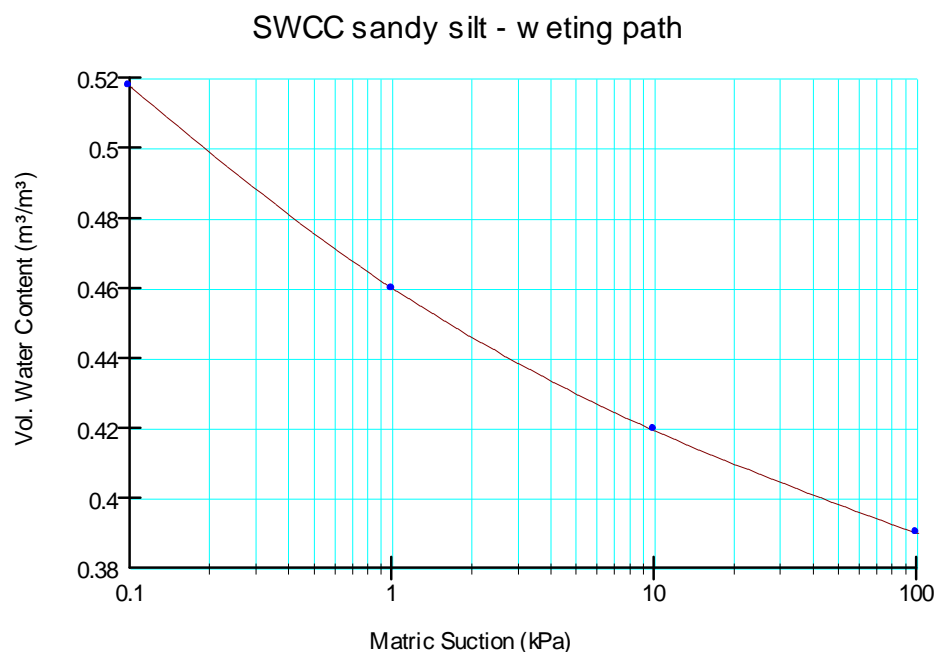


Figure 4.2: SWCC used for analysis - Sandy Silt, wetting path, Vasanthan(2016)

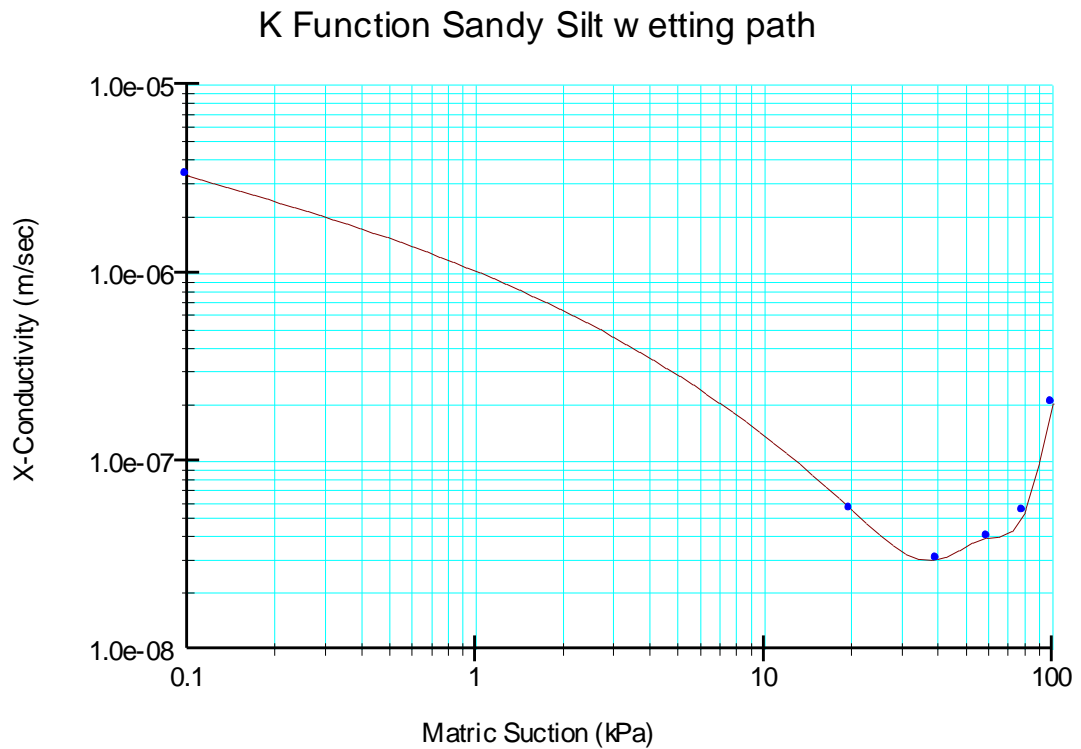


Figure 4.3: K function used for the analysis, - Sandy Silt– wetting path, Vasanthan (2016)

4.1.3 Boundary conditions and mesh properties

The geometry of the construction slope was considered for the analysis. Although there were boudinage structures identified, the slope was modeled to be made of a uniform residual soil (sandy silt) in this idealization.

Suitable boundary conditions were applied to the soil profile to represent the actual seepage conditions of the slope as mentioned in Figure 4.4. Variation of rainfall intensity with time was applied to the soil surface of A-B, B-C and C-D. Zero total flux was applied to the side of the slope above the water table at A-G and D-E to simulate the non-lateral flowing of infiltrated water. Zero total flux was also applied to the bottom of the profile at F-H to simulate no flow of ground water to further down. Initial total heads, h_t , were applied at the sides of the slope below the water table at E-F and G-H, to maintain the minimum depth to ground water table.

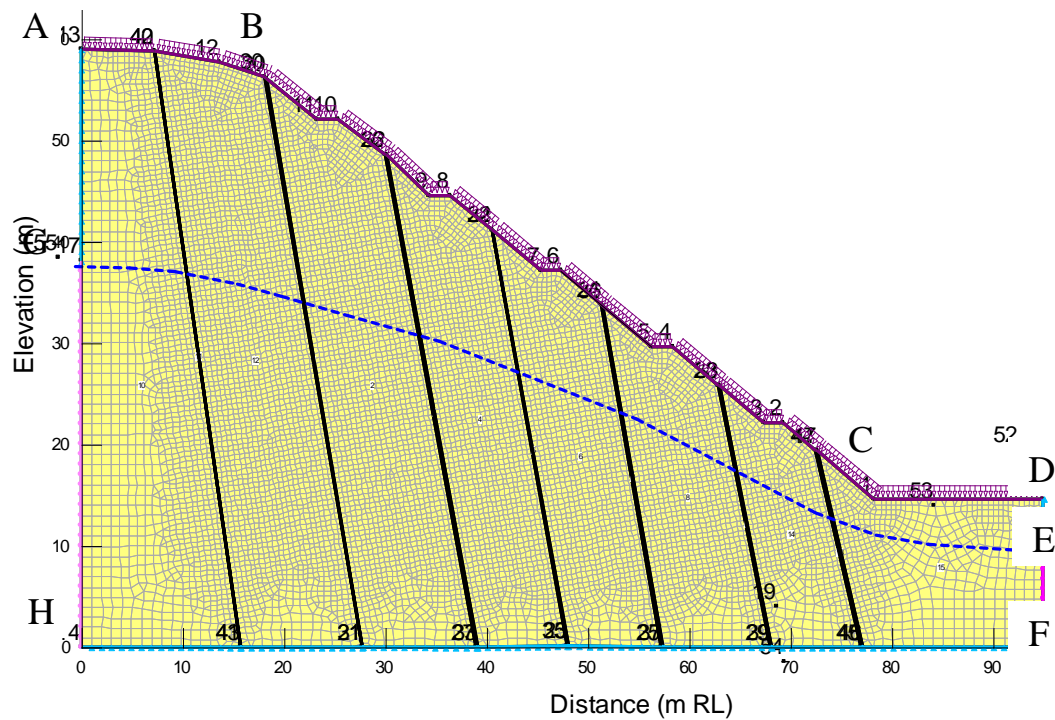


Figure 4.4: Slope with applied Boundary conditions

4.1.4 Type of Analysis

There are two fundamental types of finite element seepage analysis; steady state and transient. In definition means steady state is not changing with time and transient means always changing. In a steady state analysis all of the boundary conditions are fixed. But in a transient analysis the boundary conditions can also be functions of time or response to flow amounts.

Transient type study has been done in this back analysis. Which implies this include predicting the time it takes the soil profile to get saturated with water infiltration. Therefore, in order to move further, we must define what the pore water pressure conditions at the beginning of the time period. Therefore, initial water table was identified using the data collected in piezometers during the rectifications.

4.1.5 Modeling of Infiltration behavior

Input parameters and boundary conditions were incorporated to the Seep/W software to generate the rainwater infiltration model of slope at 42+340 to 42+400 in Walipanna at southern expressway.

The joint patterns in the rock were identified by visual observations. An idea about the presence of relict joints and their orientation were obtained with various observations made during the rectification work. The presence of water under significant pressure in the relict joints was also identified at that time. Therefore in this research initially a parametric study was done for the determination of infiltration behavior of the slope with and without the presence of relict joints.

Considering many possible variabilities and uncertainties that existed, the back analysis of the failure was done in the form of parametric analysis incorporating all possible variable conditions. As there was evidence that surface drainage measures implemented were disturbed to some extent analysis were done both with and without the drainage measures.

- (a) Infiltration analysis without any surface drainage measures (4.2.1)
 - Without relict joints (4.2.1.1)
 - With relict joints (4.2.1.2)
- (b) Infiltration analysis with surface drainage measures (4.2.2)

4.2 Results of Infiltration analysis

4.2.1 Without surface drainage measures

4.2.1.1 Homogeneous Residual soil without Relict joints

Infiltration of water during the observed rainfall at the nearby rain gauges is modeled using the SEEP/W-2007 software. Initial analysis was done for a slope without any relict joints.

The pore water pressure distribution with depth prior to the rainfall was assumed to be hydrostatic below the ground water table and negative above it in the unsaturated soil mass. The negative pore water pressures were given a cutoff value of 100 kN/m^2

The result of the analysis is presented in the form of plot, pore water pressure distribution along the vertical sections A-A to F-F of the slope in Figure 4.5 for the idealized rainfall.

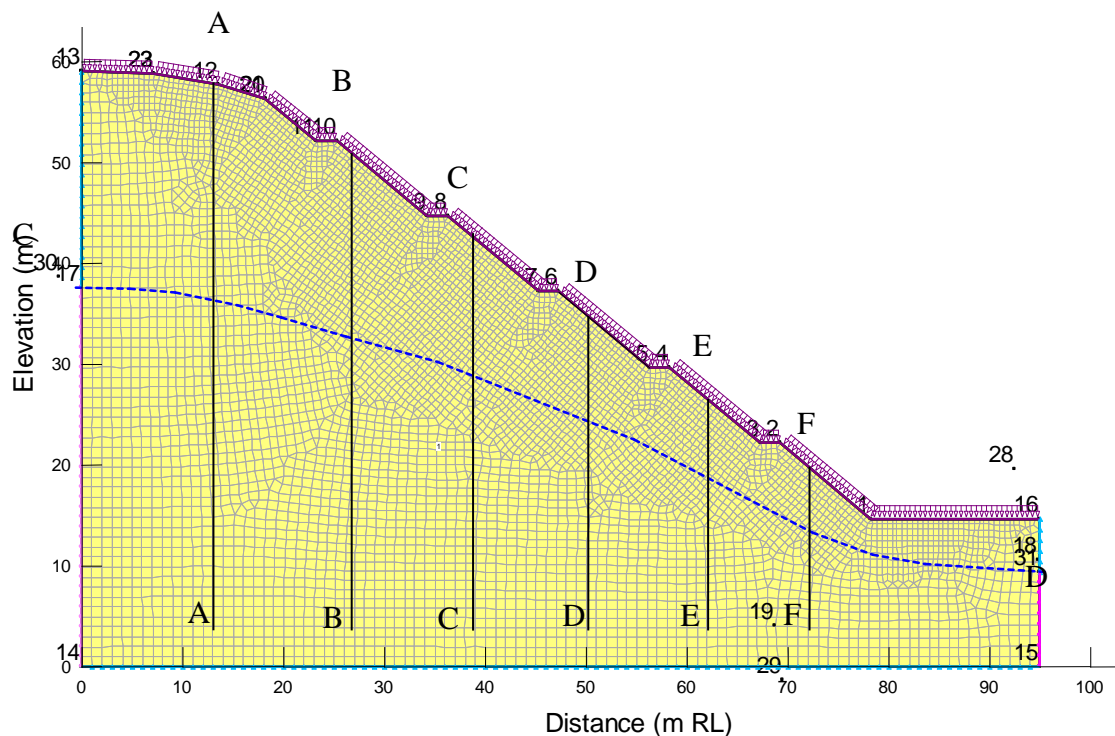


Figure 4.5: Analyzed slope

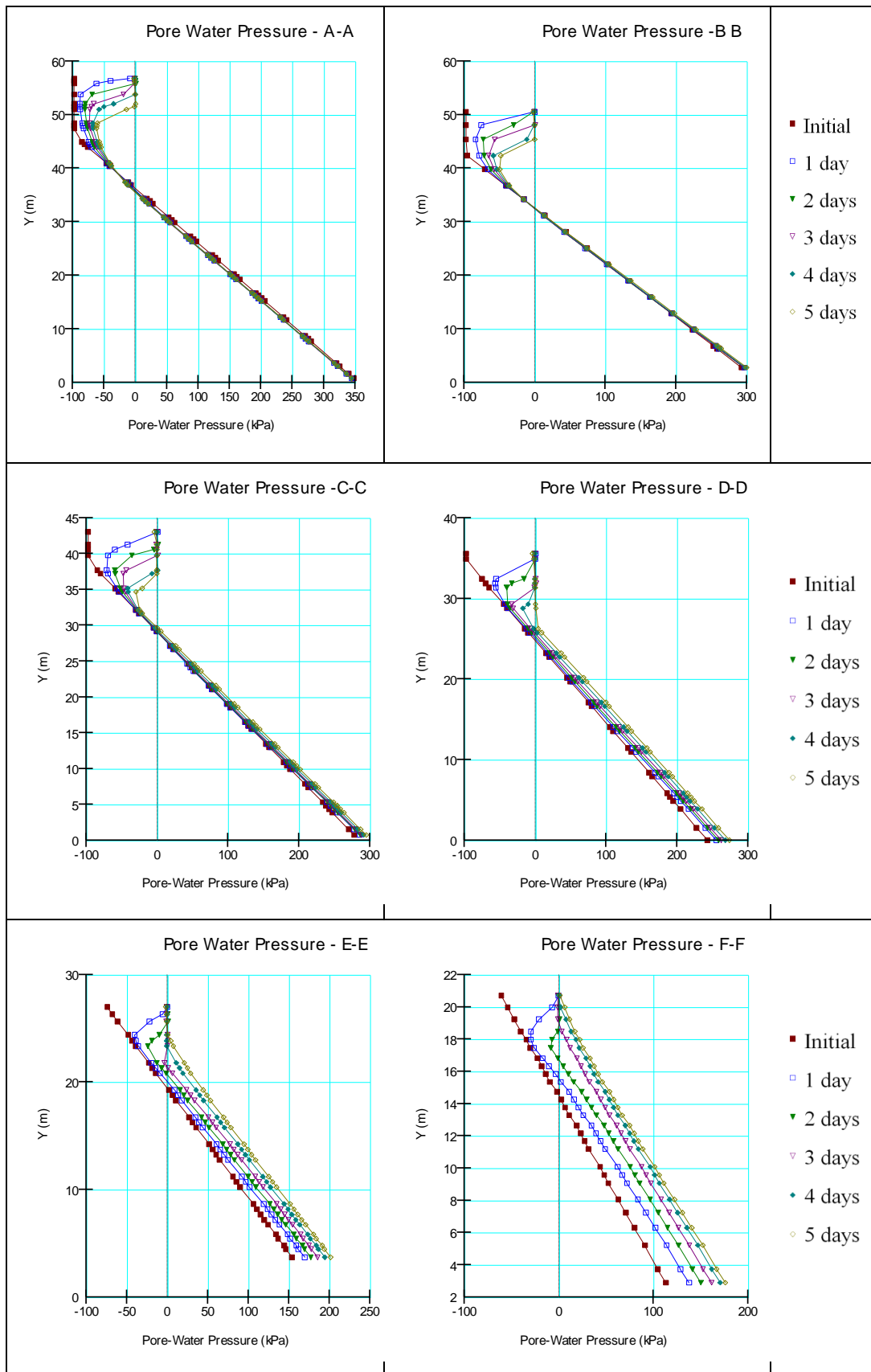


Figure 4.6: Pore water distribution vs depth in sections A-A to F-F for the idealized rainfall

With the infiltration of the rainwater the soil gets saturated near the surface and water moved to deeper levels of the slope. The changes to the pore pressure regime with the prolonged rainfall is illustrated by the pore water pressure distributions plotted along Section A-A to Section F-F. (Figure 4.6).

The result of the analysis shows that as rainfall continues the matric suction values are gradually eliminated and pore water pressure become zero or just positive (negative pore water pressure). It reveals the development of thin perched water table at the surface (Figure 4.7). As rainfall continues the loss of matric suction advances to greater depths. (The wetting front progresses downward).

In the meantime the water table also moves upwards. Effect of progression of wetting front and the rise of ground water table is more prominent towards bottom levels of the slope, in section D-D, E-E and F-F.

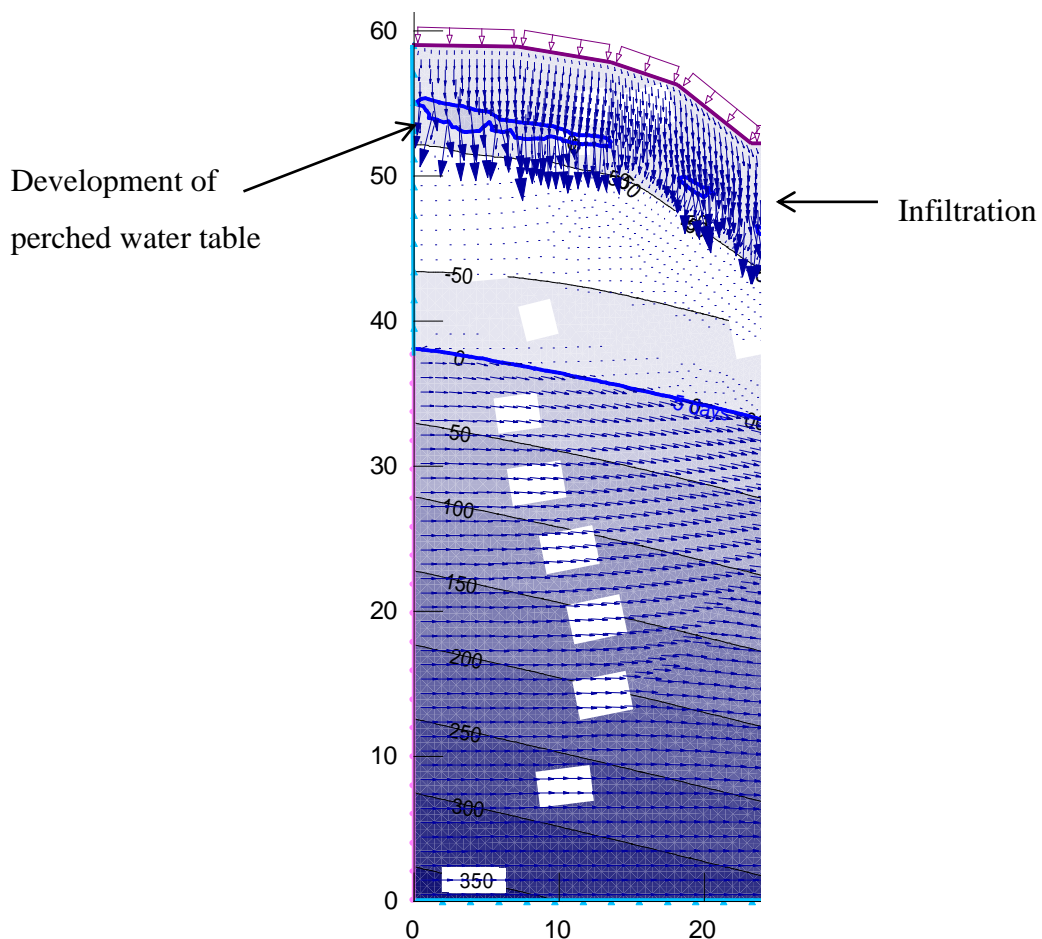


Figure 4.7: Figure shows the rain infiltration through slope profile

4.2.1.2 Homogeneous Residual soil with Relict joints

Presence of relict joints is incorporated into the analysis thereafter as shown in Figure 4.8. The result of the analysis is presented in the form of plot of pore water pressure distribution along the vertical sections A-A to F-F for the idealized rainfall. The relict joints were assumed to be of width 100mm and filled with loose material. The SWCC and Permeability functions assumed for the material in relict joints are presented in Figure 4.9 and Figure 4.10 respectively.

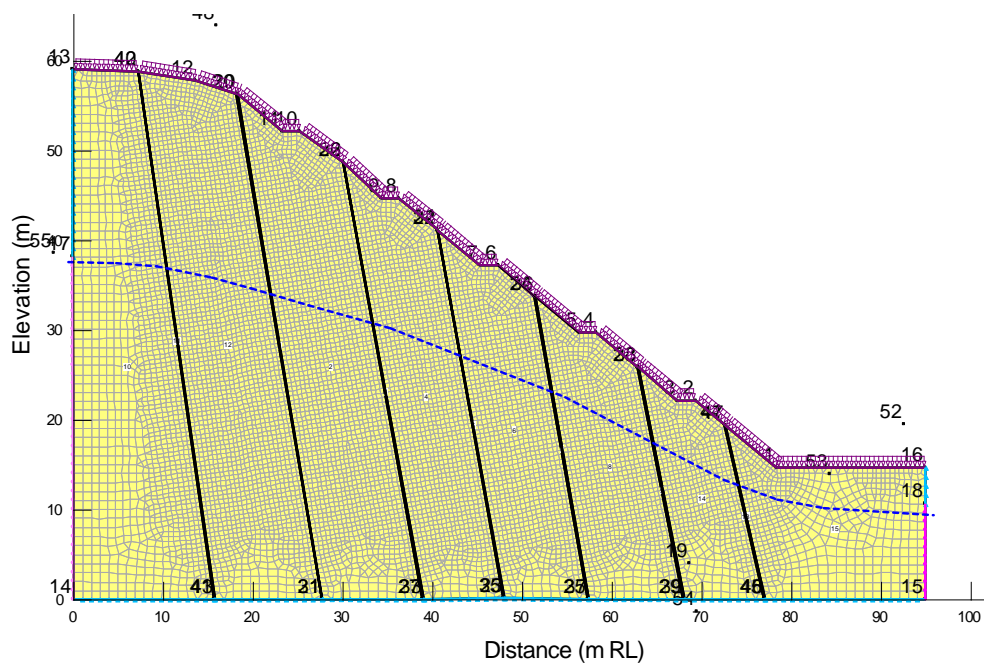


Figure 4.8: Analyzed slope with relict joints

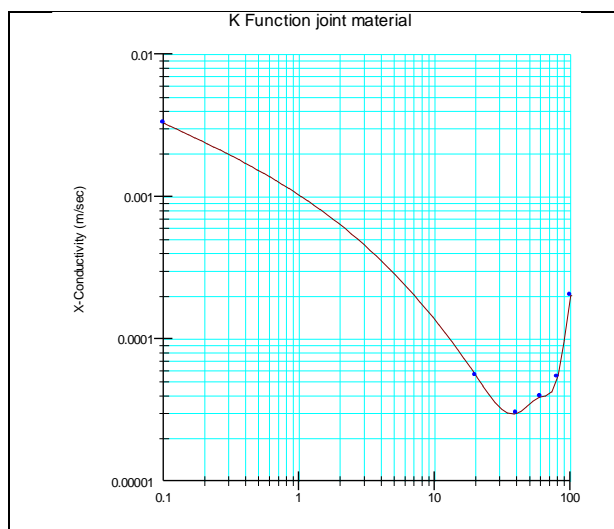


Figure 4.9: K function used for the material in relict joints

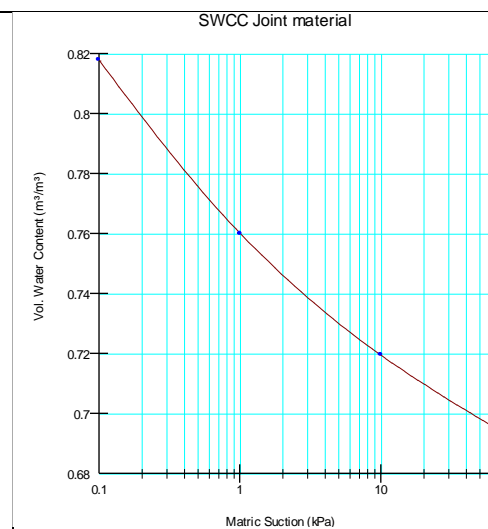


Figure 4.10: SWCC used for the material in relict joints

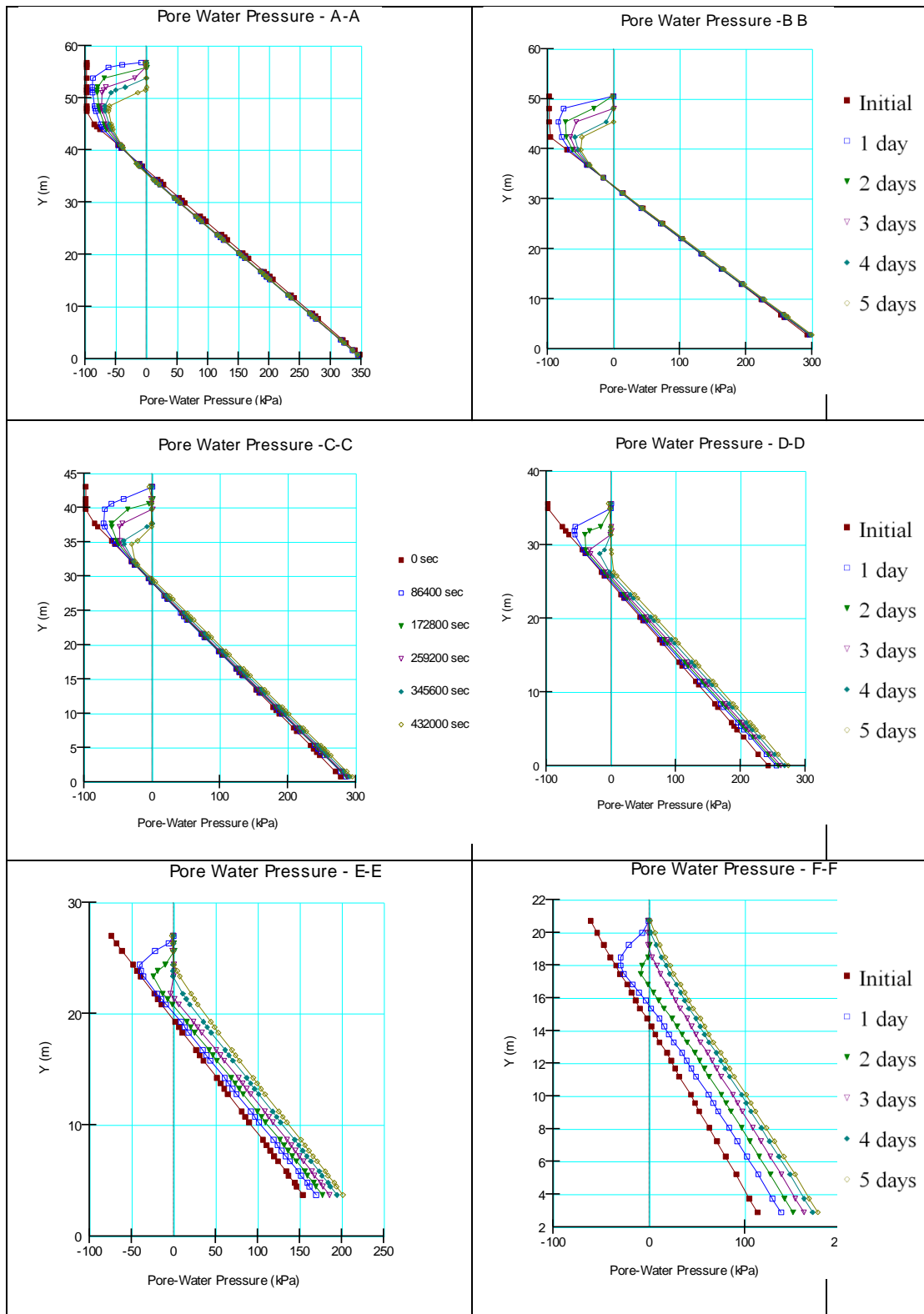


Figure 4.11: Pore water distribution vs depth in sections A-A to F-F

The result of the analysis shows that as rainfall continues the matric suction values (negative pore water pressure) eliminated and pore water pressure become zero or just positive. It reveals the development of thin perched water table at the surface. As rainfall continues the loss of matric suction advances to greater depths. (The wetting front progresses downward). It is more significant towards the lower end of the slope. Matric suction is completely destroyed there.

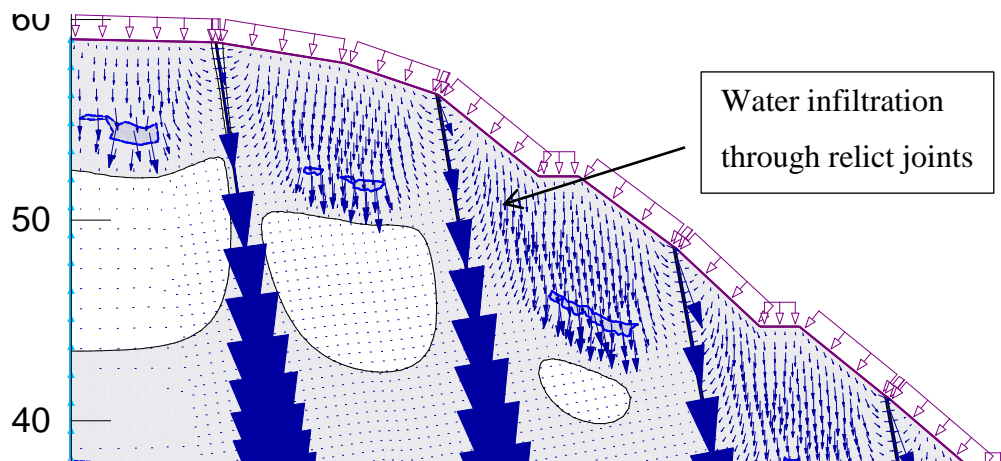


Figure 4.12: Rain infiltration through slope profile and relict joints

In the meantime the water table also moves upwards. Rising of ground water table is more prominent in infiltration model prepared with relict joints than in the model without relict joints. This is due to the presence of high permeable loose filling material in relict joints, water penetrates into the deeper level of the slope without stagnating at the surface as Figure 4.12. When relict joints are not present, the excess rainfall could not infiltrate further and contributed to runoff. It will not contribute to changes in propagation of wetting front or loss of matric suction. This emphasize that, presence of relict joints is a significant feature in slope satiability analysis.

With relict joints effect of progression of wetting front and the rise of ground water table is more prominent towards the lower end of the slope in section D-D, E-E and F-F.

4.2.2 Infiltration analysis for slope with surface drainage improvement

The surface drainage of the cut slope had been enhanced by providing concrete paved berm drains on each berm and cascade drains for free flowing of water runoff from upper slope. Together, the slope is covered with grass cover to control the erosion.

The influence of said surface drainage measures were modeled with the software SEEP/W by incorporating a 100mm thick layer of very low permeability 10^{-20} m/s over the berms for berm drains and a 100 mm thick layer of low permeability 10^{-7} m/s and/or 10^{-8} m/s over the slope surface for vegetation cover.

A comparison of the changes to the pore pressure regime due to a prolong rainfall; without any relict joints and with relict joints while the surface is covered with vegetation is presented in Figure 4.13 and Figure 4.14 respectively for the idealized rainfall.

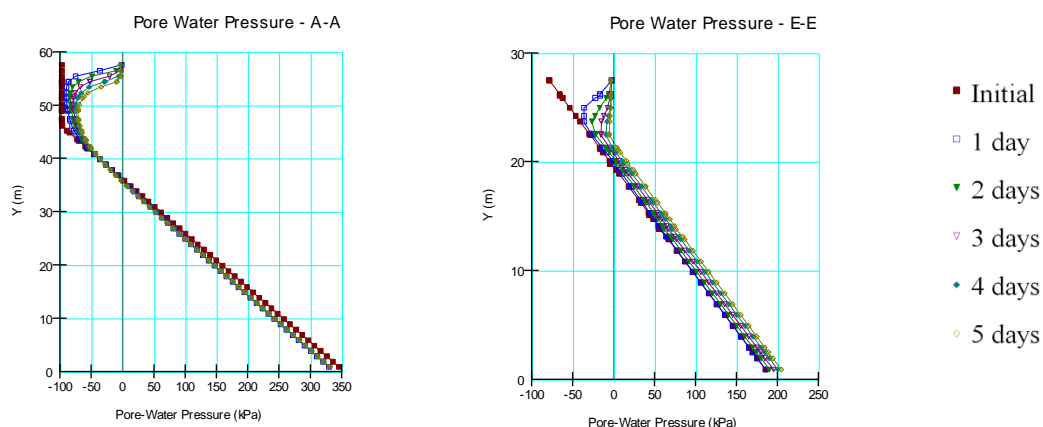


Figure 4.13: Pore water distribution vs depth in sections A-A and E-E for slope without relict joints and with surface drainage improvement (Permeability of vegetation layer = 10^{-7} m/s)

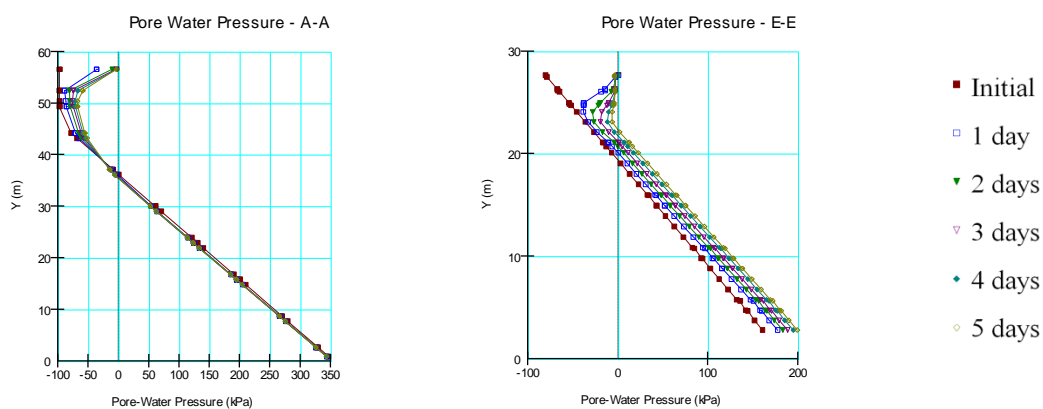


Figure 4.14: Pore water distribution vs depth in sections A-A and E-E for slope with relict joints and with surface drainage improvement (Permeability of vegetation layer = 10^{-7} m/s)

The result of the analysis shows that as rainfall continues under the conditions of improved surface drainage, complete loss of matric suction is prevented at both section A-A and section E-E. Some matric suction remained even after 5 days of rainfall. In the meantime, rise of water table at section E-E is also reduced.

This implies, with the presence of a vegetation layer of low permeability, the infiltration of water is restricted and excess rainfall has contributed to the runoff.

4.2.3 Infiltration analysis for slope with rainfall of high intensity

The influence of high rainfall intensity on infiltration was modeled with the software SEEP/W by applying 20mm/hr continuous rain for 5 days. The changes to the pore pressure regime with the prolonged rainfall under different condition of vegetation cover is illustrated by the pore water pressure distributions plotted along Section A-A and Section E-E. The Figure 4.15, Figure 4.16 and Figure 4.17 presents the cases for; no vegetation cover, vegetation cover with permeability 10^{-7} m/s and vegetation cover with permeability 10^{-8} m/s respectively.

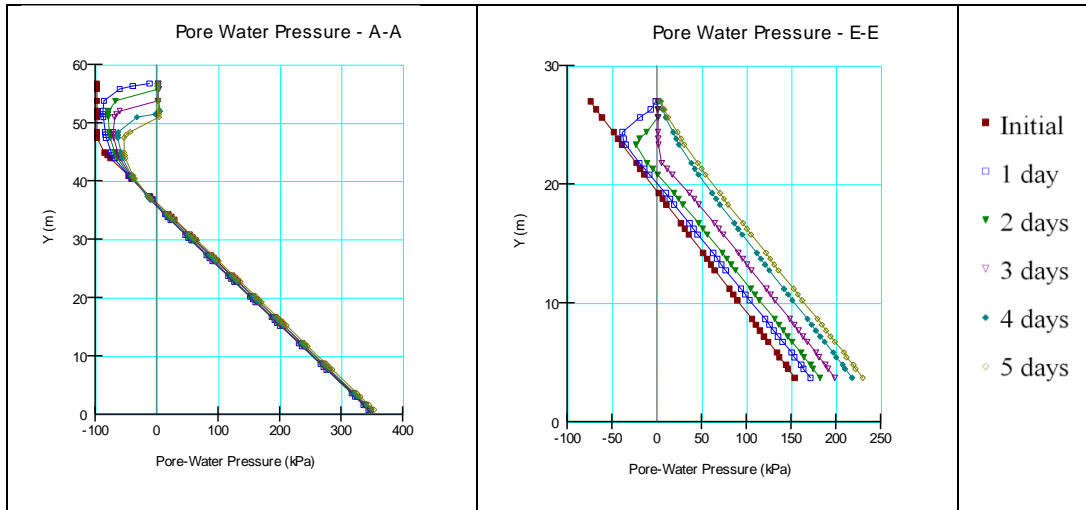


Figure 4.15: Pore water distribution vs depth in sections A-A and E-E for slope without surface drainage improvement and 20mm/hr rainfall

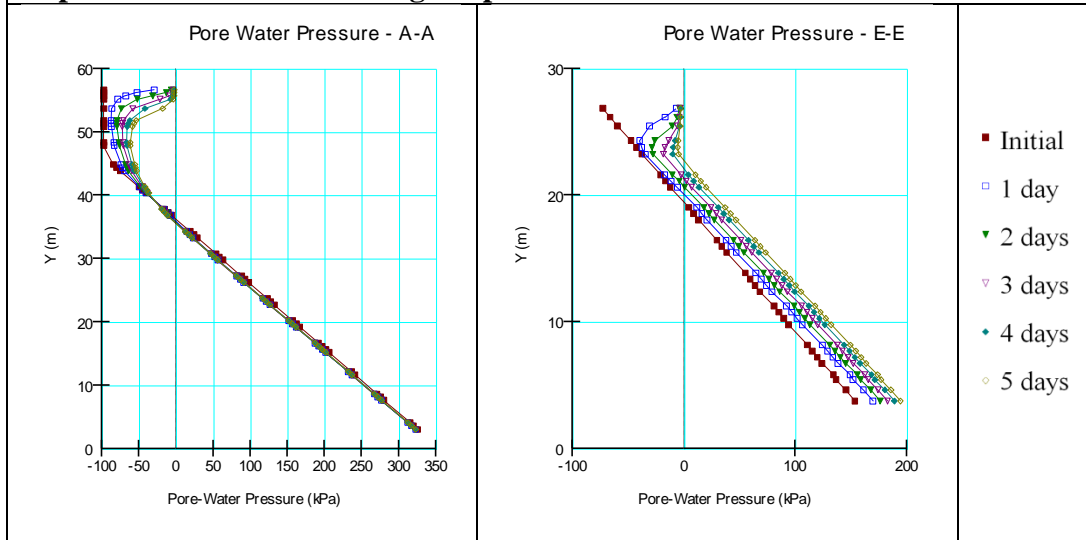


Figure 4.16: Pore water distribution vs depth in sections A-A and E-E for slope with 10^{-7} m/s permeable vegetation layer and 20mm/hr rainfall

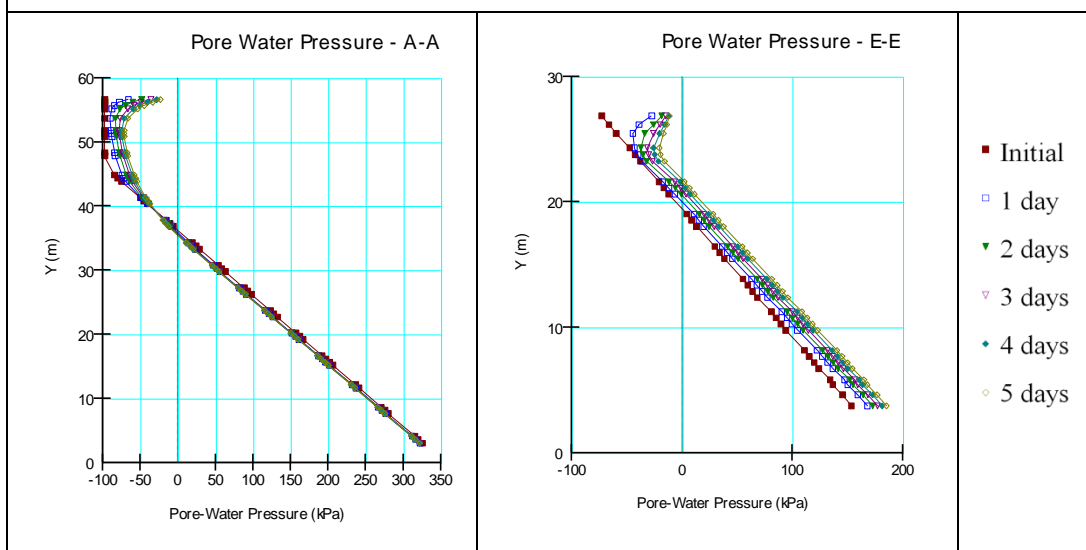


Figure 4.17: Pore water distribution vs depth in sections A-A and E-E for slope with 10^{-8} m/s permeable vegetation layer and 20mm/hr rainfall

The result of the analysis of slope with drainage improvement shows that as even with high rainfall intensity, complete loss of matric suction is prevented at both section A-A and section E-E (Figure 4.16 and Figure 4,17). Some matric suction remained even after 5 days of rainfall. The rise of water table at section E-E is also retarded but higher than for the low intensive rainfall. The effect of progression of wetting front and the rise of ground water table is lesser when the permeability of the vegetation layer is lower.

4.3 Slope Stability analysis

An analysis of the stability of the slope was done at the end of each day after incorporating the pore water pressure distributions obtained from the seepage analysis incorporating the idealized rainfall. Slope/W computer software was used to estimate the minimum factor of safety to determine the stability of slope. Soil profile, shear strength parameters, geological features, pore water pressure obtained from Seep/W analysis are the main input parameters of Slope/W.

Both circular and non circular shape slope failures were analysed. Circular trial failure surfaces were selected by the use of grid and radius approach. The potential non circular failure surfaces were plotted through the block specified approach.

4.3.1 Sub soil profile and shear strength parameters

The slope was formed of unsaturated residual soils. After the failure, seven bore holes were drilled. Based on the information gathered in the borehole investigation, the sub soil is found to be silty sands. Three undisturbed box samples were collected from top, middle and bottom part of the slope section near the failure. Direct shear tests performed on them after saturation of the samples to determine unsaturated shear strength parameters which are presented in Table 4.1.

Table 4.1: Shear strength parameters of the soil profile

Soil type	Unit Weight (γ_{eff})	Effective Cohesion (c')	Friction angle (ϕ')
Sandy Silt	19 kN/m ³	10 kPa	33 °

Parameters of filling material in relict joints were deduced based on the experiences on similar soils.

Table 4.2: Shear strength parameters of the filling material in relict joints

Filing material	Unit Weight (γ_{eff})	Effective Cohesion (c')	Friction angle (ϕ')
Loose fill	12 kN/m ³	2 kPa	15 °

4.3.2 Analysis Type

Analyses were done using the Spencer's method considering both circular and non circular shaped slope failures. As the slip surface option of GeoSlope 2007 package, Grid and Radius approach was adopted for the circular failure type and Block specified approach was adopted for the non-circular failure surfaces.

Parametric analysis were done for the variable conditions outlined in section 4.2.1. Both circular and non circular failure surfaces were considered for each case. Sections are summerised as follows.

4.4.1 Slope without any surface drainage improvement

4.4.1.1 Slope without relict joints

- (a) Circular failure surface
- (b) Non circular failure surface

4.4.1.2 Slope with relict joints

- (a) Circular failure surface
- (b) Non circular failure surface

4.4.2 Slope with surface drainage improvement

4.4.2.1 Slope without relict joints

- (a) Circular failure surface
- (b) Non circular failure surface

4.4.2.2 Slope with relict joints

- (a) Circular failure surface
- (b) Non circular failure surface

4.4 Results of slope stability Analysis

Infiltration analysis indicated that, the negative pore water pressure becomes zero or just positive near the surface level. This shear strength reduction caused by this process have adverse effects on the stability of slope. The influence on strength parameters can be expressed by,

$$\tau_f = c' + (\sigma_n - u_a) \tan \phi' + (u_a - u_w) \tan \phi^b \quad \text{Eq(25)}$$

With the diminishing of matric suction;

$$(u_a - u_w) \rightarrow 0$$

Therefore the shear strength is reduced. The factor of safety (F) is defined as;

$$F = \frac{\tau_f}{\tau_m} \quad \text{Eq(26)}$$

The SLOPE/W Software conducts the stability analysis incorporating the above changes.

4.4.1. Slope without any surface drainage improvement

4.4.1.1 Slope without Relict joints

(a) Slope without Relict joints -Analysis of circular failure surfaces

The critical failure surfaces corresponding to each day are presented from Figure 4.18 to Figure 4.23 and minimum factor of safety values obtained through the analysis are presented in Table 4.3. The potential failure surfaces considered are only circular and is done through the grid and radius approach.

Table 4.3: Minimum Factor of Safety for Circular slip surfaces – Without relict joints

Peak rainfall from Bombuwawa and Beddagama Rg	FOS
Initial	1.185
1 st day	1.182
2 nd day	1.164
3 rd day	1.121
4 th day	1.087
5 th day	1.057

At the beginning of the rainfall (day1), the slope had a safety margin of 1.185 which was quite stable. But with the progression of rainfall the matric suction has been destroyed decreasing the shear strength and reducing the safety margin.

Thus the slope is gradually moving towards instability and factor of safety is reduced to a value almost equal to unity, 1.057 by the fifth (Figure 4.23) day indicating closeness to failure. However, the shape of the critical slip surface corresponding to this stage is quite different to the observed failure. The upward movement of the ground water table and development of a slight perched water table could be identified when the series of figures are compared.

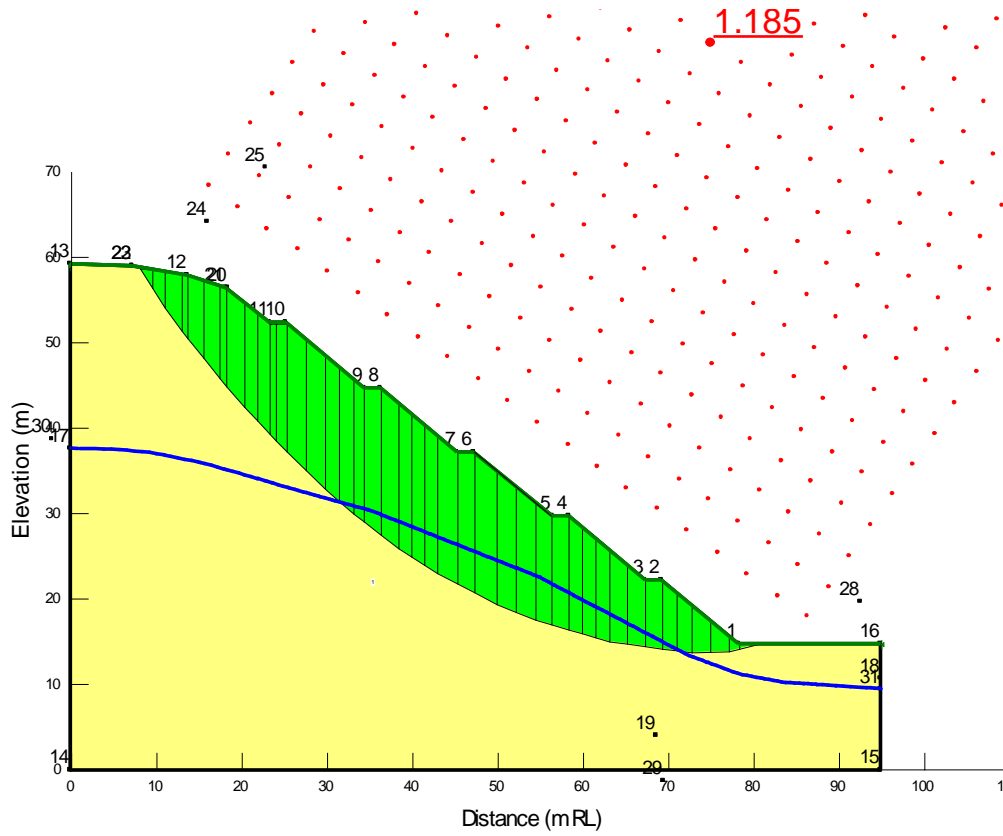


Figure 4.18: Slope stability analysis of the initial day

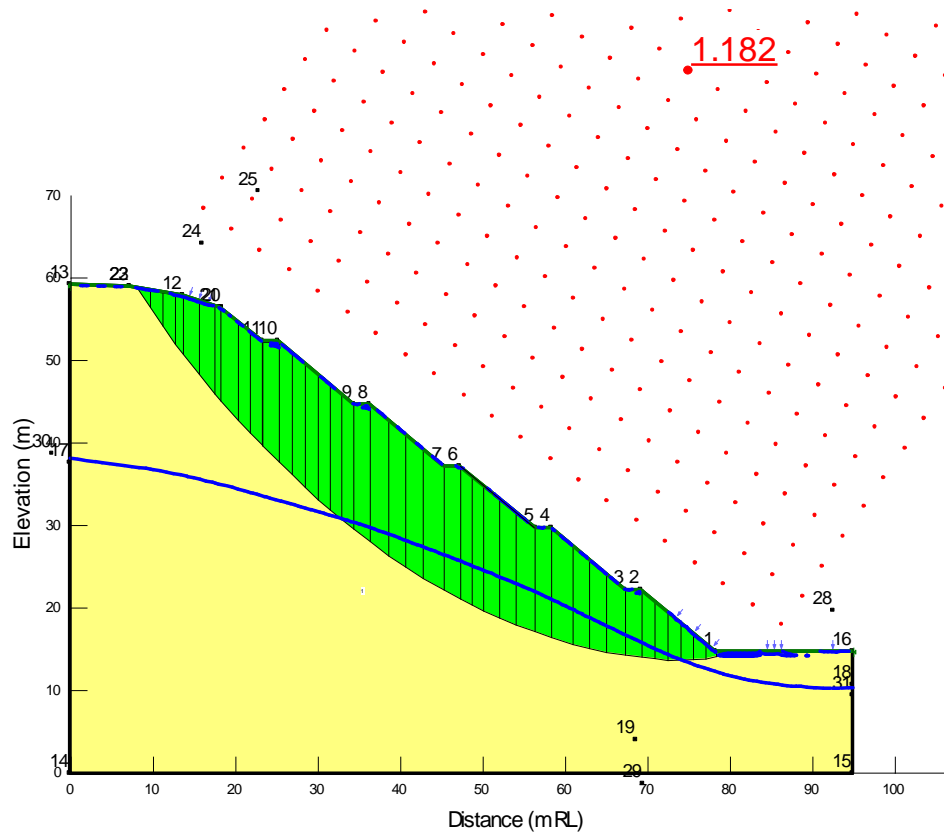


Figure 4.19: Slope stability analysis of the 1st day

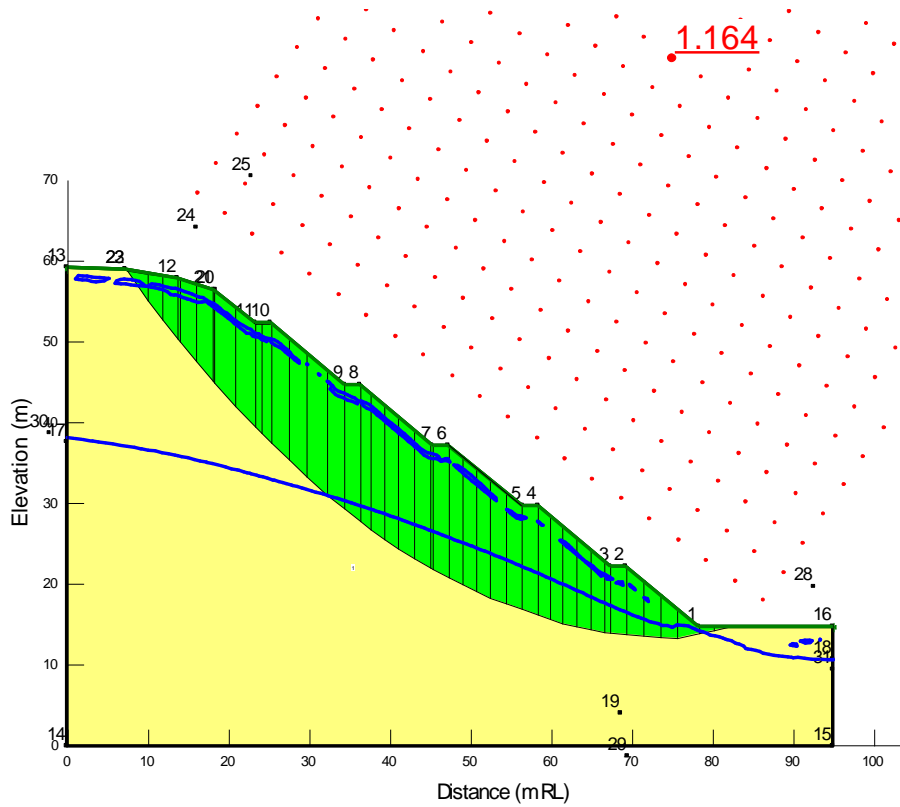


Figure 4.20: Slope stability analysis of the 2nd day

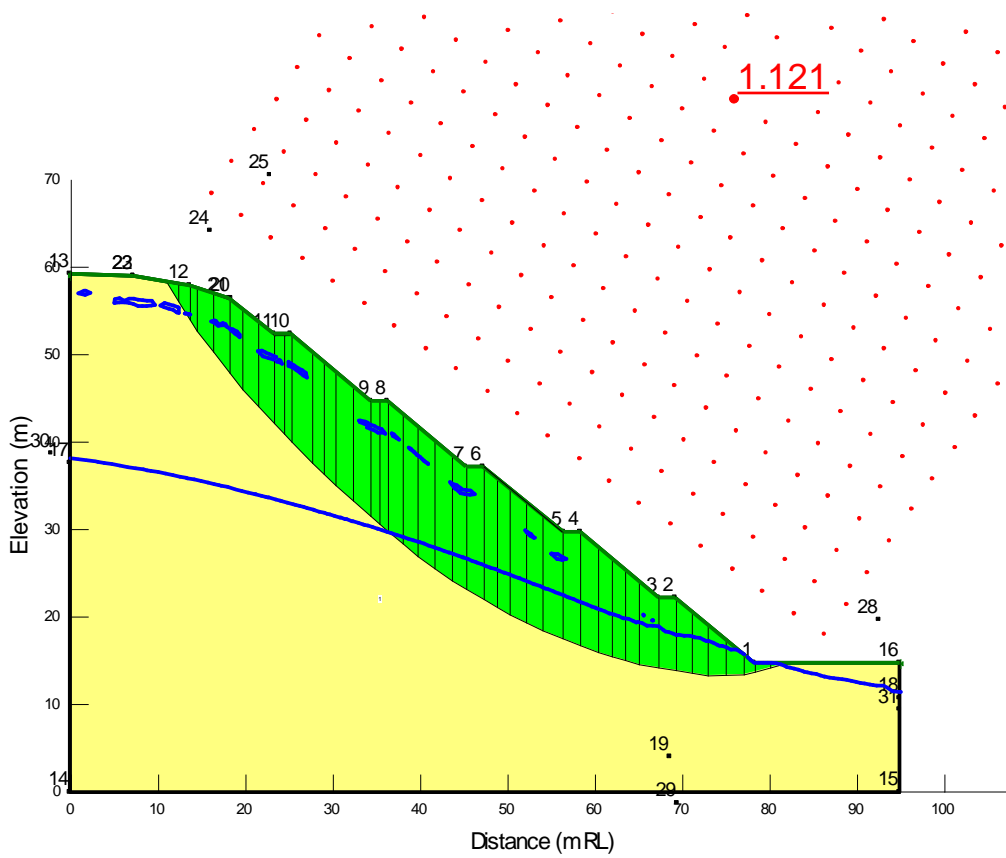


Figure 4.21: Slope stability analysis of the 3rd day

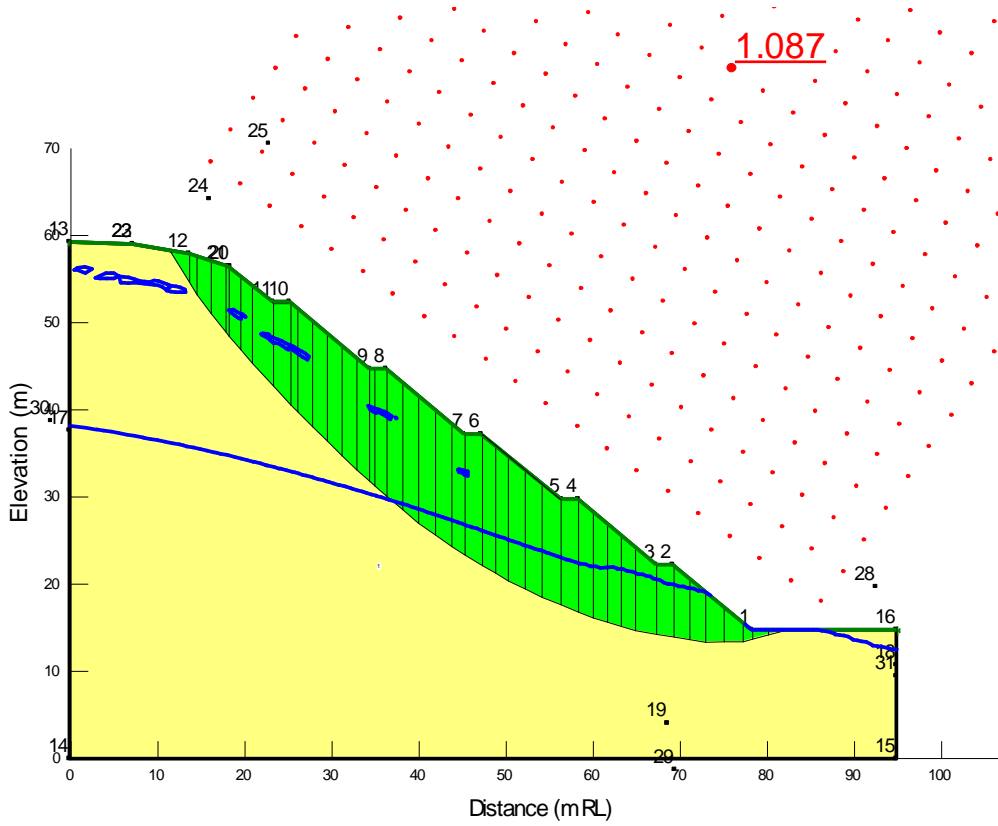


Figure 4.22: Slope stability analysis of the 4th day

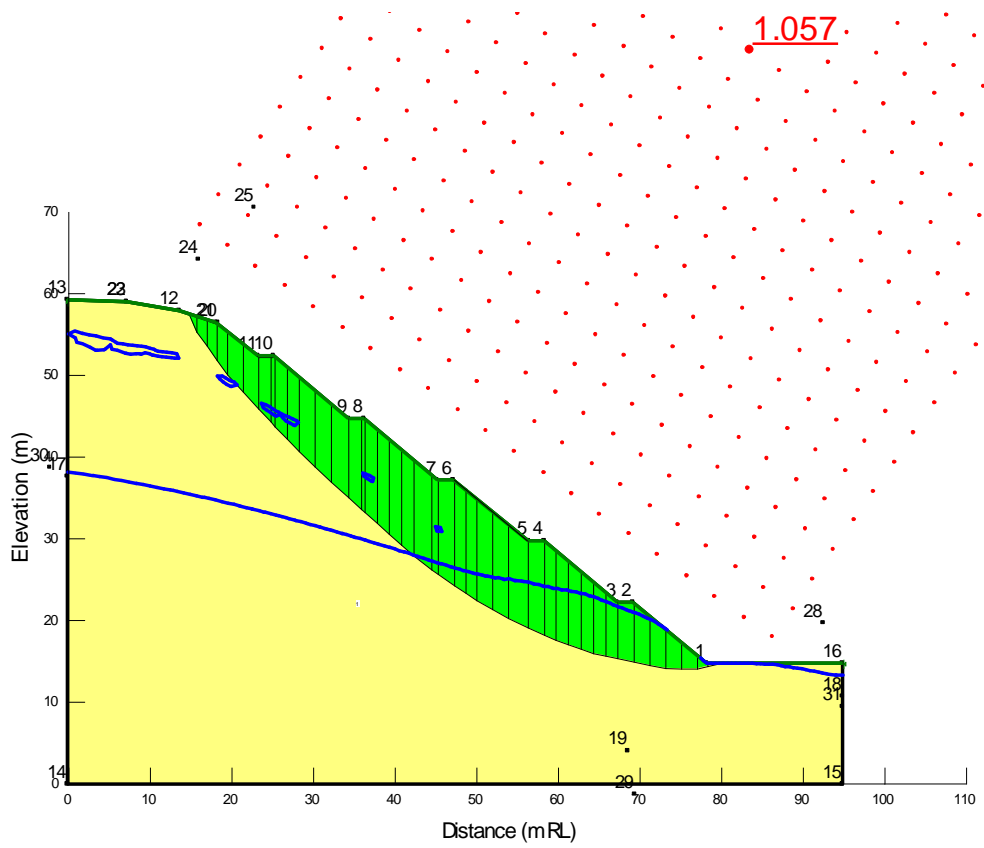


Figure 4.23: Slope stability analysis of the 5th day

(b) Slope without Relict joints – Analysis of Non-Circular slip surfaces

The preceding analysis restricted the instability to only through circular mode of failure. However with uneven infiltration non circular failure modes are quite possible. As such, by the block specified approach the potential non circular failure surfaces also were considered thereafter.

The critical failure surfaces corresponding to each day are presented from Figure 4.24 to Figure 4.29 and minimum factor of safety values obtained through the analysis are presented in Table 5.4.

Table 4.4: Minimum Factor of Safety for non-circular slip surfaces – without relict joints

Peak rainfall from Bombuwawa and Beddagama Rg	FOS
Initial	1.257
1 st day	1.251
2 nd day	1.247
3 rd day	1.185
4 th day	0.992
5 th day	0.934

The factor of safety values obtained for the early staged of the rainfall are slightly larger than for the corresponding stages of circular failure surface analysis. But on the 4th and 5th day the values are much smaller compared to the circular failure surface analysis. On the 4th and 5th day the FOS values are lower than unity indicating the slope should have failed. However, the failure take place only on the 5th day. A closer examination of the failure modes on 4th(Figure 4.28) and 5th day (Figure 4.29) indicates this is not feasible kinematically.

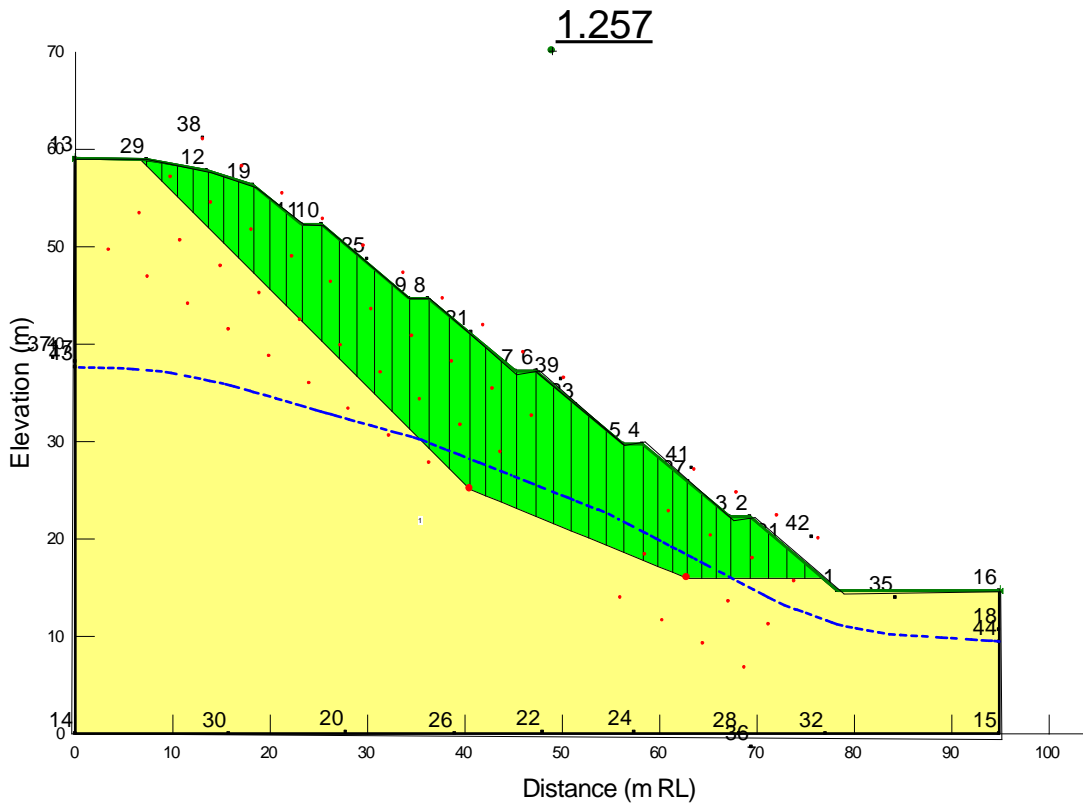


Figure 4.24: Slope stability analysis of the initial day

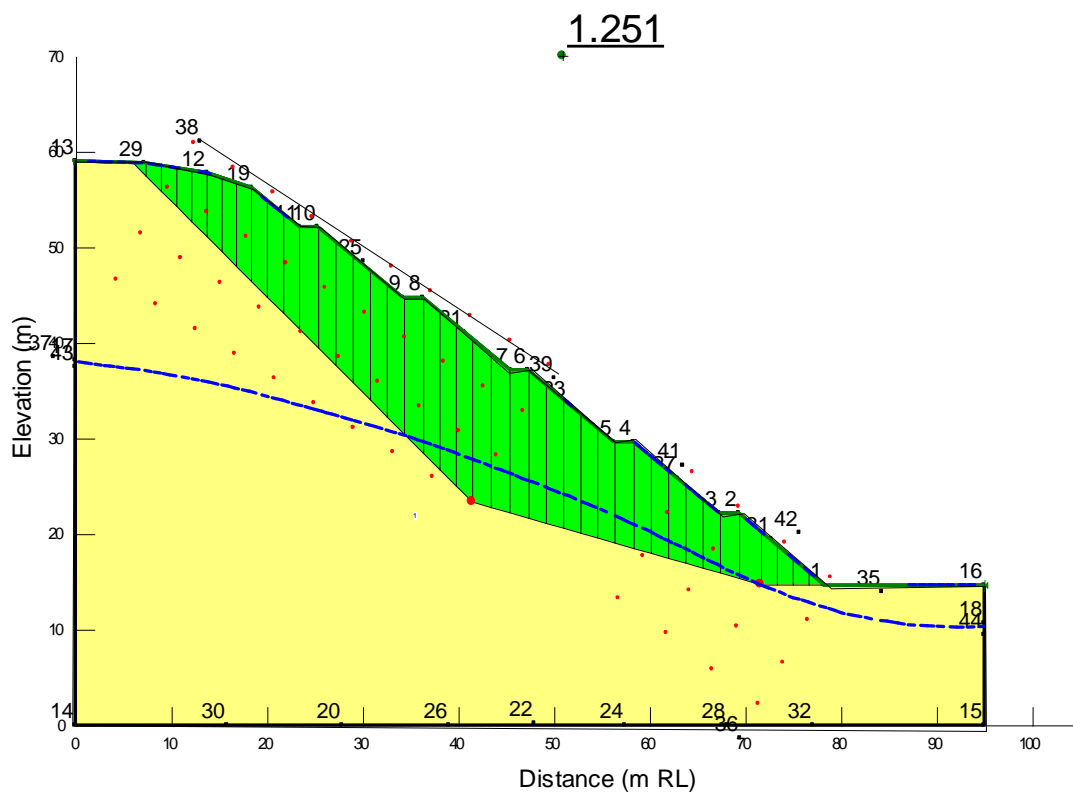


Figure 4.25: Slope stability analysis of the 1st day

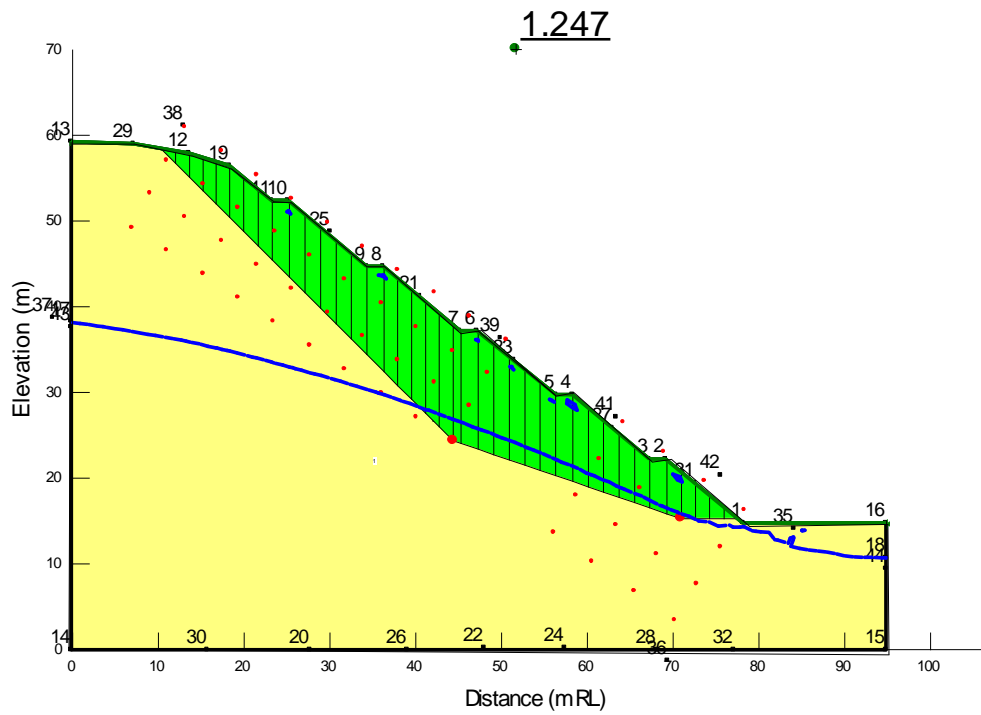


Figure 4.26: Slope stability analysis of the 2nd day

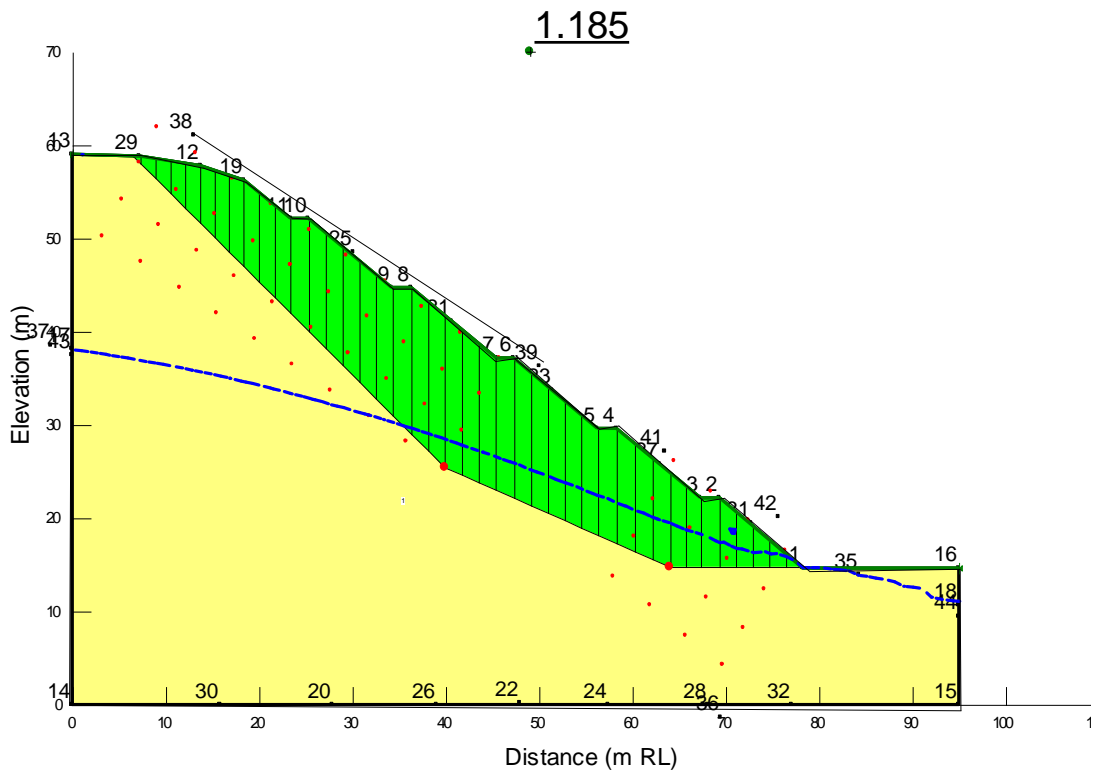


Figure 4.27: Slope stability analysis of the 3rd day

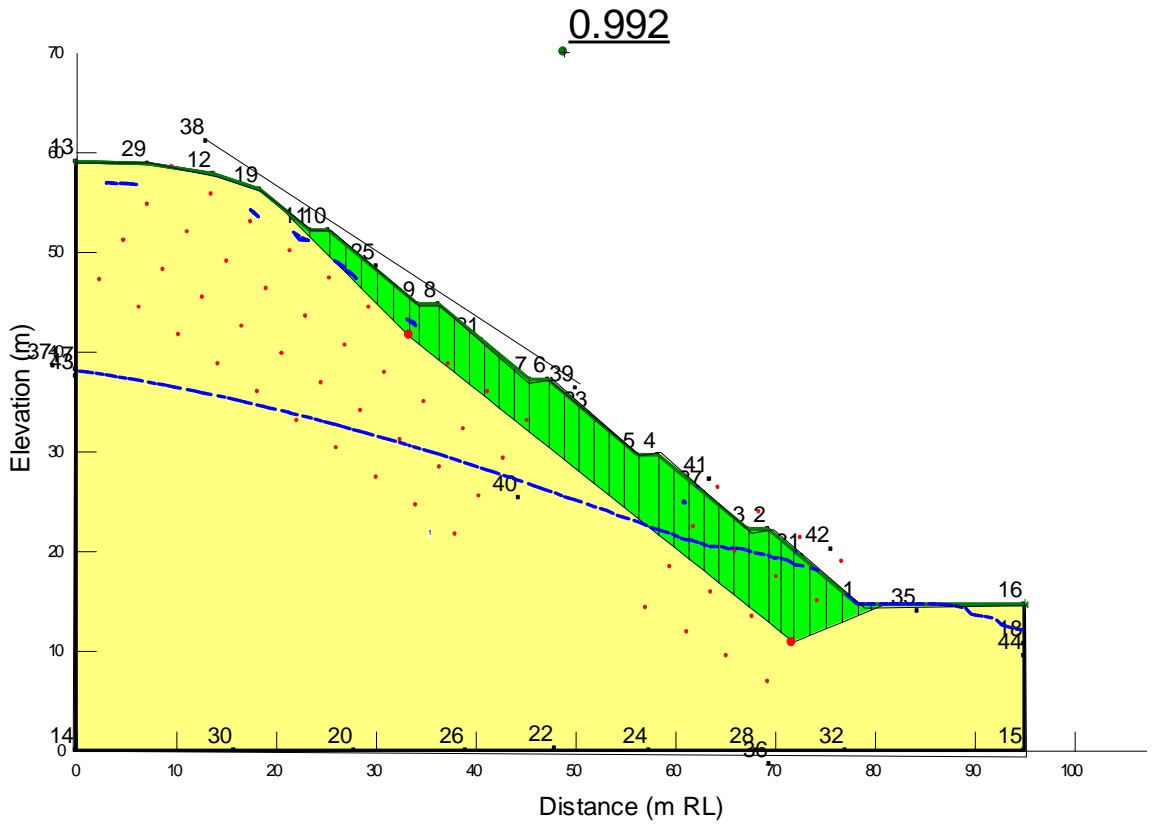


Figure 4.28: Slope stability analysis of the 4th day

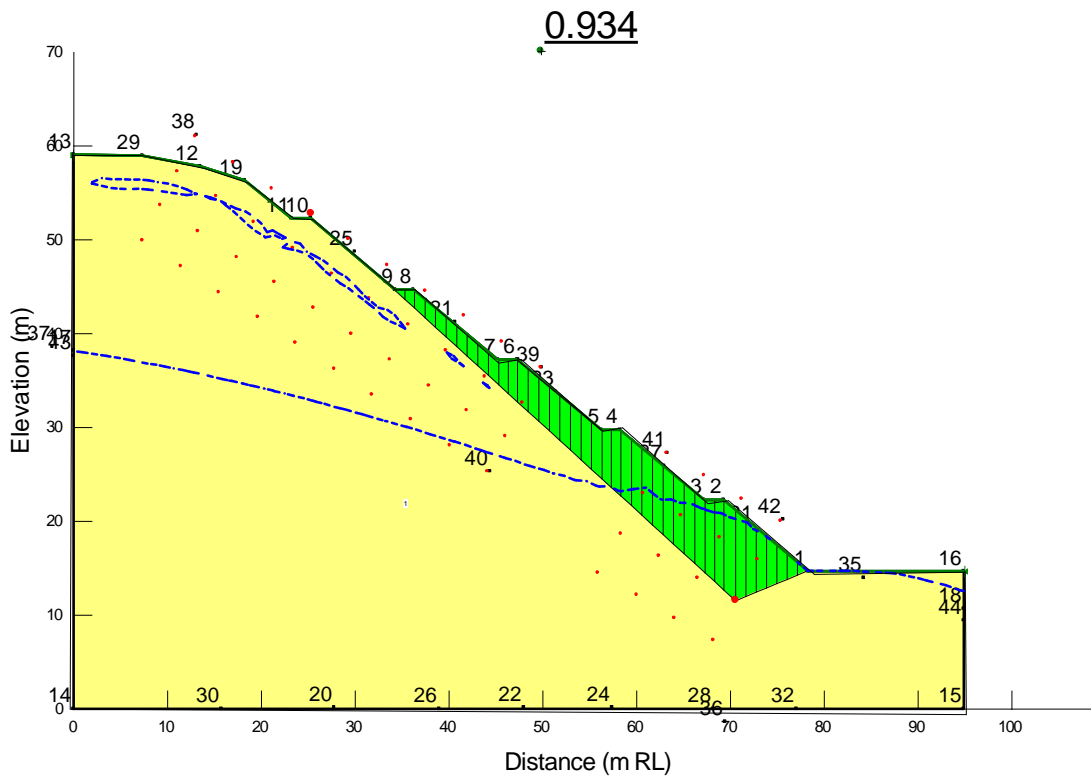


Figure 4.29: Slope stability analysis of the 5th day

4.4.1.2. Slope with Relict joints

(a) Slope with Relict joints – Analysis of Circular slip surfaces

Thereafter, the slope stability analysis was conducted accounting for the presence of relict joints. The pore water pressures obtained from the infiltration analysis done with relict joints' being present is used for this stability analysis. Critical failure surfaces are presented in Figure 4.30 to Figures 4.35. Factor of safety values obtained through the analysis are presented in Table 4.5. The system of relict joints considered is also represented in the Figures.

Table 4.5: Minimum Factor of Safety for Circular slip surfaces – With Relict joints

Peak rainfall from Bombuwawa and Beddagama Rg	FOS
Initial	1.176
1 st day	1.151
2 nd day	1.113
3 rd day	1.070
4 th day	1.033
5 th day	0.989

The comparison of the factor of safety values with the case without relict joints indicate that at each day FOS for the case with relict joints is slightly lower than the case without relict joints at the corresponding time.

The infiltration analysis performed earlier indicated that the destruction of matric suction and/or increase of positive pore water pressure is more significant when relict joints are present. The FOS approached unity (1.033) by the 4th day (Figure 4.34) and went below unity slightly on 5th day. The actual failure was seen on the 5th day. The critical failure surface with FOS greater than unity on earlier days are quite deep. The failure surface on the 5th day is much shallower and corresponds closely with the observed failure surface (Figure 4.35).

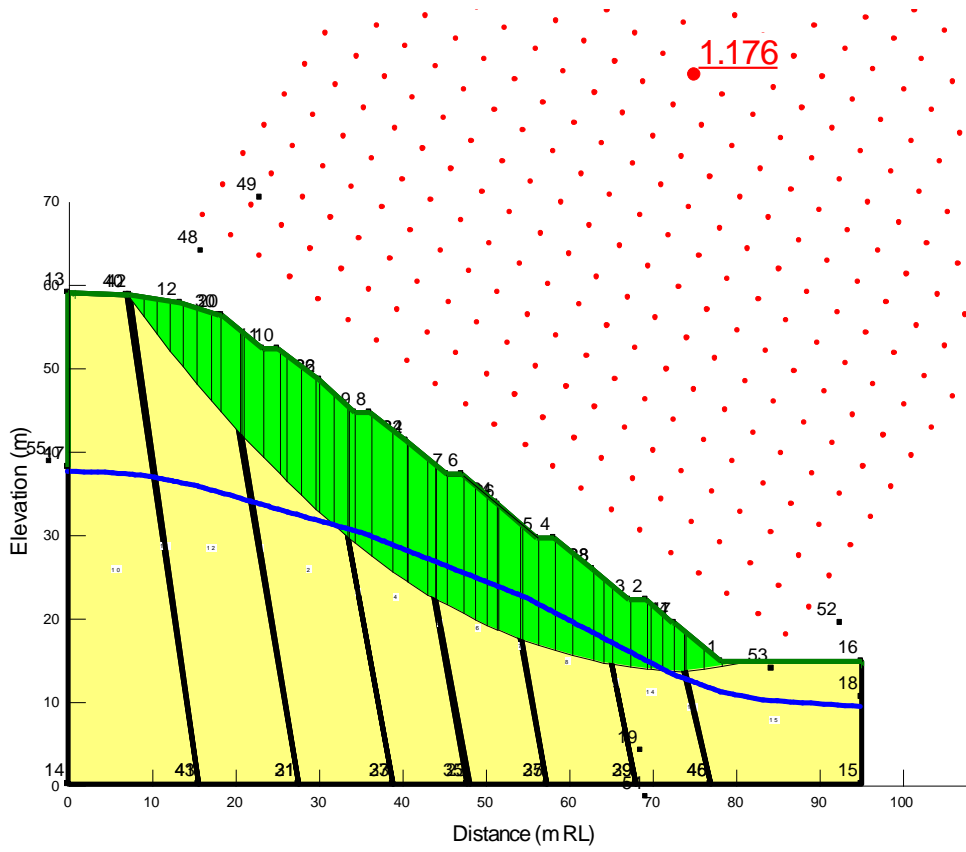


Figure 4.30: Slope stability analysis of the initial day

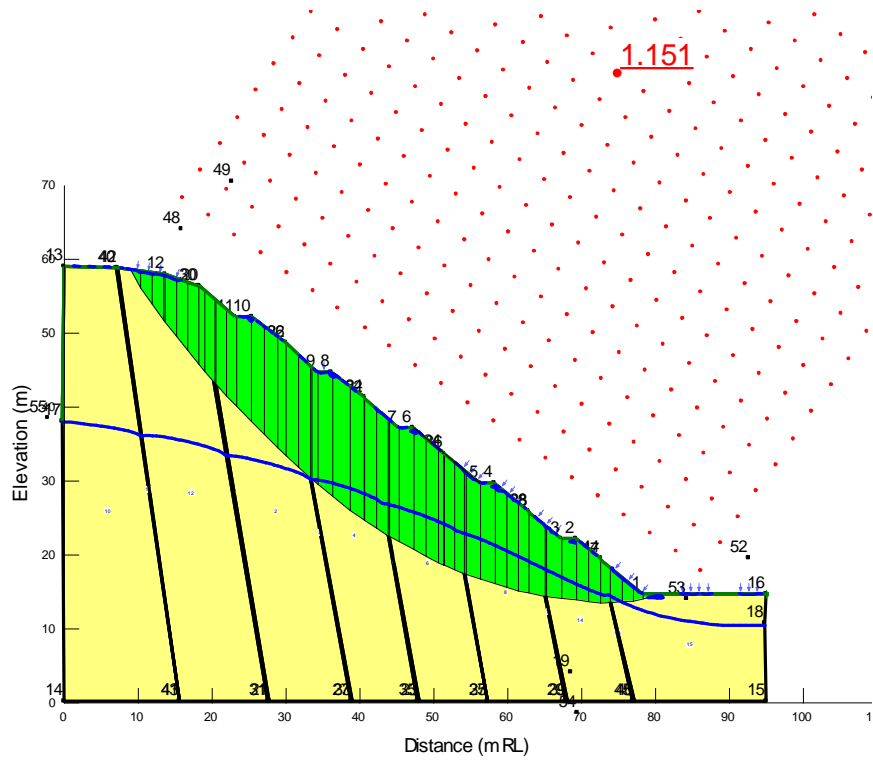


Figure 4.31: Slope stability analysis of the 1st day

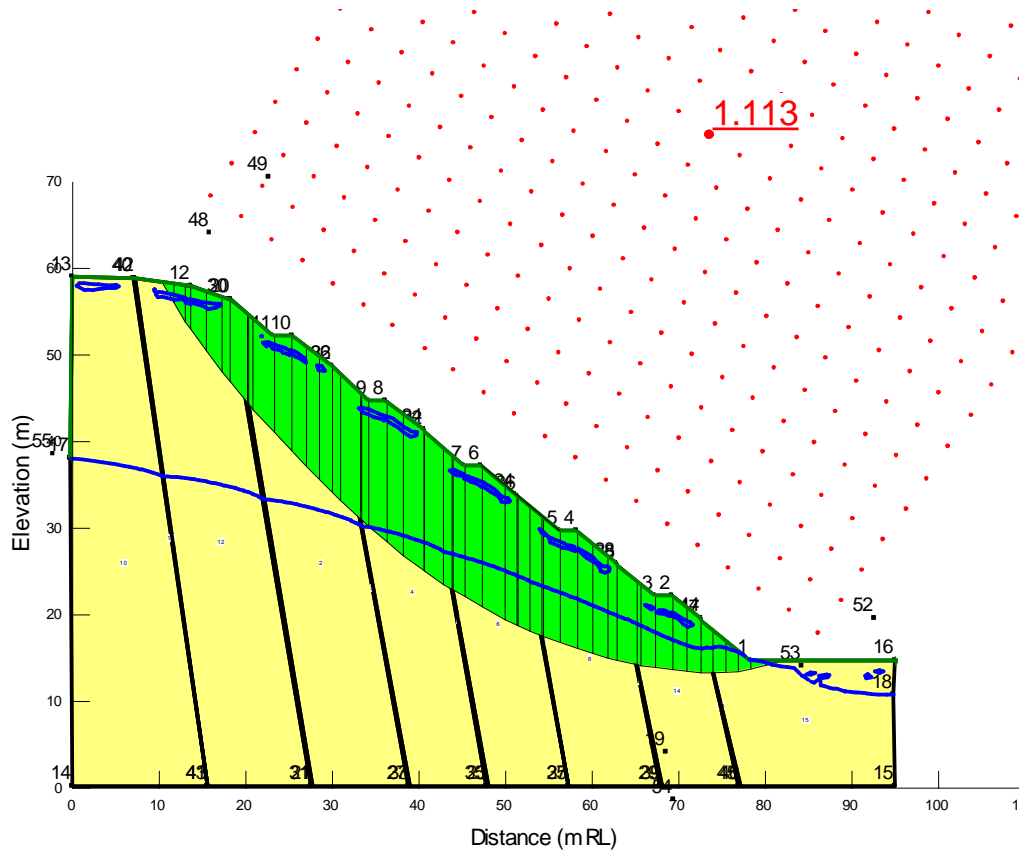


Figure 4.32: Slope stability analysis of the 2nd day

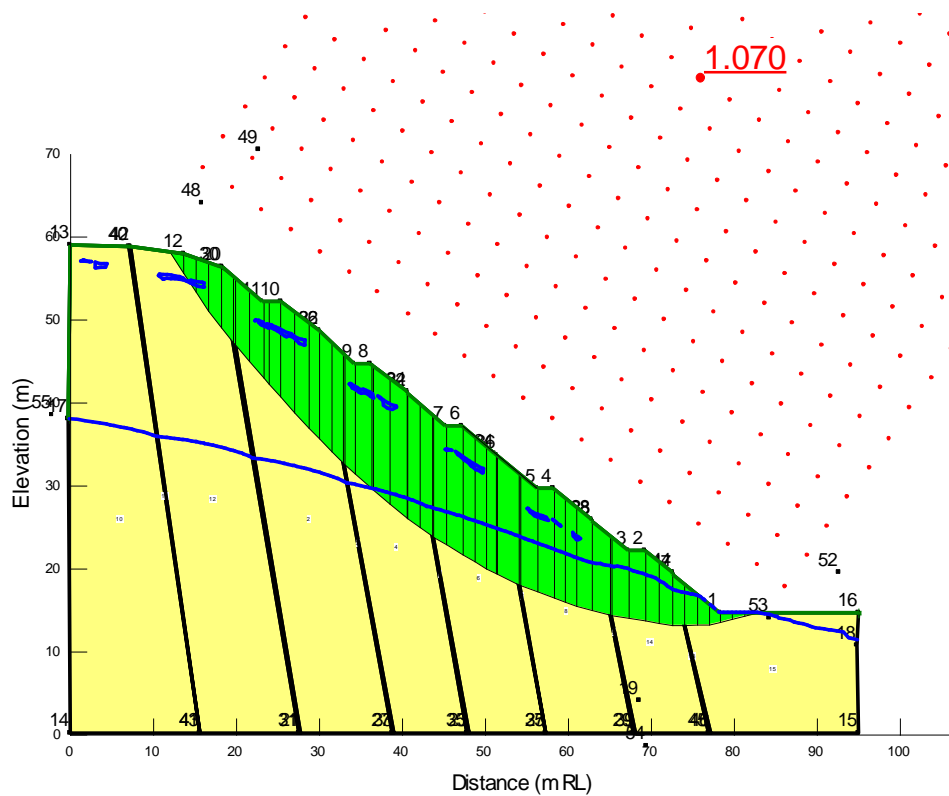


Figure 4.33: Slope stability analysis of the 3rd day

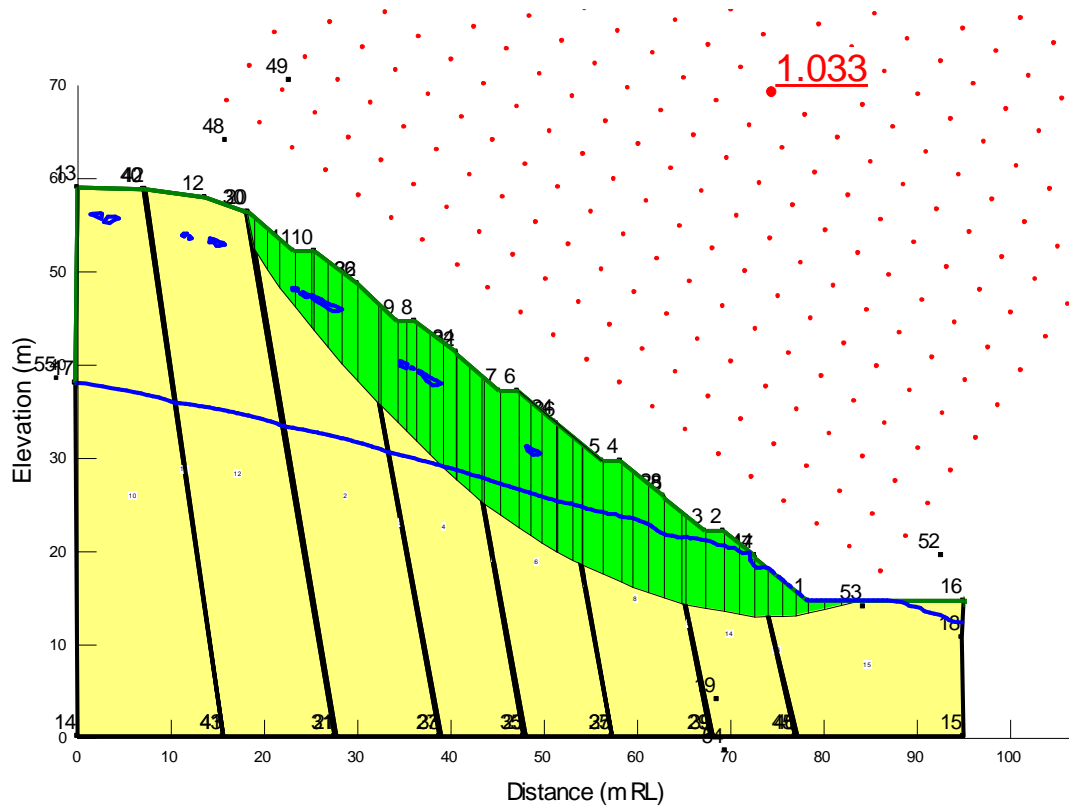


Figure 4.34: Slope stability analysis of the 4th day

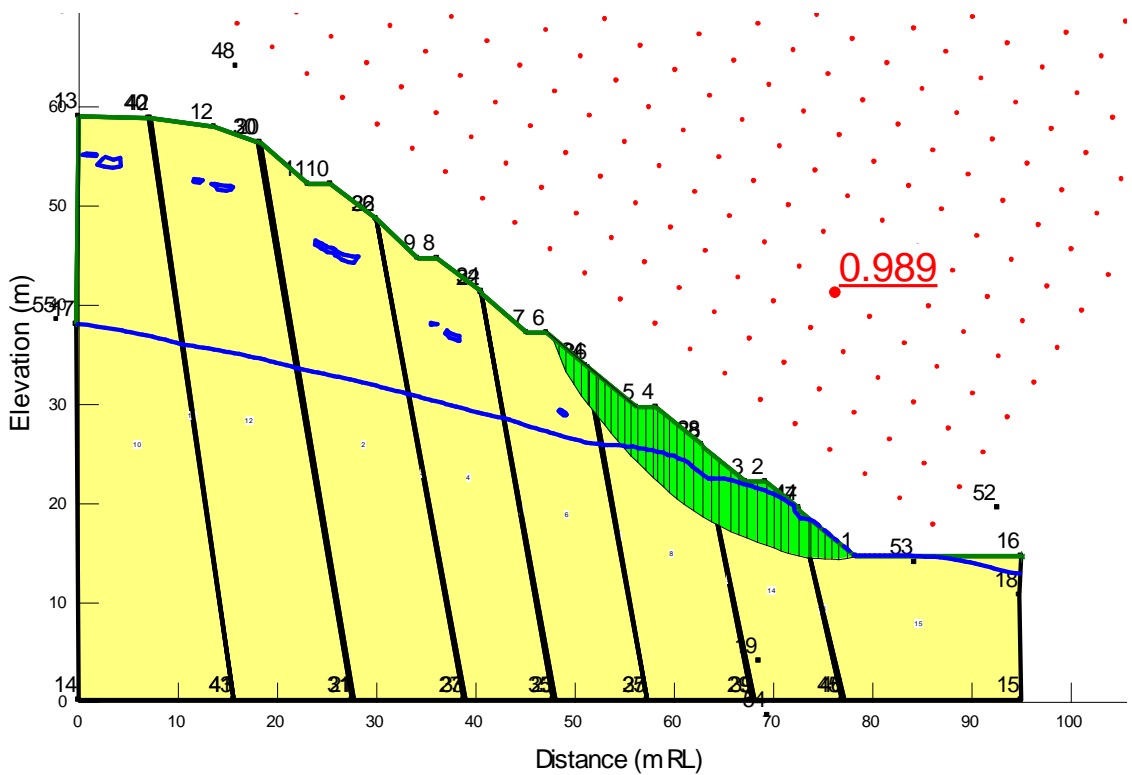


Figure 4.35: Slope stability analysis of the 5th day

The analysis closely simulates the actual event of failure at the site. Actual failure occurred at 42+340 to 42+400 in Walipanna at southern expressway has length of around 50 m along the road and extends over a height of around 20 m. Berm drains at three levels and a cascade drain were damaged by the slope failure. The failure surface is quite shallow.

On the 5th day of this analysis where the safety margin is lower than unity, failure surface has height of 22m and berm drains at three levels were failed.

(b) Slope with Relict joints – Analysis of Non -Circular slip surfaces

The pore water pressure changes obtained from the infiltration analysis done under the present of relict joints was thereafter used to analyse the instability through potential non circular failure surfaces. The results of the analysis are presented in Figure 4.36 to 4.41 and minimum factor of safety values obtained through the analysis are presented in Table 4.6.

Table 4.6: Minimum Factor of Safety for Non Circular slip surfaces – With Relict joints

Peak rainfall from Bombuwawa and Beddagama Rg	FOS
Initial	1.249
1 st day	1.246
2 nd day	1.209
3 rd day	1.115
4 th day	0.946
5 th day	0.828

The factor of safety values obtained for the early staged of the rainfall are slightly larger than to the corresponding stages of circular failure surface analysis. But on the 4th and 5th day the values are much smaller compared to the circular failure surface analysis. On the 4th and 5th day (Figure 4.40 and Figure 4.41) the FOS values are lower than unity indicating the slope should have failed. However, the failure take place only on the 5th day. A closer examination of the failure modes on 4th and 5th day indicates this is not feasible kinematically.

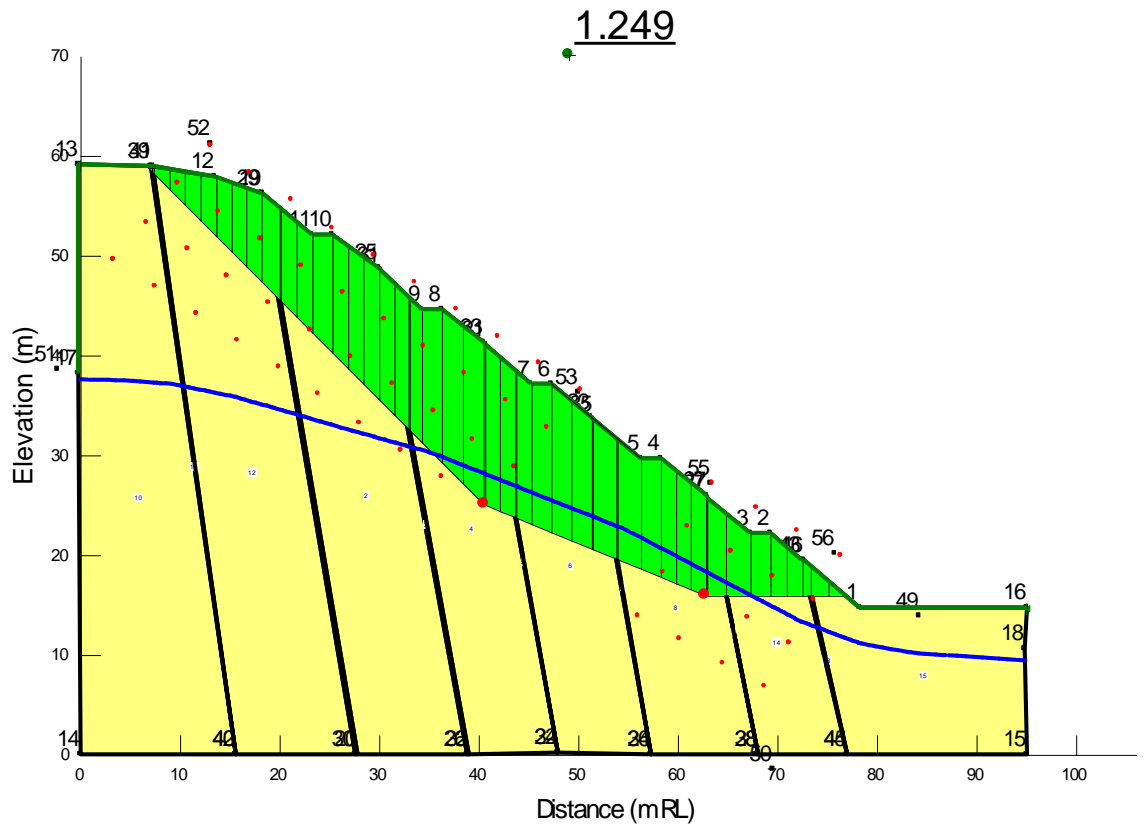


Figure 4.36: Slope stability analysis of the initial day

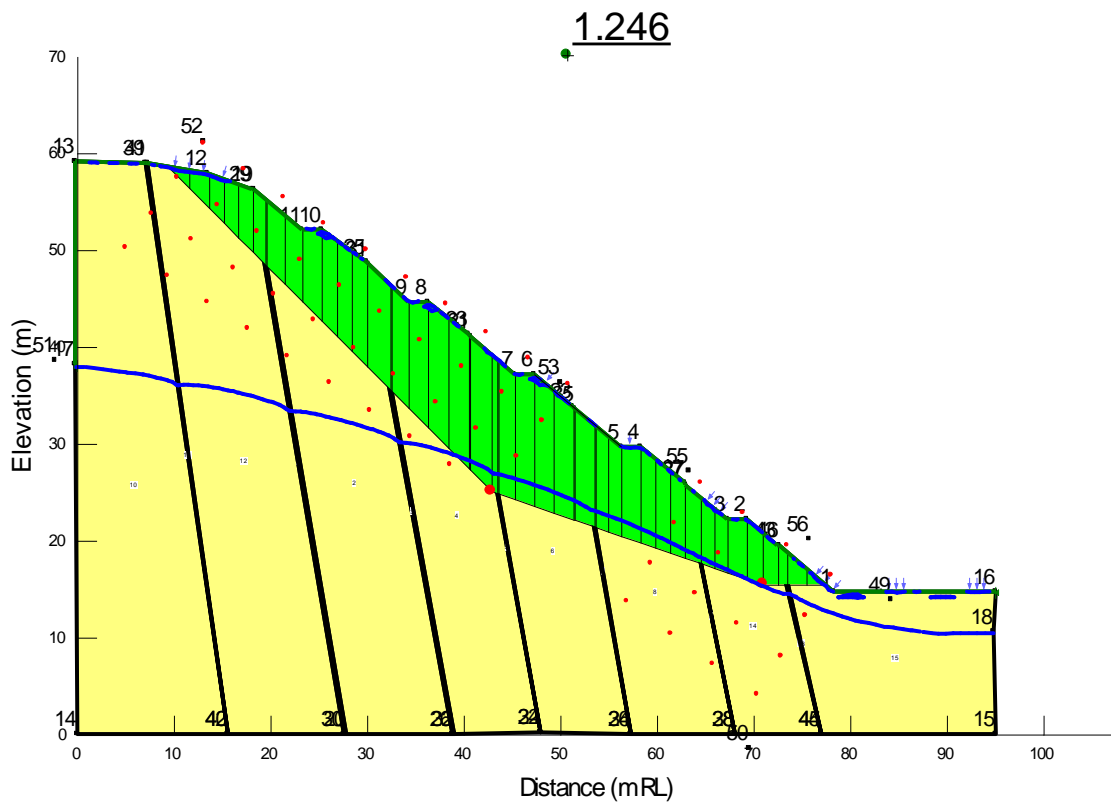


Figure 4.37: Slope stability analysis of the 1st day

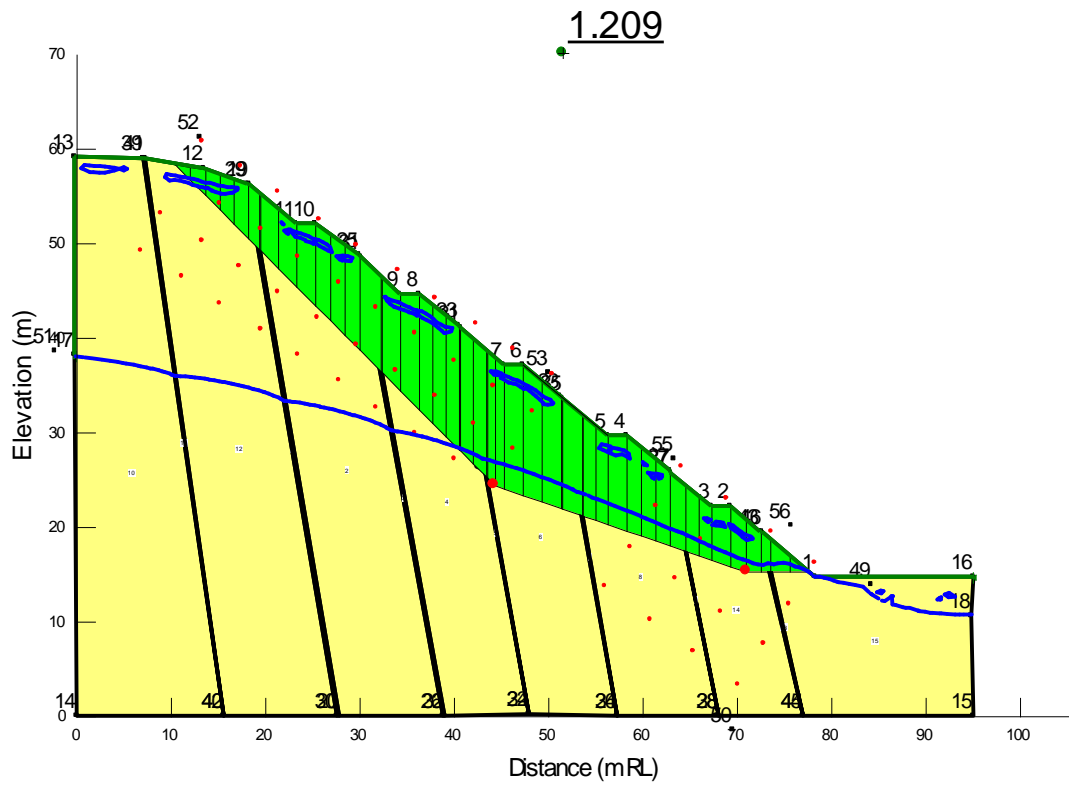


Figure 4.38: Slope stability analysis of the 2nd day

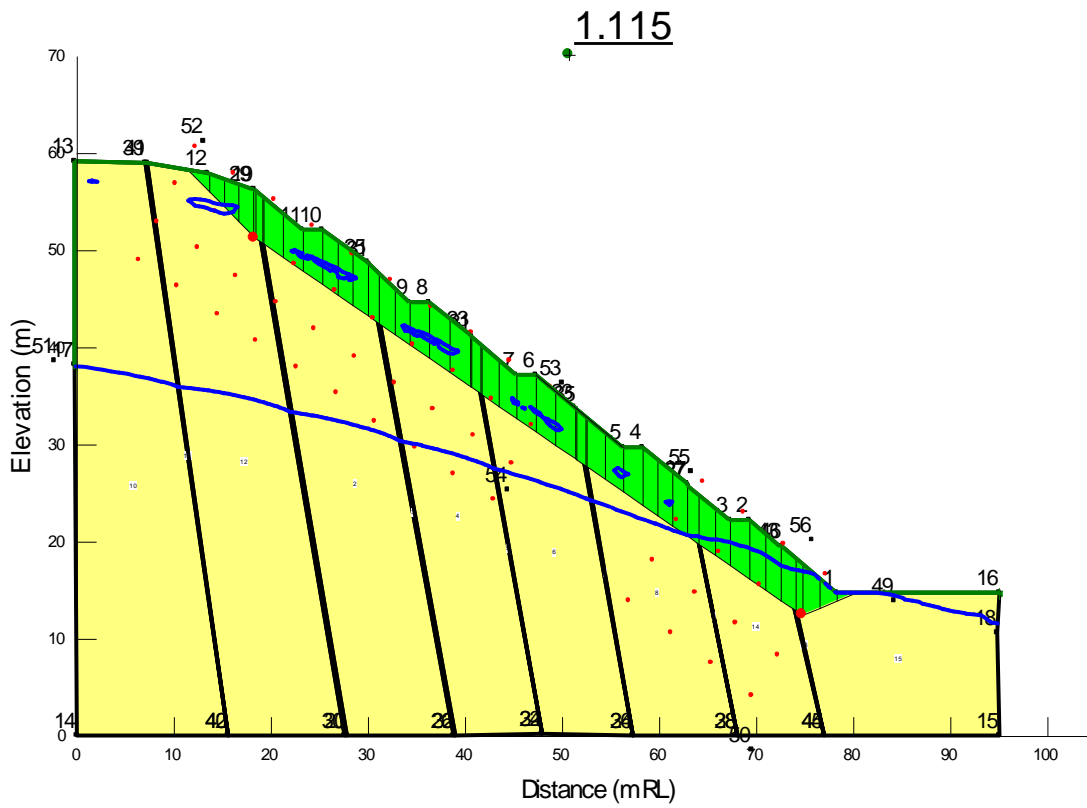


Figure 4.39: Slope stability analysis of the 3rd day

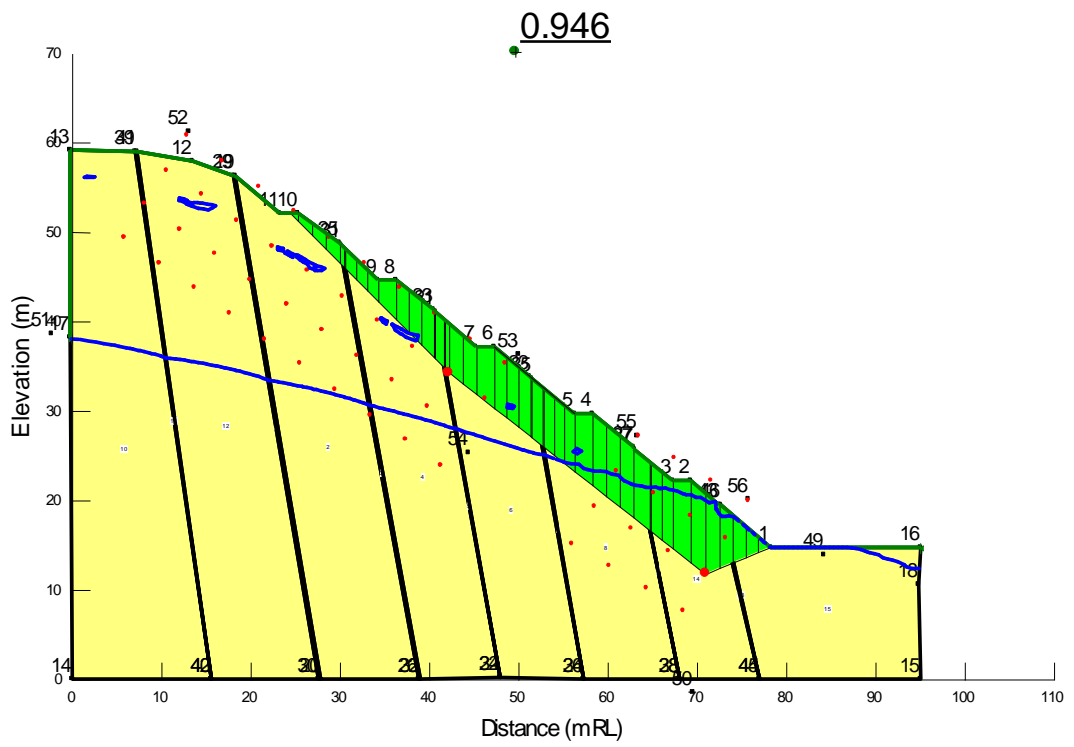


Figure 4.40: Slope stability analysis of the 4th day

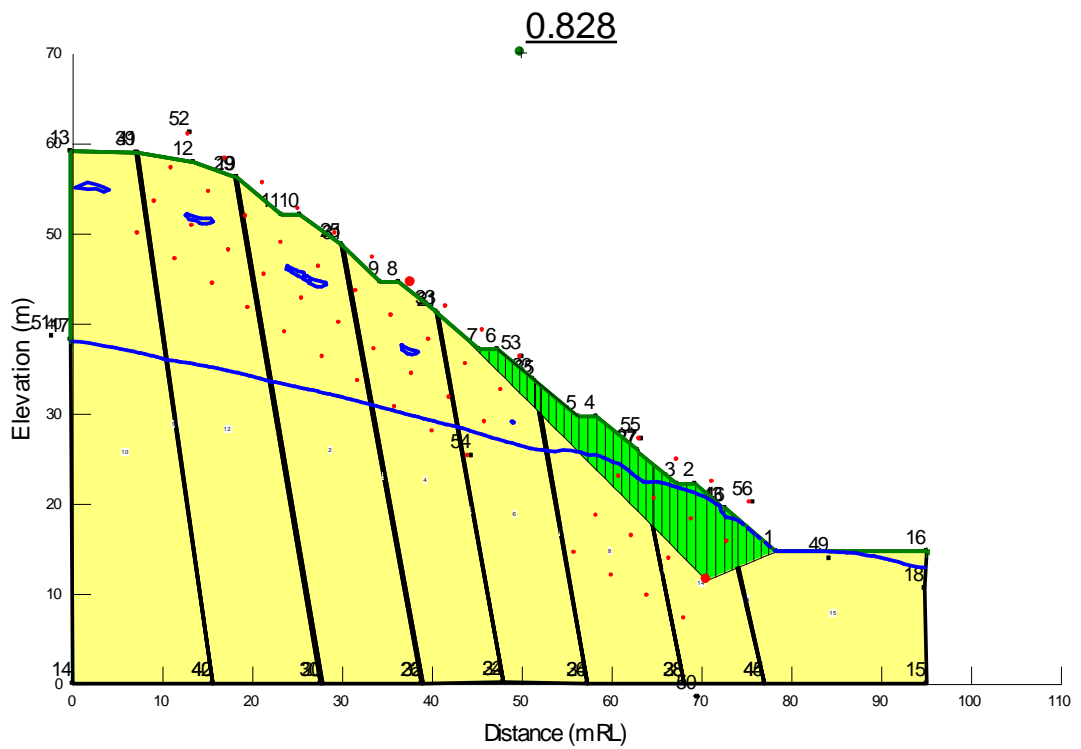


Figure 4.41: Slope stability analysis of the 5th day

4.4.2 Slope with surface drainage improvement

4.4.2.1 Slope without Relict joints

(a) Slope without Relict joints and with surface drainage improvement - Circular failure surfaces

The preceding analysis modeled the infiltration without accounting for the presence of any surface drainage measures such as; berm drains, cascade drains or surface protection vegetation. The changes to the pore water pressure regime thus obtained was incorporated in the stability analysis conducted thereafter. The analyses were done for the two possible cases; without relict joints and with relict joints.

In this section the presence of surface drainage measures and erosion protecting vegetation is considered. The changes to the pore water pressure regime computed under these conditions are incorporated into the stability analysis presented in this section.

The critical failure surfaces corresponding to each day, with the surface drainage improvement of berm drains and vegetation cover of 10^{-7} m/s and 10^{-8} m/s permeability are presented. The critical failure surfaces are presented from Figure 4.42 to Figure 4.47 and minimum factor of safety values obtained through the analysis are presented in Table 4.7.

Table 4.7: Minimum Factor of Safety for Circular slip surfaces – Without relict joints – For rainfall recorded at Bombuwawa and Beddegama

Date	FOS	
	Vegetation – Permeability 10^{-7} m/s	Vegetation – Permeability 10^{-8} m/s
Initial	1.203	1.203
1 st day	1.203	1.203
2 nd day	1.190	1.191
3 rd day	1.171	1.178
4 th day	1.145	1.161
5 th day	1.122	1.142

At the beginning of the rainfall event, the slope had a safety margin of 1.201 which implies reasonable stability. The rainfall infiltration is lower compare to the slope without surface drainage improvement as illustrated in section 4.2.3. With more impermeable vegetation covers infiltration is more restricted.

With the improvement of surface drainage, no development of perched water table condition could be identified. The matric suction has been gradually destroyed decreasing the shear strength and factor of safety reduced to a value of 1.122 (Figure 4.47(a)) and 1.142 (Figure 4.47 (b)) for vegetation layer of 10^{-7} m/s permeability and 10^{-8} m/s permeability respectively. It indicated by the fifth day slope is still in a stable condition.

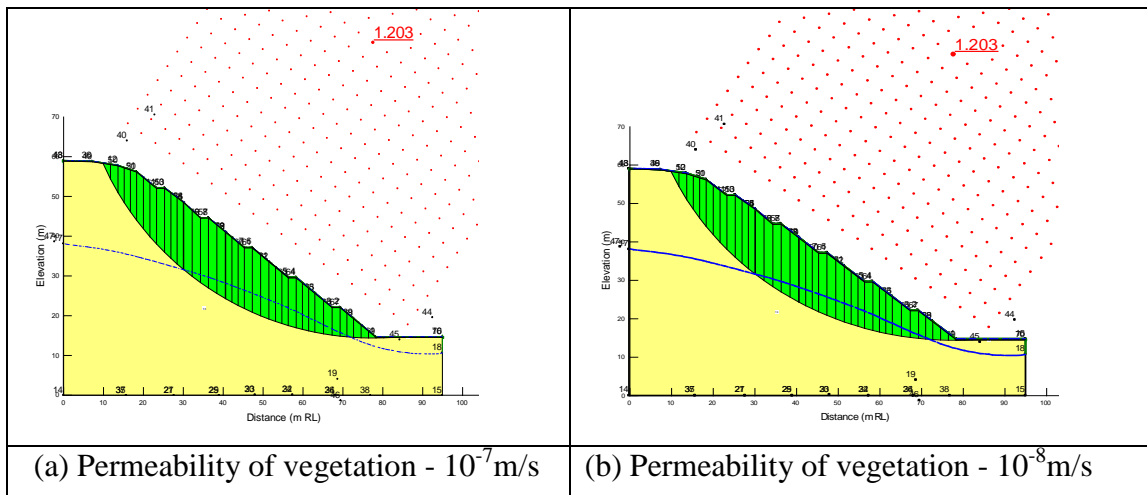


Figure 4.42: Slope stability analysis of the initial day

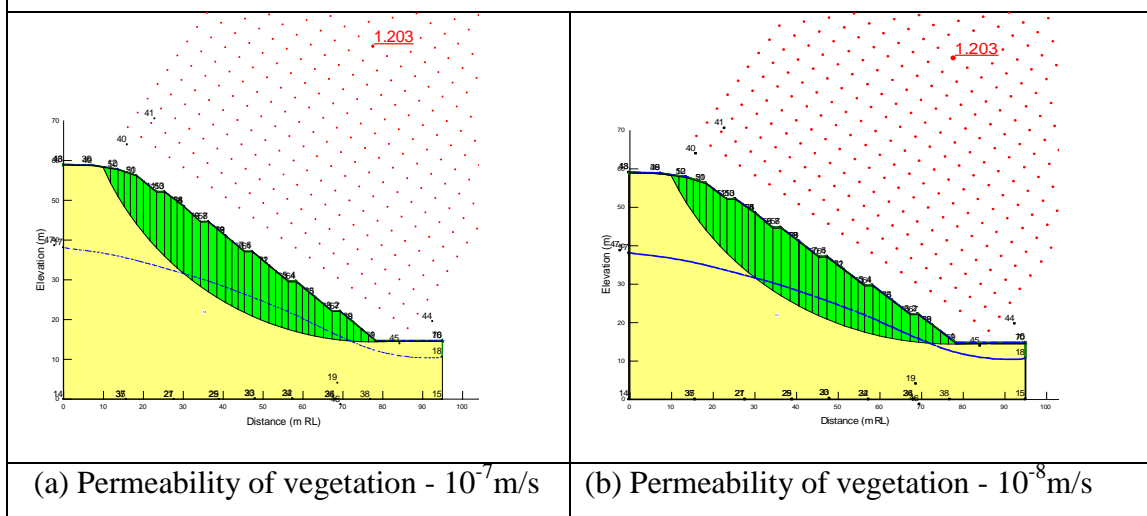
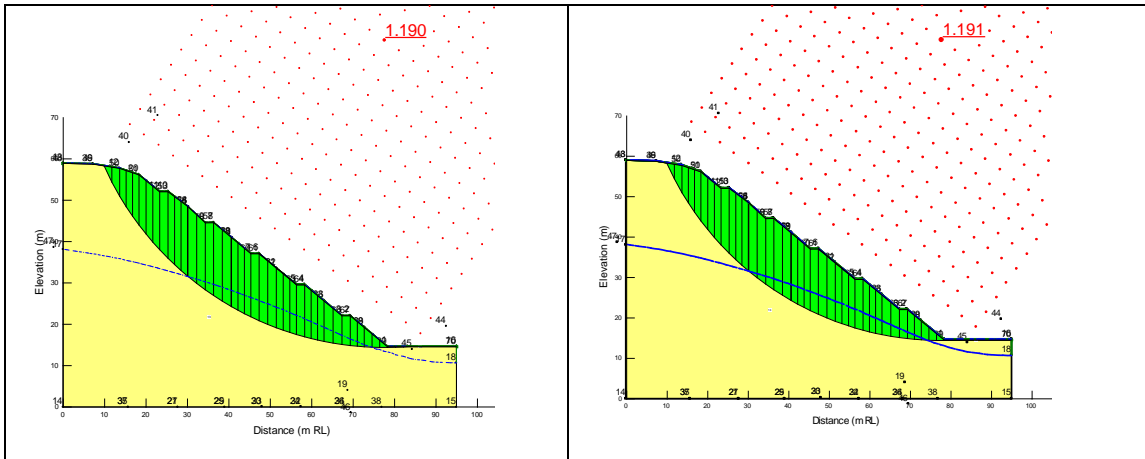


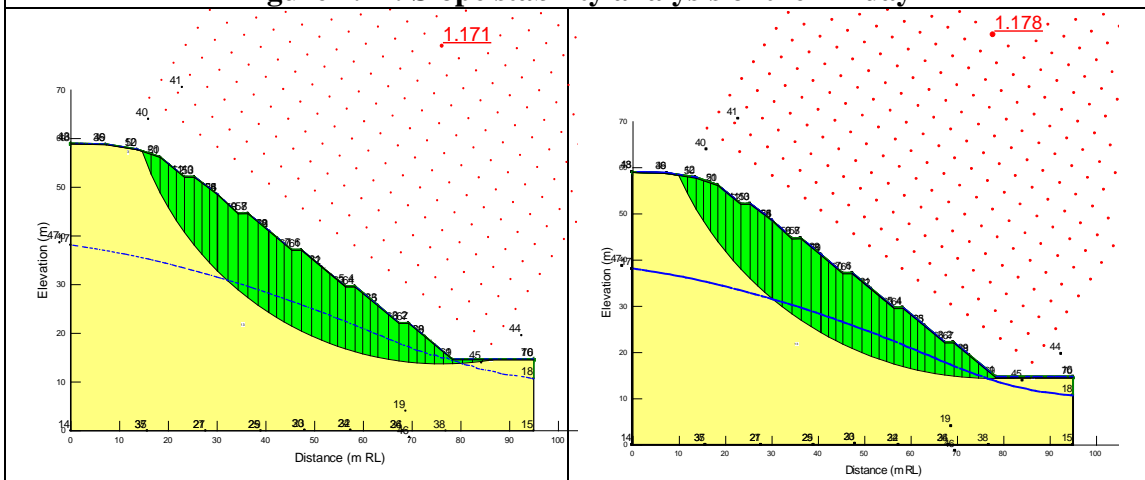
Figure 4.43: Slope stability analysis of the 1st day



(a) Permeability of vegetation - 10^{-7} m/s

(b) Permeability of vegetation - 10^{-8} m/s

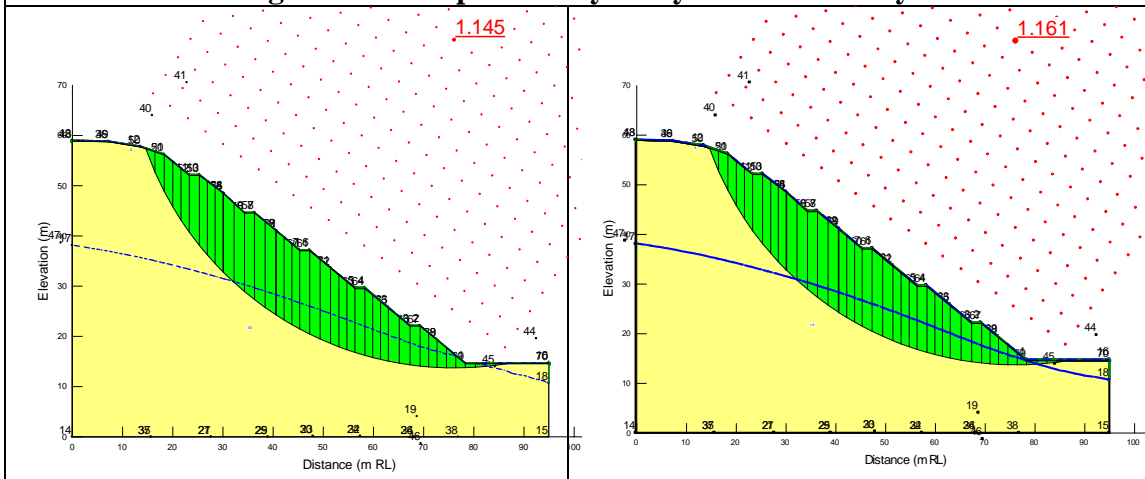
Figure 4.44: Slope stability analysis of the 2nd day



(a) Permeability of vegetation - 10^{-7} m/s

(b) Permeability of vegetation - 10^{-8} m/s

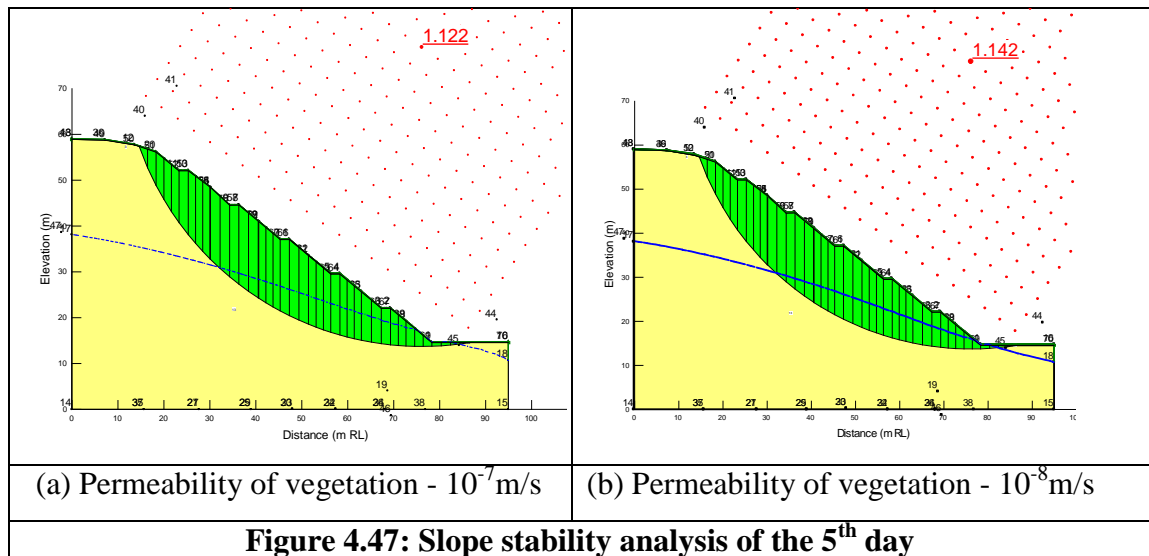
Figure 4.45: Slope stability analysis of the 3rd day



(a) Permeability of vegetation - 10^{-7} m/s

(b) Permeability of vegetation - 10^{-8} m/s

Figure 4.46: Slope stability analysis of the 4th day



(b) Slope without Relict joints and with surface drainage improvement – Non-Circular slip surfaces

The critical failure surfaces corresponding to each day, for non circular slip surfaces with the surface drainage improvement of berm drains and vegetation cover of 10^{-7} m/s and 10^{-8} m/s permeability are analysed. The results are presented from Figure 4.48 to Figure 4.53. Minimum factor of safety values obtained through the analysis are presented in Table 4.8.

Table 4.8: Minimum Factor of Safety for non-circular slip surfaces – without relict joints

Peak rainfall from Bombuwawa and Beddagama Rg	FOS	
	Vegetation Permeability 10^{-7} m/s	Vegetation Permeability 10^{-8} m/s
Initial	1.234	1.234
1 st day	1.229	1.229
2 nd day	1.215	1.216
3 rd day	1.195	1.201
4 th day	1.168	1.183
5 th day	0.989	1.159

With the vegetation cover of permeability 10^{-7} m/s the factor of safety values obtained until the 4th day of the rainfall under non circular condition (Table 4.8) are slightly larger than to the corresponding stages of circular failure surfaces (Table 4.7). But on the 5th day the value is much smaller compared to the circular failure surface and it is lower than the unity indicating the slope should have failed. However, closer examination of the failure modes on 5th day indicates this mode of failure is not feasible kinematically (Figure 4.53).

But with vegetation layers of much lower permeability 10^{-8} m/s the factor of safety values obtained until the 5th day of the rainfall are slightly larger than to the corresponding stages of circular failure surface analysis. It shows in column 2 of Table 4.7 and Table 4.8.

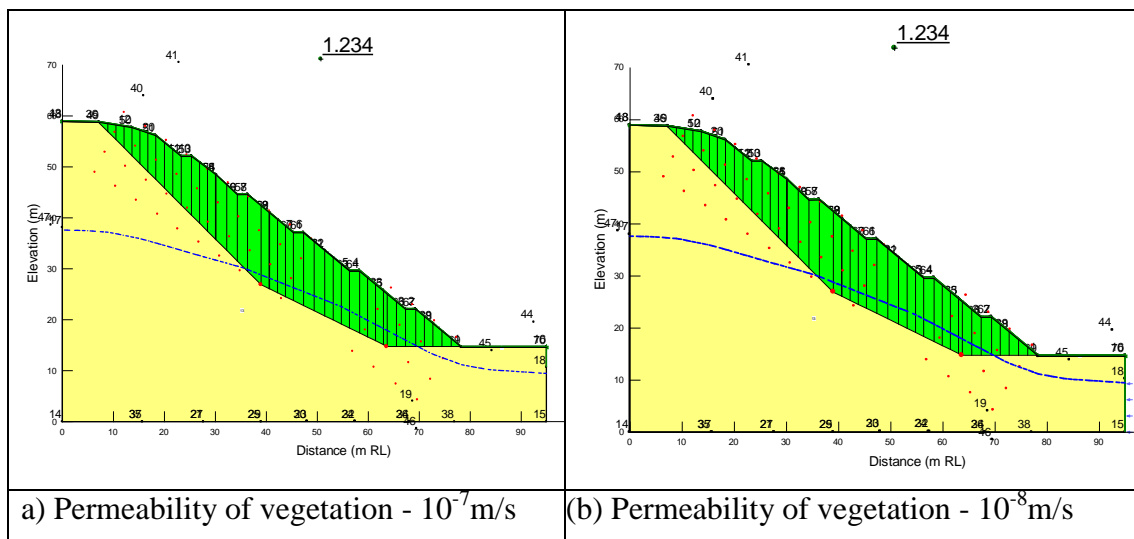


Figure 4.48: Slope stability analysis of the initial day

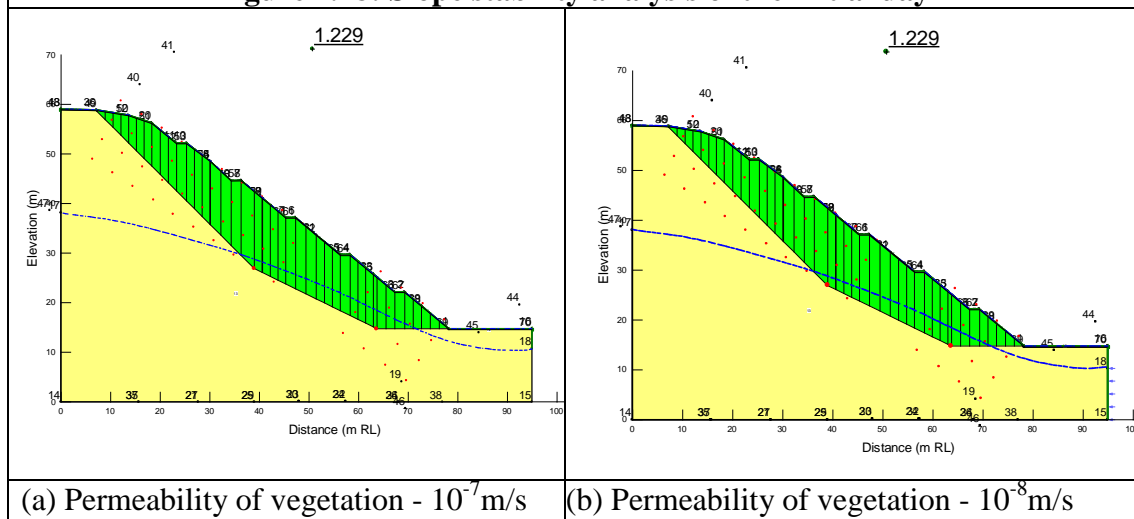


Figure 4.49: Slope stability analysis of the 1st day

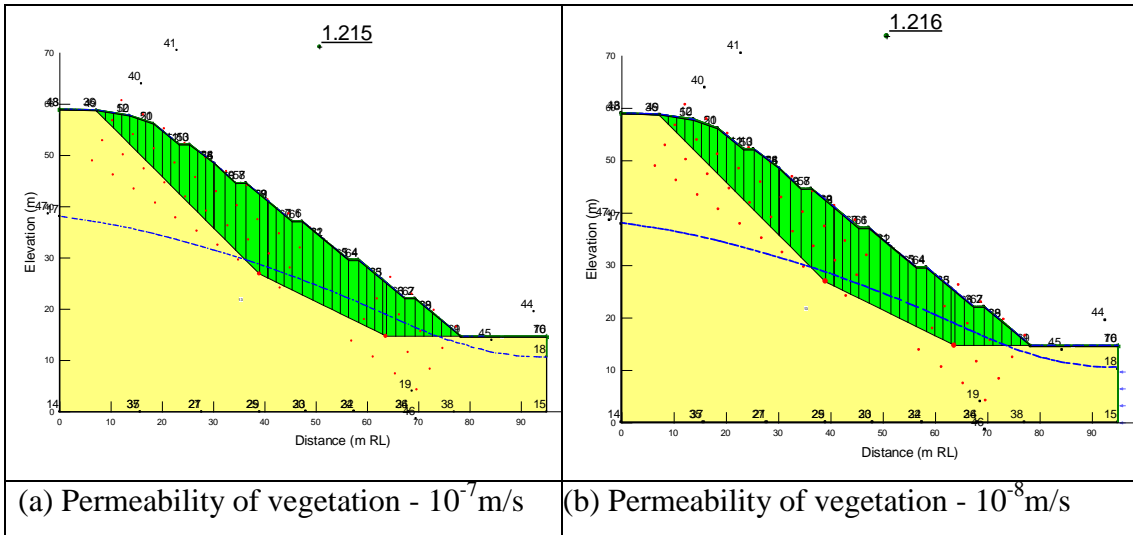


Figure 4.50: Slope stability analysis of the 2nd day

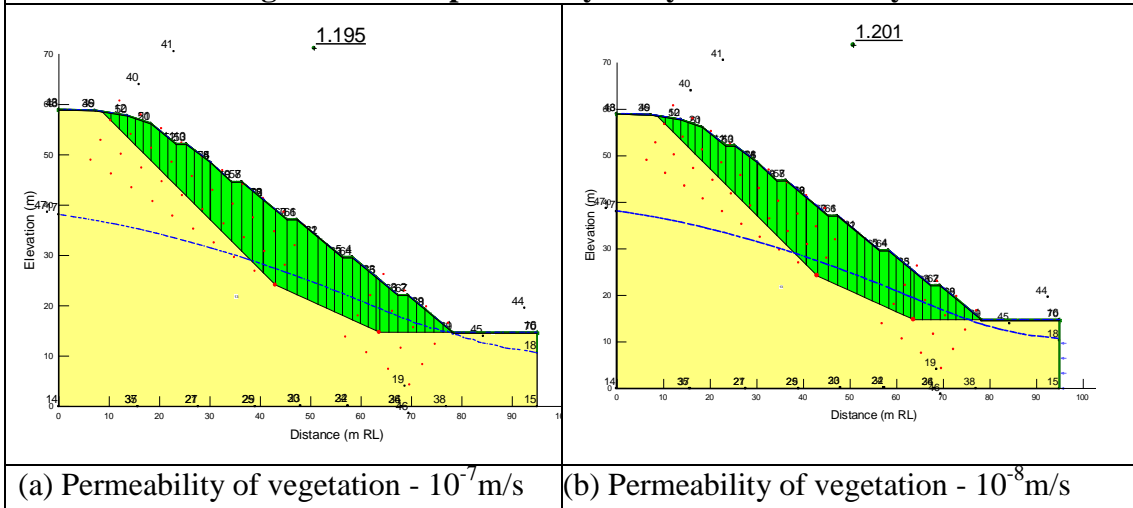


Figure 4.51: Slope stability analysis of the 3rd day

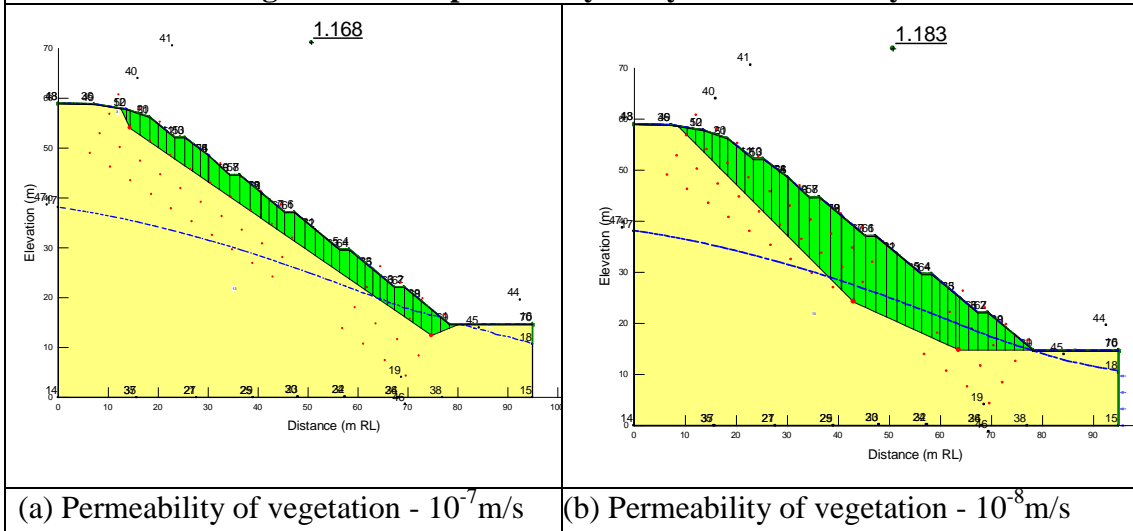
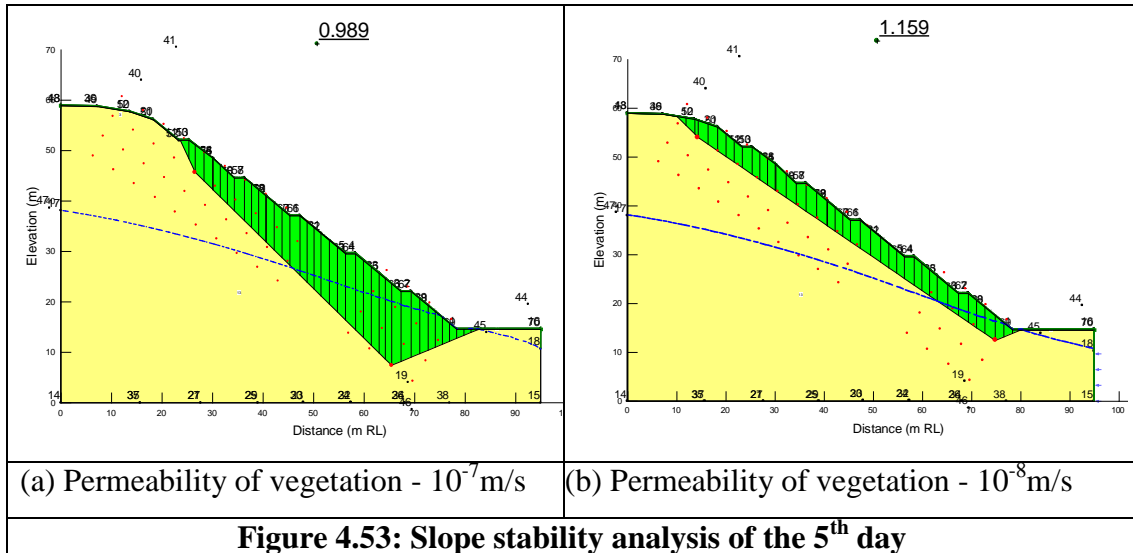


Figure 4.52: Slope stability analysis of the 4th day



4.4.2.2 Slope with surface drainage improvement and with relict joints

(a) Slope with Relict joints and surface drainage improvement – Circular slip surfaces

The critical failure surfaces corresponding to each day when the relict joint are encountered and surface drainage improvement of berm drains and vegetation cover of 10^{-7} m/s and 10^{-8} m/s permeability are applied is analysed thereafter. The pore pressure values obtained from the infiltration analysis under the same conditions is incorporated in this stability analysis. The critical failure surfaces are presented from Figure 4.54 to Figure 4.59 and minimum factor of safety values obtained through the analysis are summarised in Table 4.9.

Table 4.9: Minimum Factor of Safety for Circular slip surfaces – With Relict joints- Peak rainfall from Bombuwawa and Beddagama Rg

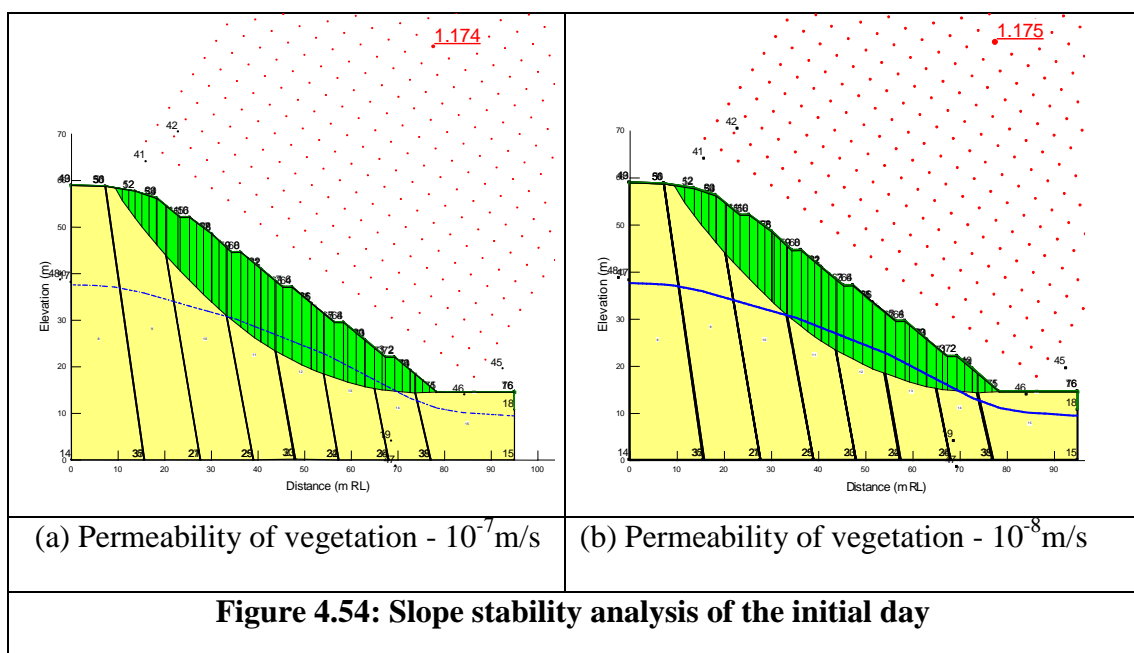
Date	FOS	
	Vegetation – Permeability 10^{-7} m/s	Vegetation – Permeability 10^{-8} m/s
Initial	1.174	1.175
1 st day	1.155	1.158
2 nd day	1.128	1.137
3 rd day	1.094	1.117
4 th day	1.056	1.092
5 th day	1.032	1.068

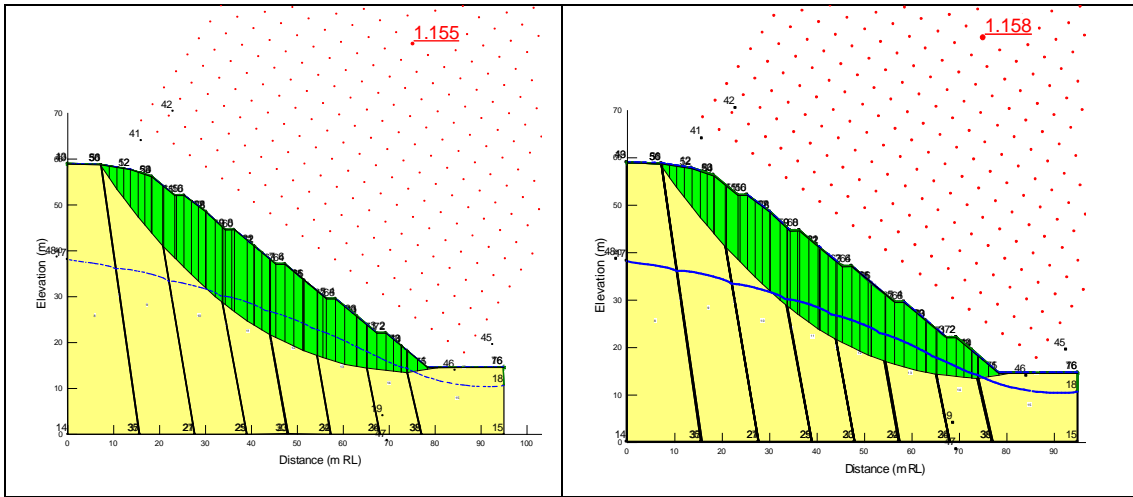
FOS values obtained are higher than those for the similar slope without surface drainage improvement at the corresponding time.

When surface drainage is not present, the failure surface on the 5th day is corresponding closely with the actually observed failure surface. FOS has become lower than unity. But with the improvement of the surface drainage FOS approached unity, 1.032 and 1.068 with different permeability values on 5th day, which indicates the slope is still remaining stable. The critical failure surfaces are also quite deep which does not simulate the actual event of failure.

This indicates that the surface drainage improvement by vegetation cover and berm drains along with cascades reduced the infiltration and loss of matric suction, which had been effective in maintaining a significant margin of safety during the prolonged rainfall.

When there is no surface drainage improvement, the factor of safety reduced significantly as the rain persists. When the surface drainage improvement is present the reduction of the factor of safety with the prolonged rainfall is very minimal.

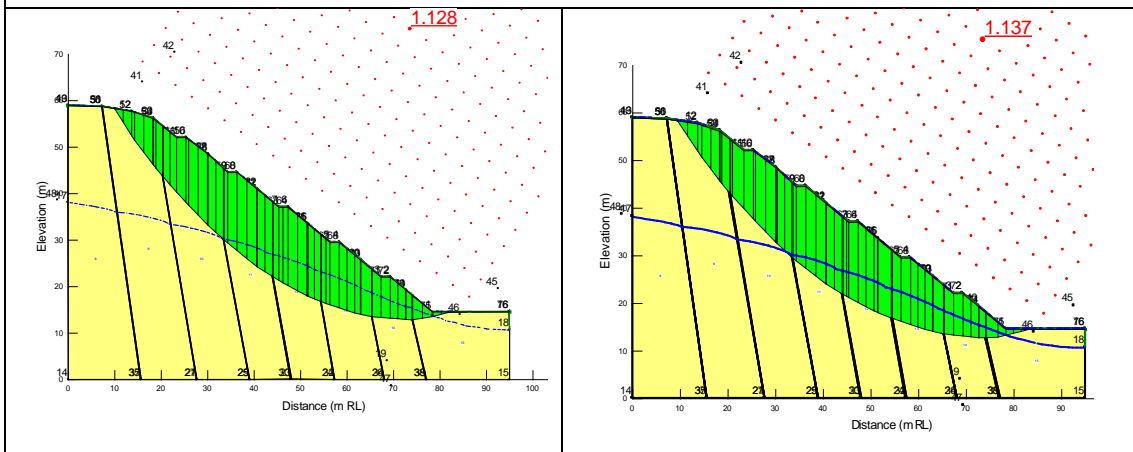




(a) Permeability of vegetation - 10^{-7} m/s

(b) Permeability of vegetation - 10^{-8} m/s

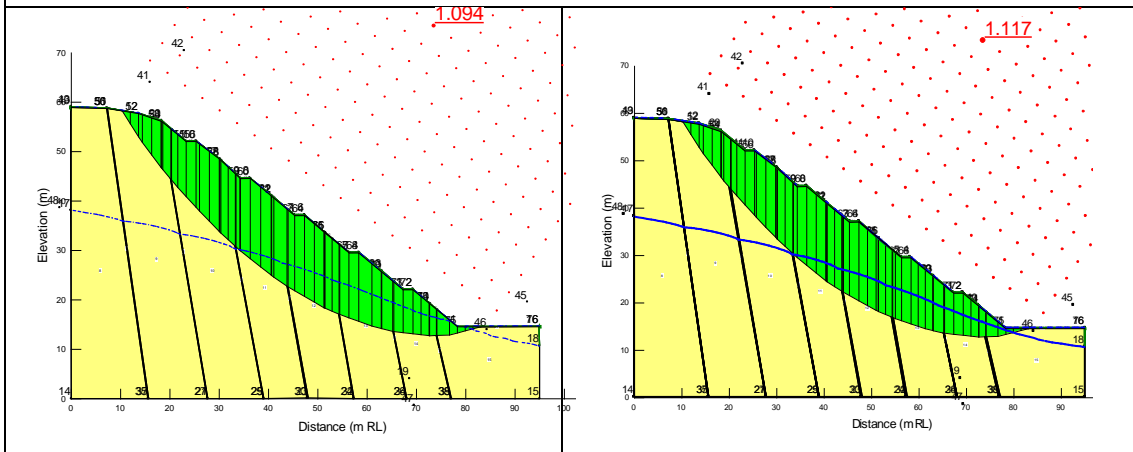
Figure 4.55: Slope stability analysis of the 1st day



(a) Permeability of vegetation - 10^{-7} m/s

(b) Permeability of vegetation - 10^{-8} m/s

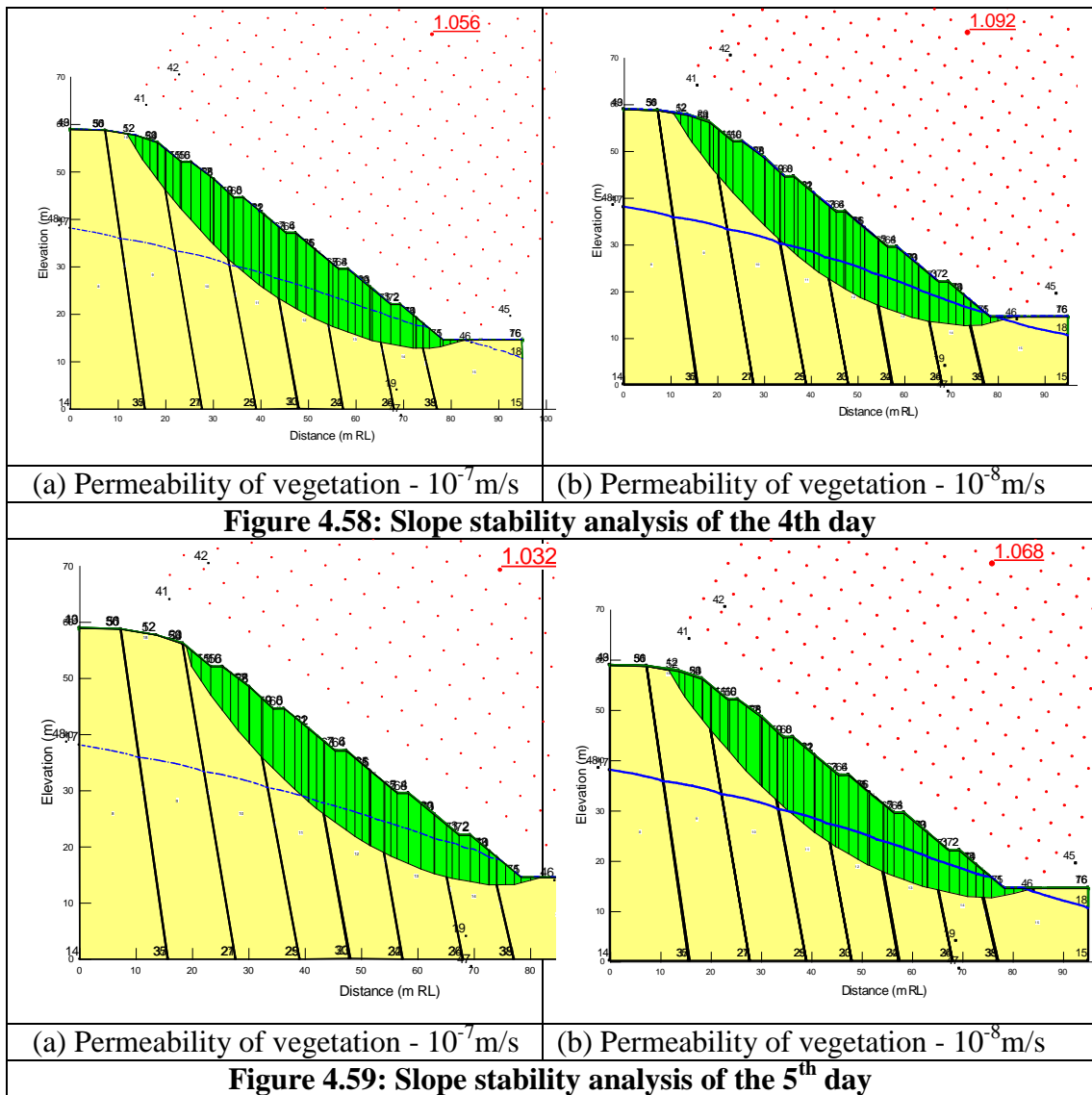
Figure 4.56: Slope stability analysis of the 2nd day



(a) Permeability of vegetation - 10^{-7} m/s

(b) Permeability of vegetation - 10^{-8} m/s

Figure 4.57: Slope stability analysis of the 3rd day



(b) Slope with Relict joints and with surface drainage improvement – Non - Circular slip surfaces

The critical failure surfaces corresponding to each day for non circular slip surfaces when the relict joint are encountered and surface drainage improvement of berm drains and vegetation cover of 10^{-7} m/s and 10^{-8} m/s permeability are applied is analysed thereafter. The critical failure surfaces are presented from Figure 4.60 to Figure 4.65. Minimum factor of safety values obtained through the analysis are summarised in Table 4.10.

Table 4.10: Minimum Factor of Safety for Non circular slip surfaces – With Relict joints

Peak rainfall from Bombuwawa and Beddagama Rg	FOS	
	Vegetation Permeability 10^{-7} m/s	Vegetation Permeability 10^{-8} m/s
Initial	1.227	1.227
1 st day	1.206	1.210
2 nd day	1.181	1.189
3 rd day	1.151	1.167
4 th day	0.927	1.145
5 th day	0.872	0.913

The factor of safety values obtained for the early staged of the rainfall are slightly larger than to the corresponding stages of circular failure surface analysis. But FOS reduced with time and became much smaller compared to the circular failure surface analysis on the 5th day. FOS values on 4th and 5th day have become lower than unity indicating the slope should have failed. However, a closer examination of the failure modes indicates this mode is not feasible kinematically (Figure 4.65).

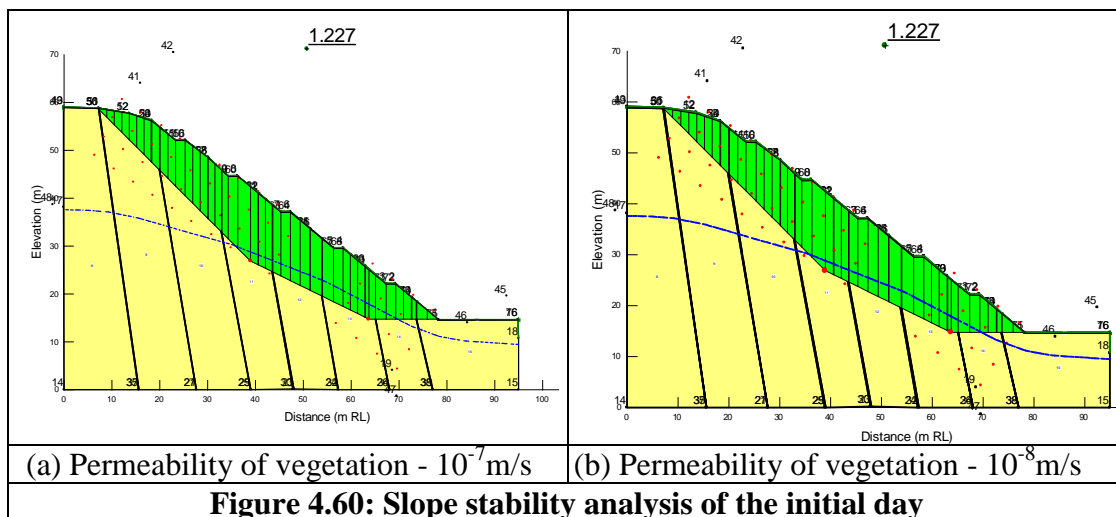


Figure 4.60: Slope stability analysis of the initial day

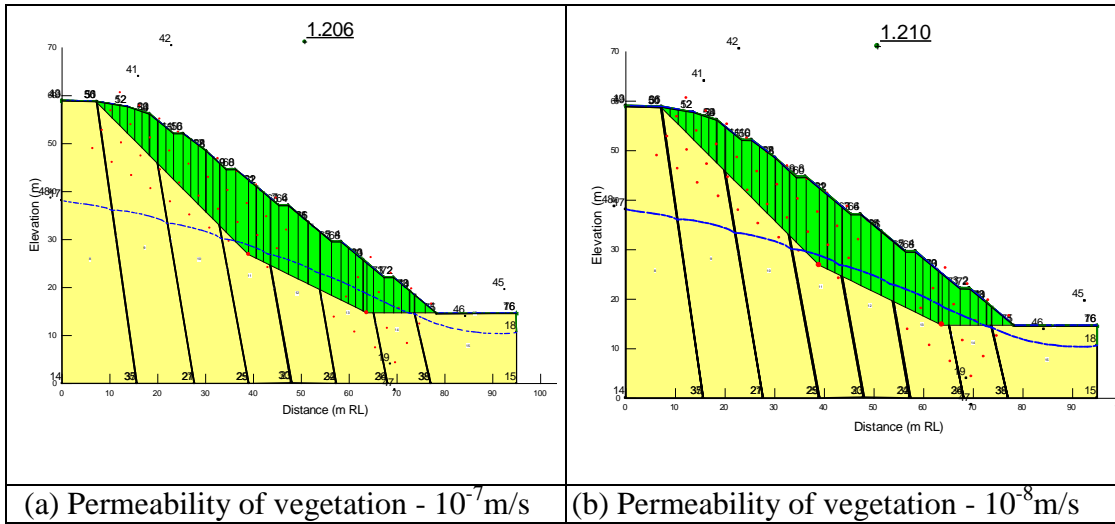


Figure 4.61: Slope stability analysis of the 1st day

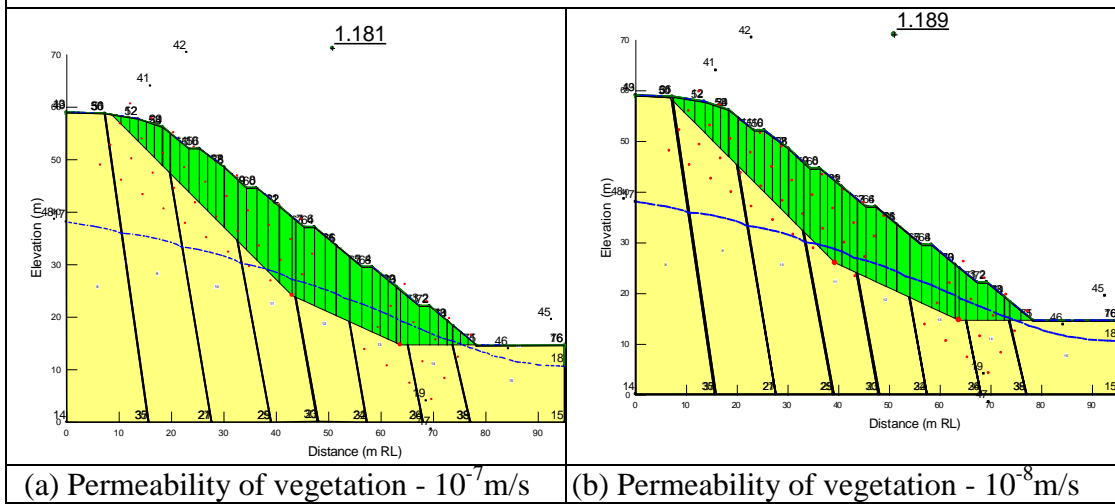


Figure 4.62: Slope stability analysis of the 2nd day

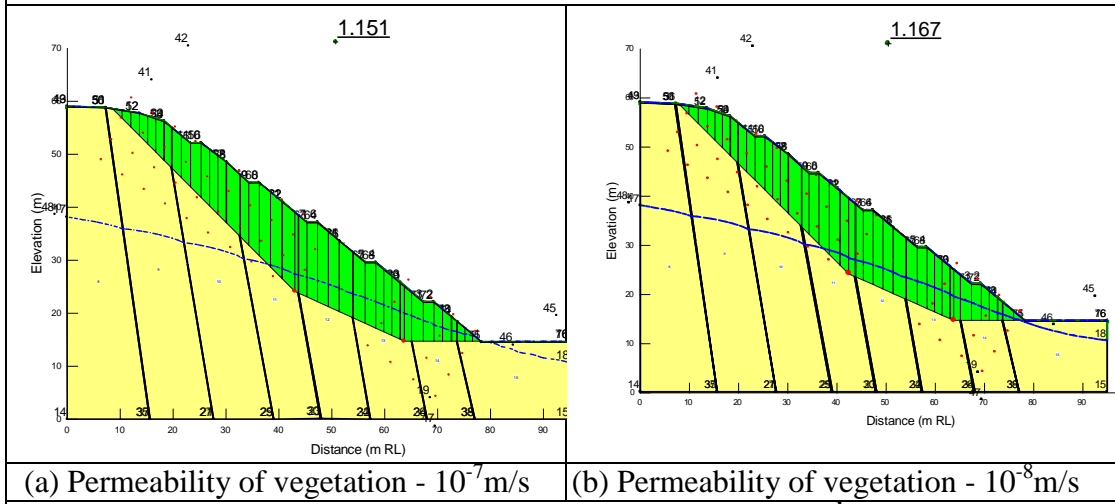
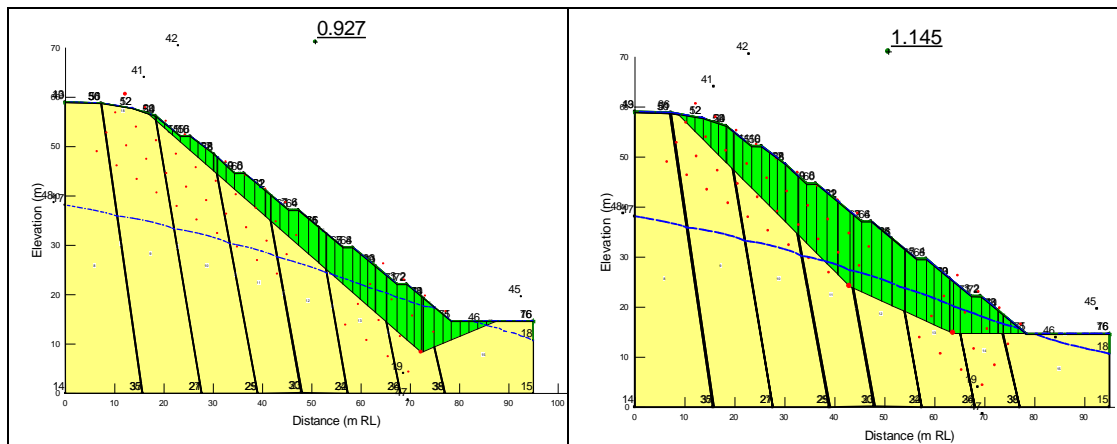
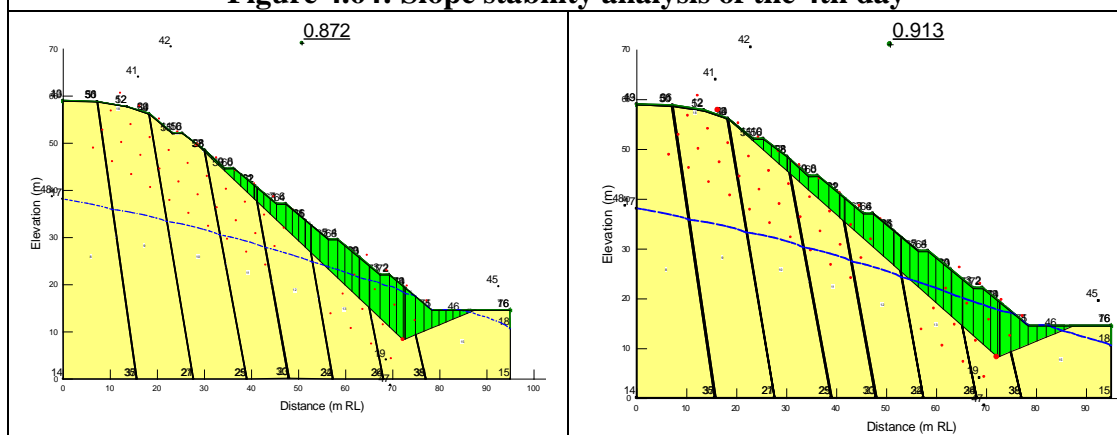


Figure 4.63: Slope stability analysis of the 3rd day



(a) Permeability of vegetation - 10^{-7} m/s (b) Permeability of vegetation - 10^{-8} m/s

Figure 4.64: Slope stability analysis of the 4th day



(a) Permeability of vegetation - 10^{-7} m/s (b) Permeability of vegetation - 10^{-8} m/s

Figure 4.65: Slope stability analysis of the 5th day

4.4.3 Summary of Results

The factor of safety variation with the progression of the rainfall under different condition is summarized for the case without any surface drainage improvement in Table 4.11. The same values are graphically presented in Figure 4.66.

The comparison of results indicate that the factor of Safety values obtained for the non circular slip surfaces are lower than the corresponding stages of circular failure surfaces on later staged of the rainfall. But, when the shaped of the critical failure surfaces are compared some of the non circular failure modes appear to be not feasible kinamatically.

The FOS values for each day is lower when relict joints are present for the cases of both circular and non circular failure surfaces. The seepage analysis also indicated

that more destruction to the pore pressure regime takes place when the relict joints are present. The safety margin should thereafter be lower.

Table 4.11: Summary of the minimum Factor of Safety values – Slope without surface drainage improvement

Time	Without Relict joints		With Relict joints	
	Circular slip surfaces	Non Circular slip surfaces	Circular slip surfaces	Non Circular slip surfaces
Initial	1.185	1.257	1.176	1.249
1 st day	1.182	1.251	1.151	1.246
2 nd day	1.164	1.247	1.113	1.209
3 rd day	1.121	1.185	1.070	1.115
4 th day	1.087	0.992	1.033	0.946
5 th day	1.057	0.934	0.989	0.828

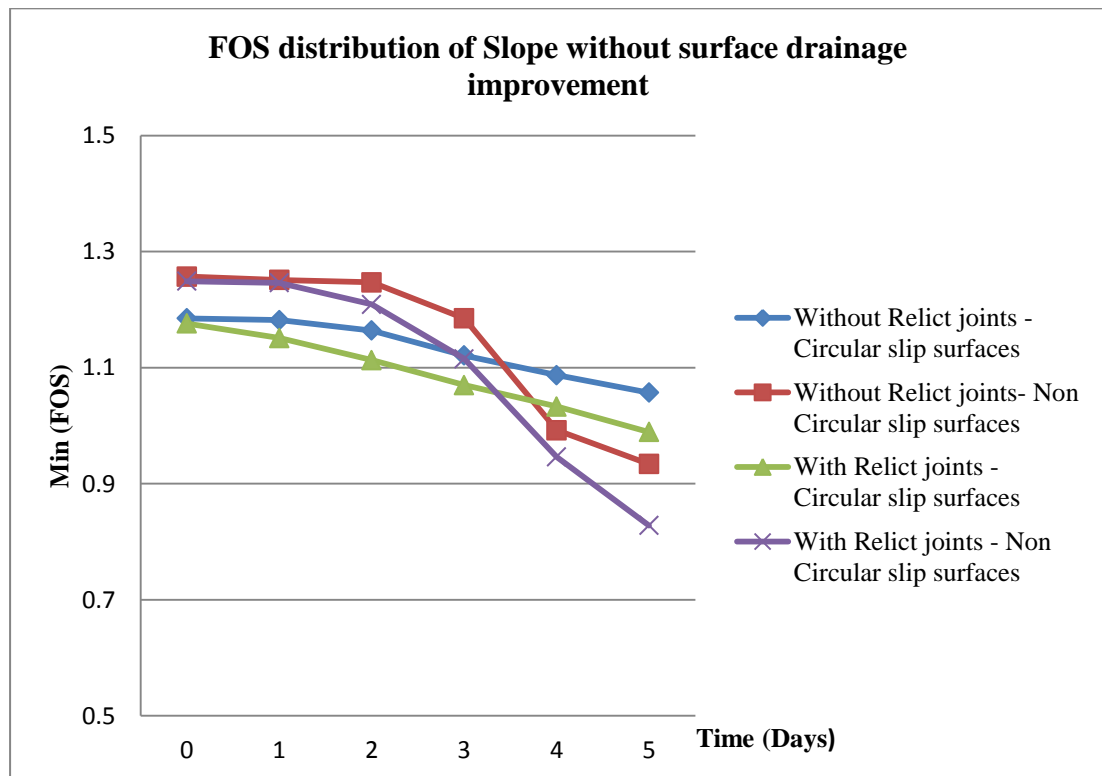


Figure 4.66: FOS distribution of Slope without surface drainage improvement

The variation of the factor of safety with the progression of the rainfall when surface drainage measures and surface protection vegetation is provided for different conditions with and without relict joints is summarised in Table 4.12. The data are graphically presented in Figure 4.67.

Table 4.12: Summary of the minimum Factor of Safety values – Slope with surface drainage improvement

Time	Without Relict joints				With Relict joints			
	Circular slip surfaces		Non Circular slip surfaces		Circular slip surfaces		Non Circular slip surfaces	
	Vegetation – Permeability							
	10 ⁻⁷ m/s	10 ⁻⁸ m/s	10 ⁻⁷ m/s	10 ⁻⁸ m/s	10 ⁻⁷ m/s	10 ⁻⁸ m/s	10 ⁻⁷ m/s	10 ⁻⁸ m/s
Initial	1.203	1.203	1.234	1.234	1.174	1.175	1.227	1.227
1 st day	1.203	1.203	1.229	1.229	1.155	1.158	1.206	1.210
2 nd day	1.190	1.191	1.215	1.216	1.128	1.137	1.181	1.189
3 rd day	1.171	1.178	1.195	1.201	1.094	1.117	1.151	1.167
4 th day	1.145	1.161	1.168	1.183	1.056	1.092	0.927	1.145
5 th day	1.122	1.142	0.989	1.159	1.032	1.068	0.872	0.913

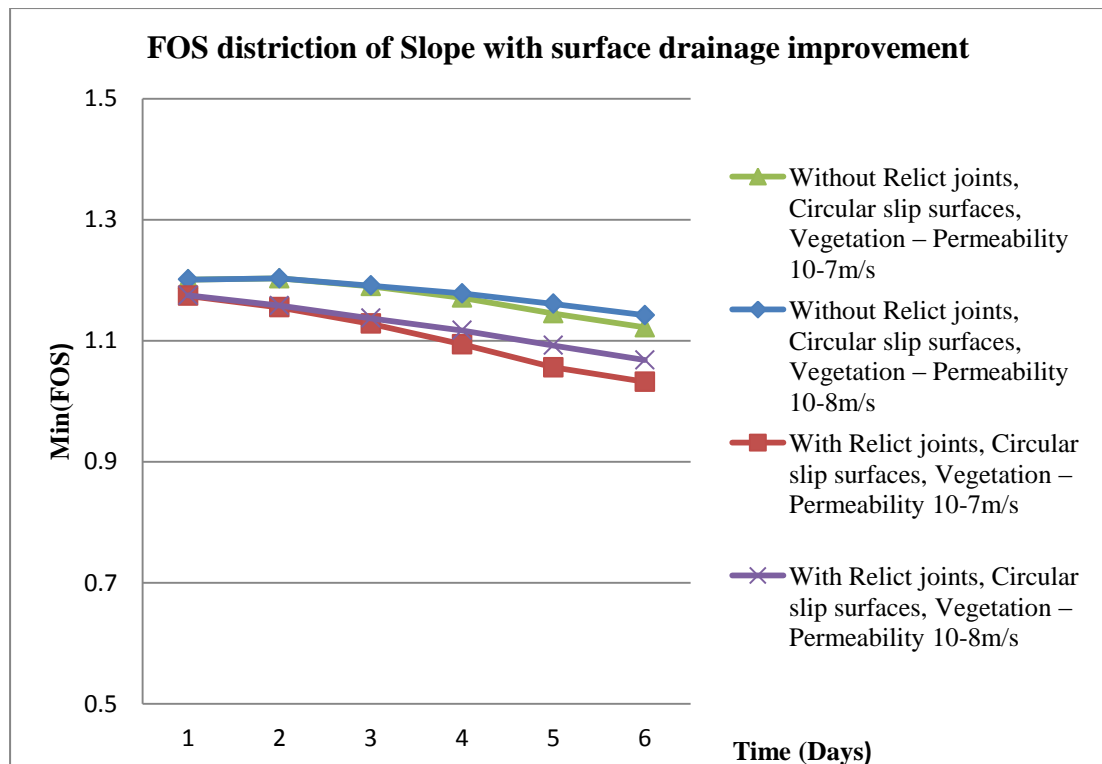


Figure 4.67: FOS distribution of Slope with surface drainage improvement

The comparison of the factor of safety values with the case without surface drainage improvement and with surface drainage improvement proved that on each day FOS is slightly higher where there is surface drainage improvement.

This indicates that, if properly functioned berm drains and cascade drains along with a vegetation cover had been maintained it would help the slope to remain stable. At the field the cracking of the cascade drain just above the failure surface and possible leakage of water to the slope could be observed. That would have contributed to the initiation of failure.

With the improvement of surface drainage and use of a vegetation cover of lower permeability infiltration could be further reduced and a further increasing of FOS could be obtained.

4.4.4 Stability of the slope with higher rainfall intensity of 20mm/hr

A further parametric analysis was done to assess the effectiveness of the surface drainage measures and surface protection vegetation in the event of a prolong rainfall of much greater intensity 20mm/hr. (This is a hypothetical very heavy rain fall)

The critical failure surfaces corresponding to each day, for circular slip surfaces with the surface drainage improvement of berm drains and vegetation cover of 10^{-7} m/s and 10^{-8} m/s permeability are analysed. Minimum factor of safety values obtained through the analysis are summarised in Table 4.13. the values are graphically presented in Figure 4.68. Critical failure surfaces are presented from Figure 4.69 to Figure 4.73.

Table 4.13: Minimum Factor of Safety - 20mm/hr continuous rain

20mm/hr continuous rain for 5 days	FOS	FOS	FOS
	Without Surface Drainage improvement	Vegetation – Permeability 10^{-7} m/s	Vegetation – Permeability 10^{-8} m/s
Initial	1.176	1.175	1.175
1 st day	1.144	1.148	1.158
2 nd day	1.090	1.121	1.136
3 rd day	0.969	1.084	1.116
4 th day	0.792	1.045	1.092
5 th day	0.720	1.011	1.057

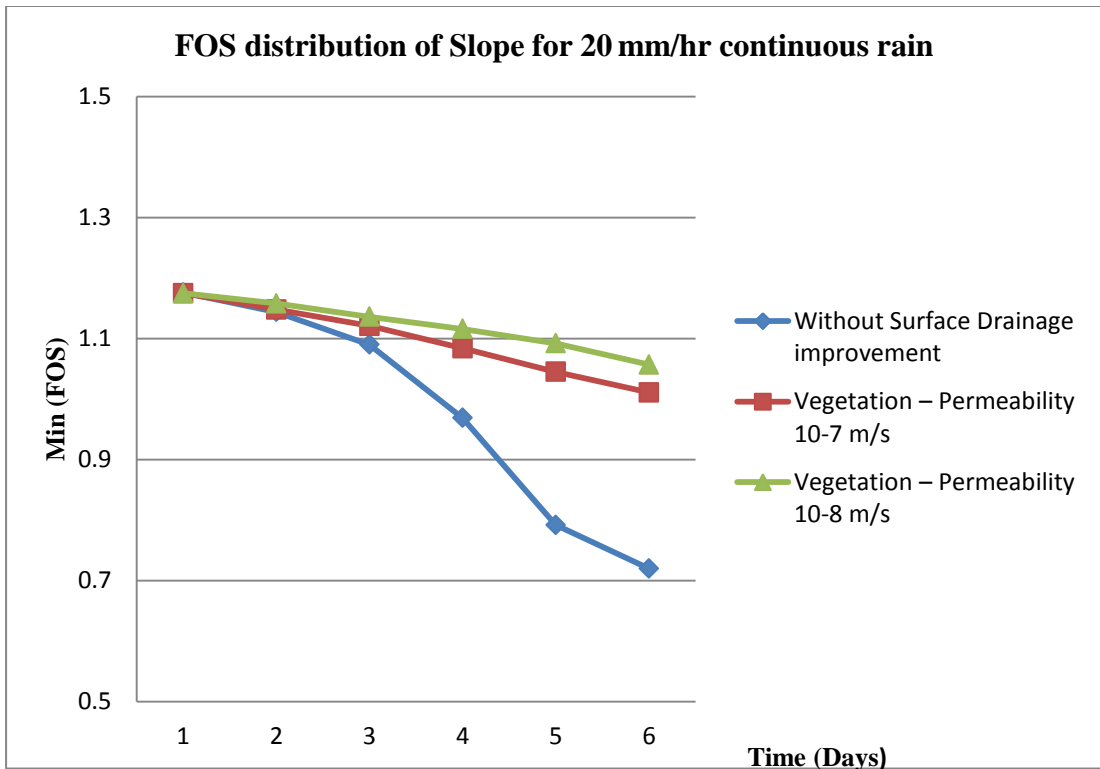


Figure 4.68: FOS distribution of Slope for 20mm/hr continuous rain

When surface drainage improvement is not present, safety margin of the slope reduced significantly with the rainfall of high intensity. Just after the 2nd day FOS value become lower than unity. On 3rd day critical failure surface is quite shallow and kinamatically feasible.

When surface drainage improvement of the slope is applied, even on the 5th day FOS value is close to the unity which indicates the slope remains sill stable. The critical failure surfaces are quite deep. This indicates that, surface drainage improvement of the slope is providing the positive impact on slope stability even with rainfalls of high intensity.

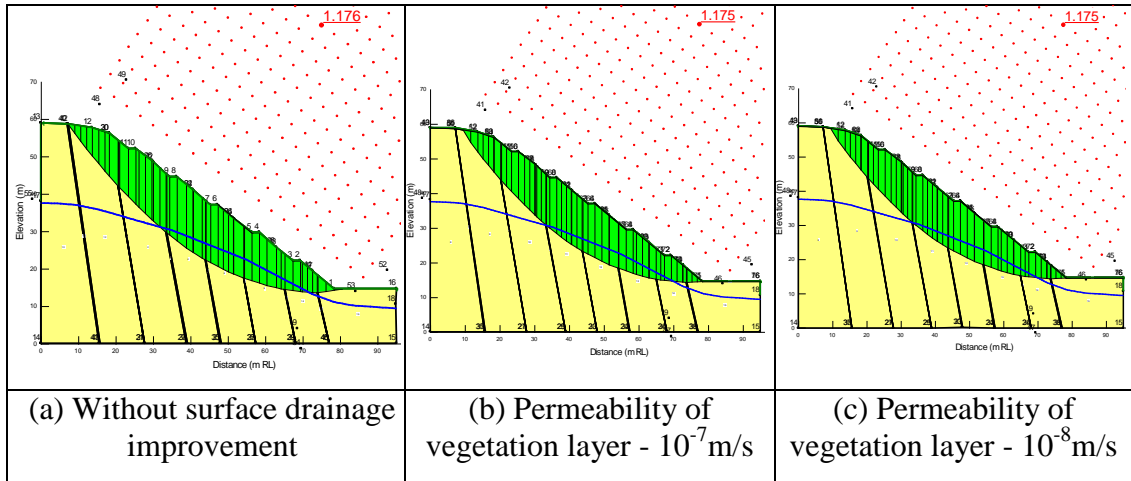


Figure 4.69: Slope stability analysis of the initial day

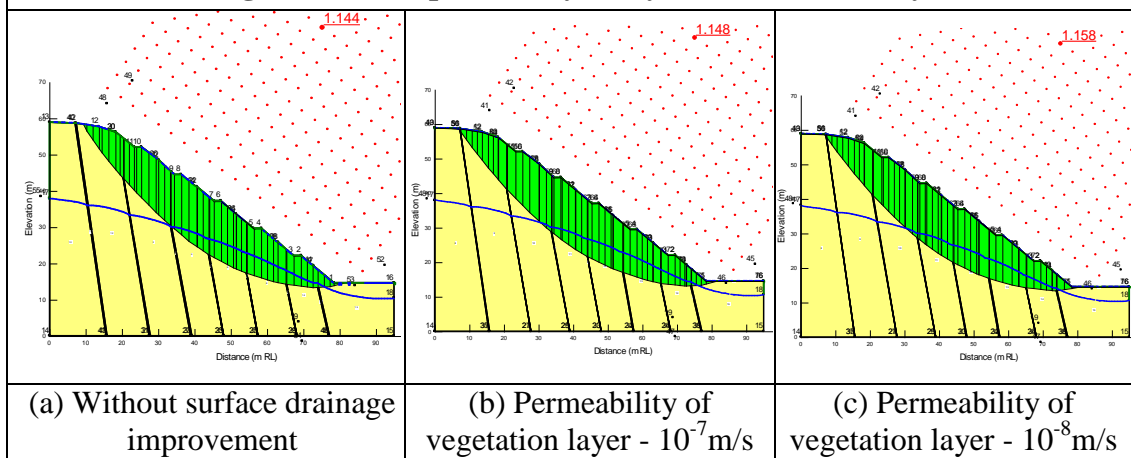


Figure 4.70: Slope stability analysis of the 1st day

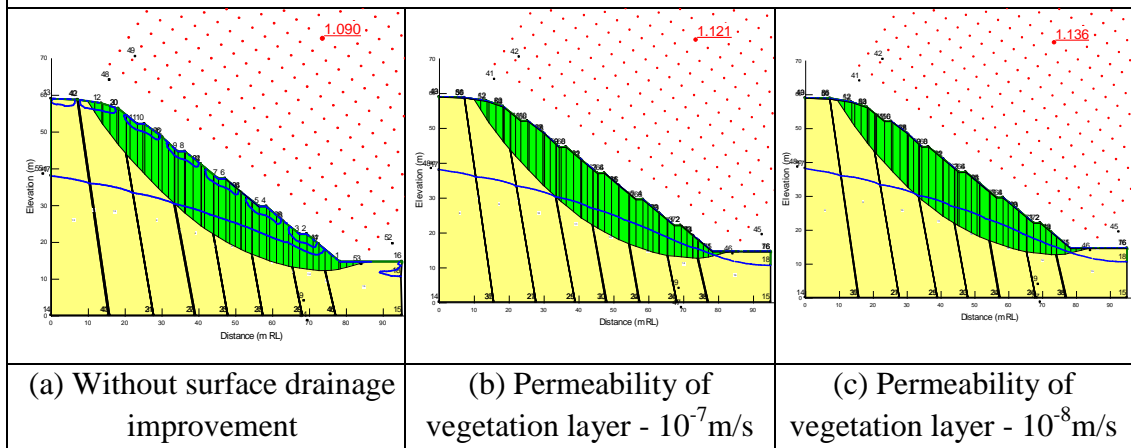


Figure 4.71: Slope stability analysis of the 2nd day

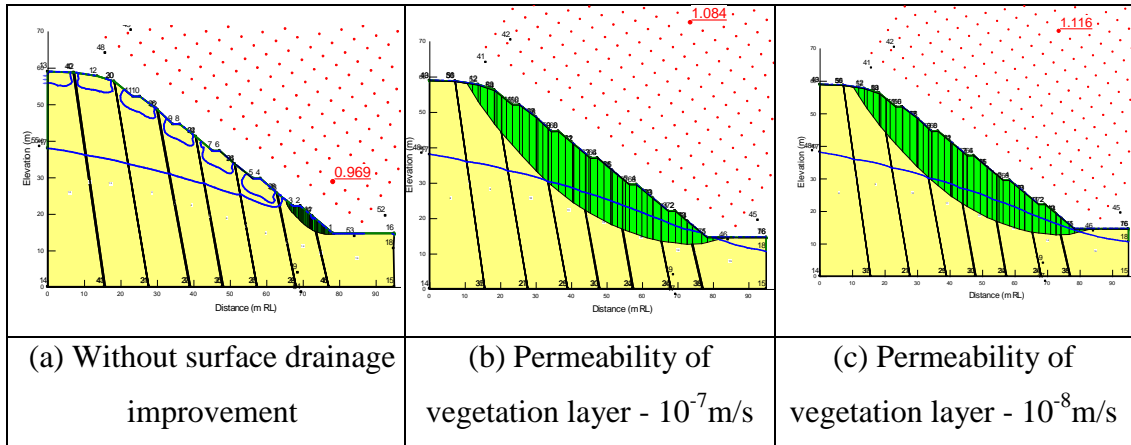


Figure 4.72: Slope stability analysis of the 3rd day

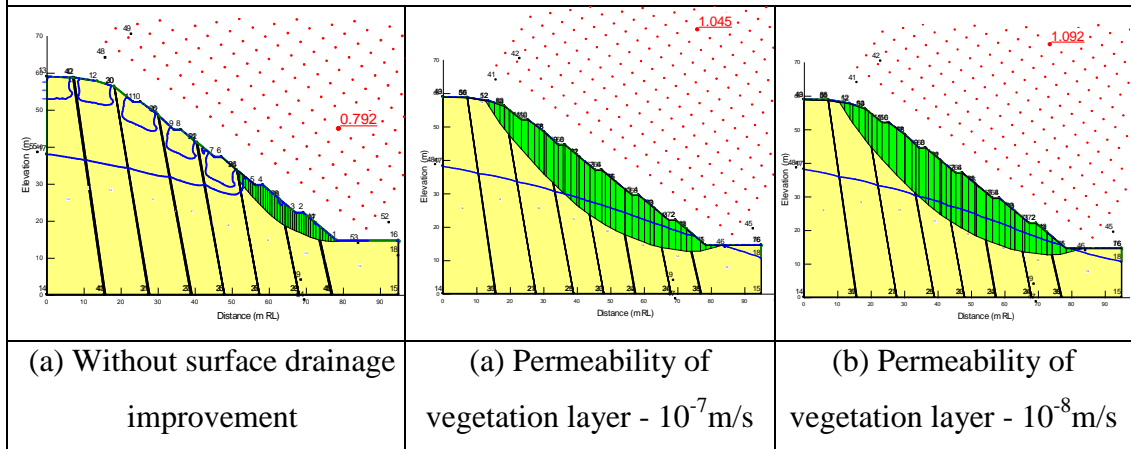


Figure 4.73: Slope stability analysis of the 4th day

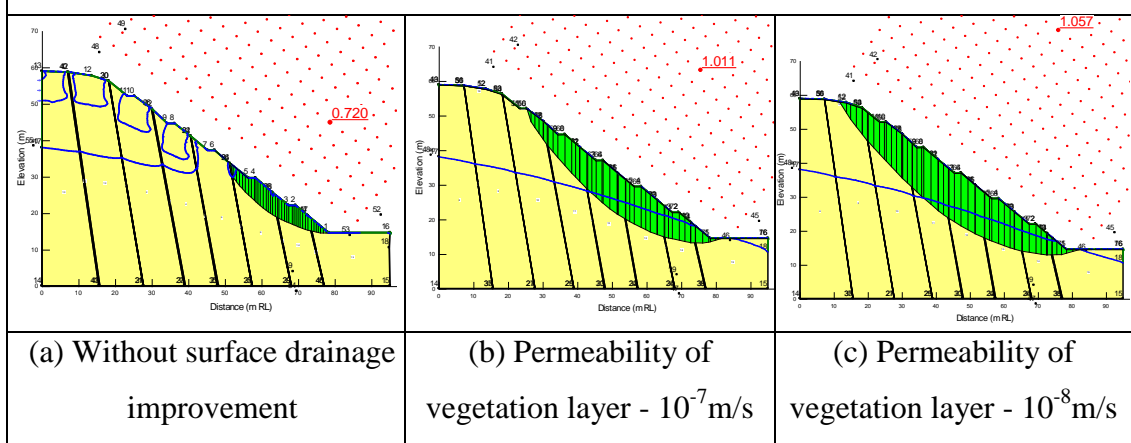


Figure 4.74: Slope stability analysis of the 5th day

CHAPTER 05: CONCLUSIONS

5.1 Failure at Walipanna in Southern Expressway

A catastrophic failure occurred in the Southern expressway at chainage 42+340 to 42+ 400 at Walipanna after few days of rain. There was no rain during the day of failure. Surface cracks (tension cracks) indicating the initiation movement, clearly demarcating the potential failure mass appeared in the morning by 9.00 am and the catastrophic failure by 5pm on the same day. This is a slope of height 45m and excavated to a slope gradient of 1:1.2 with berms at vertical height intervals of 7.5m. Berm drains were constructed on each berm and water flowing in berm drains were intercepted and sent down by several cascade drains. The slope surface was covered with surface protection vegetation.

The slope section were analysed after obtaining the sub surface profile using several boreholes at the design stage. Several undisturbed samples were obtained through box samples and consolidated drained triaxial tests were conducted after saturation of the samples to obtain the design parameters for the stability analysis.

The failure occurred in the background of compliance with proper design and construction procedures. The failure extended to the height of 3 berms and over a width of 50m. The failure is quite shallow, the debris were not with a very high water content. A whitish clayey material was seen at some locations in the exposed scar after failure. The debris of the failure was spread over one half of the road. Oozing out of water at the toe of the slope had been witnessed prior to failure.

5.2 Identification of causes of failure

In this research a back analysis of failure was done. It is necessary to model the process of infiltration and all elements of the failure in an accurate back analysis. Box samples were obtained under undisturbed condition to establish the SWCC, permeability function and shear strength parameters that are necessary for the analysis. This was done through another parallel research project.

A close examination of the site geology revealed that five different joint systems are present in the rocks exposed. At upper levels of the slope at the rear side fresh

bedrock is exposed. Drilling works during the rectification process revealed that there are relict joints in the weathered product (soil) and the systems of joints are interconnected. The presence of water entrapped under high pressure in the relict joints were also identified during the process of rectification. Boudinage structures and the unweathered rock embedded in a matrix of soil were encountered during the drilling for rectification.

Infiltration of the rainfall that was recorded in nearby rain gauges were modeled using the SWCC and permeability function derived from the tests conducted on undisturbed samples recovered from the site. Stability analyses were conducted thereafter incorporating the changes of the pore pressure regime obtained through the above infiltration modeling. The modeling of infiltration was done with SEEP/W software and the stability analysis was done with SLOP/W software.

The infiltration analysis was done under different possible alternate conditions. The different forms of analysis done are illustrated in the figure 5.1. A wide range of analysis of this form was necessary in this back analysis due to the presence of many uncertainties.

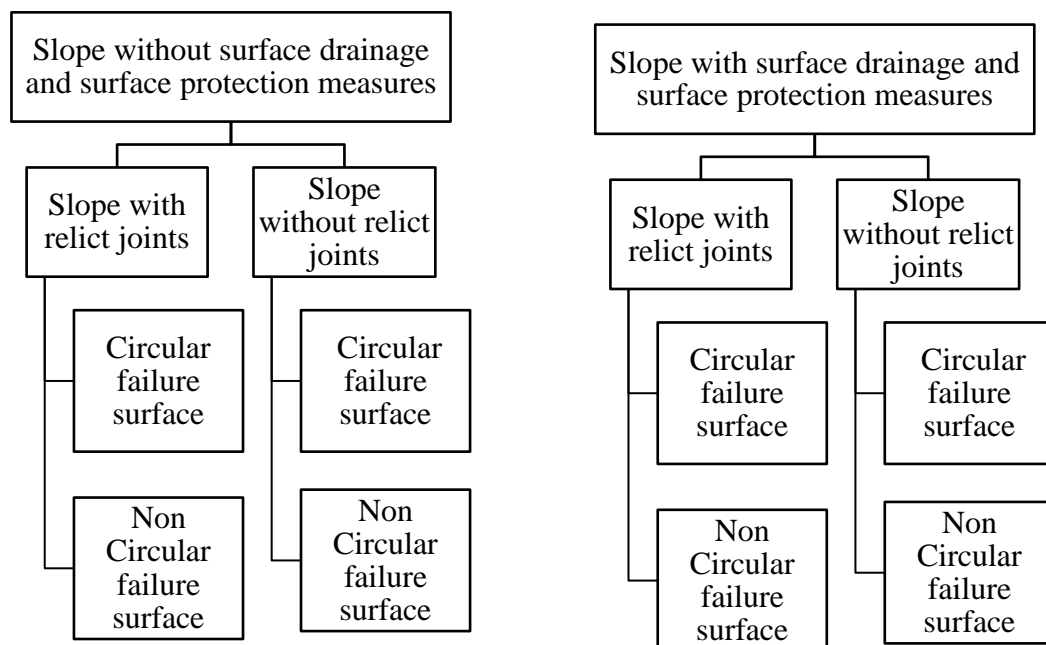


Figure 5.1: Different forms of analysis done

The results of the analysis revealed that if the drainage measures are in position in perfect working order this failure would not have occurred. Those measures were found to be capable of tolerating even a rainfall of much higher intensity than that actually occurred.

However, after the failure there were evidence to indicate that some cascade drains have cracked and there had been water seeping into the slope.

The back analysis revealed that with the presence of relict joints there is more infiltration and negative effect are much greater. The presence of relict joints was confirmed during the rectification work and the combination of the relict joints and failed surface drainage system would have contributed to the failure. Both potential circular and non circular failure surfaces were considered in the study and failure surfaces obtained for the condition in the 5th day in the circular failure surface analysis with relict joints and non effective drainage system corresponds well with the observed failure surface

5.3 Rectification process

The scar remained after failure was unstable and was stabilize by the use of soil nailing at the upper levels and the construction of a gravity retaining structure at the toe. Surface drainage measures were also applied to minimize infiltration of rainwater. In addition a number of sub horizontal drains were drilled to facilitate the release of any high pore water pressures built up in the slide.

5.4 Concluding comments/ Lessons learnt

Failure occurred at this location, after the design and implementation of all surface drainage and slope surface protection measures. If there had been close monitoring of the functioning of the constructed drainage measures, the defects in the drainage system could have been detected early and appropriate repair works could have been carried out which could have prevented this failure. Thus the importance of close monitoring of all slopes is highlighted very strongly.

5.5 Key findings

The importance of close monitoring of the surface drainage measures and any other stabilizing measures installed, and paying prompt attention to any maintenance requirements is highlighted.

The rise of ground water table due to infiltration is quite significant at the toe of the slope. Therefore when natural slopes are excavated into steeper profiles for construction of highways it is recommended to have a series of sub horizontal drains at the toe level even if the ground water table is found to be lower than the toe level.

06: REFERENCES

- Bao, C.G., Gong, B.W., and Zhan, L.T., (1998). "Keynote paper: Properties of unsaturated soils and slope stability for expansive soils." Proc., 2nd Int. Conf. on Unsaturated Soils, Vol. 2, Beijing, 71–98.
- Bishop, A.W., (1955), "The use of the slip circle in the stability analysis of slopes", *Geotechnique*, pp. 5(1): 7-17.
- Curden, D.M., (1991), "A simple definition of a Landslide", International association of Engineering Geology, Paris.
- Cruden, D.M. and Varnes, D.J., 1996, "Landslide Types and Processes, Special Report", Transportation Research Board, National Academy of Sciences, pp. 247:36-75
- Dharmasena, U.K.N.P., Bandara, K.N., Karunawardena W.A and Kulathilaka, S.A.S.,(2015) , "Back Analysis and Rectification of a Failed Cut Slope in the Southern Expressway", ICGE 2015, Sri Lanka, pp. 543-546
- Escario, V. and Juca, J., (1989), "Shear strength and deformation of partly saturated soils", Proceedings of the 12th International Conference on Soil Mechanics and Foundation Engineering, Rio de Janeiro, 2: pp. 43-46.
- Fellenius, W., (1936), " Calculation of the stability of earth dams", Proceedings of the second congress of large dams", Vol. 4, pp.445-463.
- Fredlund, D.G., Morgenstern, N.R and Widger R.A., (1978) "The shear strength of unsaturated soils." *Canadian geotechnical journal*, 15, pp. 313-321
- Fredlund, D. G. and Rahardjo, H., (1993), "Soil mechanics for unsaturated soils". New York: Wiley.
- Gan, J.K.M. and Fredlund, D.G., (1988), "Multistage direct shear testing of unsaturated soils", American Society for Testing Materials, *Geotechnical Testing Journal*, 11(2): pp. 132-138.
- GEO-SLOPE International Ltd, Second Edition, May 2007 "Stability Modeling with SLOPE/W 2007" An Engineering Methodology Calgary, Alberta, Canada.

GEO-SLOPE International Ltd, Second Edition, May 2007 “Seepage Modeling with SEEP/W 2007” An Engineering Methodology Calgary, Alberta, Canada.

Janbu, N., (1954), “Applications of composite slip surfaces for stability analysis”, Proceedings of the European conference on the stability of earth slopes, Stockholm, Vol.3, pp. 39-43.

Jotisankasa, A., Tapparnich, J., Booncharoenpanich, P., Hunsachainan, N. and Soralump, S., (2010), “Unsaturated soil testing for slope studies”, Proc. International conference on Slope, Thailand 2010, Geotechnique and Geosynthetics for Slope, Chiangmai, Thailand.

Kulathilaka, S.A.S. and Sujeevan, V. (2011), “Rain triggered slope failures in unsaturated residual soils”, Published in the Journal of the Sri Lankan Geotechnical Society, Sri Lanka, pp. 20 -26.

Kulathilaka, S.A.S. and Kumara, L.M., (2011), “Effectiveness of surface drainage in enhancing the stability of cut slopes during the periods of heavy rain”, Published in the Journal of the Institution of Engineers, Sri Lanka, pp.127-137.

Landslide Research and Risk Management Division, NBRO, “ Proposal for rectification of failed slope at Ch 42+340 to Ch 42+400 in STDP”, 2013

Morgenstern, N.R. and Price, V.E., (1965), “The analysis of the stability of general slip surfaces”, Geotechnique, Vol. 15, pp.79-93.

Nurly. G and Azman B.K, (2008), “Mechanics of Rainfall infiltration through Soil Slope”, Faculty of engineering, University of technology Malaysia, Malaysia

Sarma, S.K., (1973), “Stability analysis of Embankment and Slopes”, Geotechnique, Vol 23 (3), pp. 423-433.

Spencer, E., (1967), “A method of analysis of Embankments assuming parallel interslice forces”, Geotechnique, Vol 17 (1), pp. 11-26.s

Sujeevan, V. and Kulathilaka, S.A.S., (2011), “Rainfall infiltration analysis in unsaturated residual soil slopes”, Published in the Journal of the Sri Lankan Geotechnical Society, Sri Lanka.

US Army Corps of Engineers, (2003), “Slope Stability Engineer Manual”, Department of the Army ,Washington, USA.

Vanapalli, S.K., Fredlund, D.G. Pufahl, D.E. and Clifton, A.W., (1996), “Model for the prediction of shear strength with respect to soil suction”, Canadian Geotechnical Journal, Vol. 33, pp. 379-392.

Varnes, D.J., (1978), “ Slope movement types and process.” Transportation Research Board, National Academy of Sciences.

Vasanthan, N., (2016), “Establishment of fundamental characteristics of some unsaturated Sri Lankan residual soils”, Thesis submitted in partial fulfillment of the requirements for the degree of Master in Engineering, University of Moratuwa.

Wieczorek .G.F., (1996), “Landslide triggering mechanisms”, Special Report - National Research Council, Transportation Research Board Volume 247, pp.76-90.

Williams, P.J, (1982), “An Introduction to geotechnical science: The science of the earth”, Longman, New York.

7: APPENDICES

Appendix A:

Location plan of the bore holes which were drilled from the berms, after failure